Radiative Corrections to Semileptonic Processes in the Standard Model

by

Kyle Shiells

A Thesis submitted to the Faculty of Graduate Studies
of the University of Manitoba in partial fulfilment
of the requirements of the degree of

DOCTOR OF PHILOSOPHY

Department of Physics & Astronomy
University of Manitoba
Winnipeg

Examining Committee

Dr. Peter Blunden, Supervisor

(Department of Physics & Astronomy)

Dr. Gerald Gwinner, Departmental Member

(Department of Physics & Astronomy)

Dr. Michael Gericke, Departmental Member

(Department of Physics & Astronomy)

Dr. Eric Schippers, Internal Member

(Department of Mathematics)

Dr. Carl Carlson, External Member

(Department of Physics, College of William and Mary)

Abstract

The Standard Model (SM) is currently our most complete, fundamental, and successful theory of nature. However, despite its ability to make some of the most precise predictions in all the physical sciences, there are scenarios where it has been shown to be inadequate or incomplete. This is why SM Precision tests are very important avenues to a solution because they can inform us where the SM is incorrect, and in a manner of speaking, by how much. In this dissertation, we look at two major precision tests: the weak mixing angle and the unitarity condition sum of the top row CKM matrix elements. In order to extract either of these quantities at the level of precision required to meaningfully test the SM, we must go beyond their leading order calculation, and compute all of their 1 loop radiative corrections. The physical process we consider acts like a host to perform both the calculation and the experiment and must be somewhat practical. Semileptonic reactions are a prime candidate as nucleons and nuclei provide practical

targets in scattering experiments as well as ideal decay parents, as opposed to their leptonic alternatives. The cost of this experimental convenience are additional challenges when calculating the observables in the SM theory, as hadronic modeling becomes a necessity. This dissertation investigates some of the most troublesome radiative corrections in an attempt to reduce their hadronic uncertainties, using state-of-the-art dispersive techniques as well as update some previously calculated radiative corrections in the aforementioned test quantities. Using these methods, we have found that the CKM matrix is no longer consistent with unitarity and an updated relationship between the weak mixing angle and the weak charge of the proton is proposed.

Contents

List of Tables

List of Figures

Acknowledgements

I would like to take a few moments here to thank those who have helped make my journey in life a successful one, both as a physicist and as a person. First of all, I would like to thank my advisor, Peter Blunden. Peter provided me with an opportunity to do research in theoretical subatomic physics when both my heart and my mind knew that was what I wanted to do. After completing my coursework in quantum theory, I needed an outlet – a medium with which to take this knowledge further to eventually find myself at home with this dissertation work. My journey throughout this dissertation was truly an epic intellectual challenge, and one that required years of hard work, brainstorming, and a stubborn soul. Thank you Peter for believing in me and always giving me another angle with which to attack a problem – I think I always left your office with a new idea to try and implement in my research. You are a bona fide theorist, and a bonafide Manitoban. Working with you has been a pleasure.

During this dissertation I also had the luxury of meeting a very talented man by the name of Wally Melnitchouk from Jefferson Lab in Virginia. Wally

introduced me to the heavy-duty field of parton distribution functions, and during the way, has made me appreciate hadronic physics much much more. Thank you Wally for teaching me some new tricks from your field, and I promise I won't arbitrarily re-scale my uncertainties anymore!

During my life as a student at the University of Manitoba, I have met many inspiring people. The Department of Physics & Astronomy has been like a second home for me for over the past decade. Many of our faculty members have helped shape me as a physicist, and given me a lifelong love for the subject. In particular I would like to thank my previous supervisor, Gerald Gwinner, for taking me in as your graduate student when I was unsure about where to go in life. The opportunities you gave me, and your support acted as a potent catalyst to help me pursue a career as a physicist and get me where I am today.

I am fortunate to have an amazingly supportive family. Mom and Dad, I owe you everything. You raised me to work hard in life and to pursue my dreams no matter how big they are. You both have always loved and supported me, and I can't thank you enough for that. Thank you dad for teaching me to take pride in my work, and to pursue perfection in it. Mom, thank you for always pushing me to grow. I understand this now – the purpose of life is to keep growing. Thanks to you, I will never stop bettering myself, and I will be sure to pass this value down to my children as well.

Finally, I cannot continue this thesis until I have thanked my lovely wife Marcelle Shiells. Marcelle, I feel as if I couldn't have done this without you.

You are my better half and you have always been there for me, even during my life's toughest challenges. Thank you for putting up with me throughout this entire dissertation and listening to me talk about all these equations and particles, even if it made zero sense to you! Raising our children for the first few years of their life during graduate school was worth the extra work – I wouldn't have done it any other way, and wouldn't have done it with anyone else.

Chapter 1

Introduction

In this opening chapter, I will start by introducing the theoretical foundations of the Electroweak sector of the Standard Model. This will hopefully not only familiarize the reader with the particles and interactions needed for the calculations done in chapters 3 and 4, but to also give the reader the impression that the theory is an impressively engineered and well-oiled machine. Next, I introduce the concept of precision tests, which will ultimately be performed in chapters 4 and 5 of the thesis. Finally, I attempt to define the two processes through which we will test the Standard Model: beta decays of the neutron and parity violating electron proton scattering.

1.1 Electroweak Theory

The Standard Model (SM) aims to define the most fundamental particles in nature and all of their interactions (minus gravity). It constructs its foundations from all of our suspected imperative symmetries (e.g. Lorenz invariance) and it adheres to the rules of quantum mechanics through the more generalized framework of quantum field theory (QFT). In the theory, our 'tactile' matter of the universe is made of spin 1/2 particles called fermions, and these particles interact with each other as well as a special particle known as the Higgs boson. In the Electroweak sector of the SM, the weak and electromagnetic (EM) interactions are unified under a $SU(2)_L \times SU(1)_Y$ gauge group, where the L implies that the $SU(2)$ part is thought to only act on left-handed fermions and Y is called the weak hypercharge. This theoretical construct was first proposed by Glashow [1] in 1961, and has since become our 'standard' picture of particle physics, together with the $SU(3)_C$ group which defines the strong interaction. Before standard theory (ST) was established, however, weak decays were first modeled by Enrico Fermi in the 1930's in the so-called 4-Fermi model. All of the observed weak decay rates at the time were found to have the same overall order of magnitude and so the responsible interaction was thought to be of the form

$$\mathcal{L}^{npe\nu_e}_{4-Fermi} = G_F \bar{\psi}_p \psi_n \bar{\psi}_e \psi_\nu, \tag{1.1}$$

$$G_F = 1.166 \times 10^{-5} \mathrm{GeV}^{-2}, \tag{1.2}$$

for the reaction $n \rightarrow pe^{-}\nu_e$. This simple 4-particle interaction was also proposed for the other decays, such as that found in muon decay. The idea that G_F could be applied to all the weak decays is known as the universality of the weak interaction, and would not be understood until Glashow's model. Despite the ability of 4-Fermi theory to make reliable tree-level predictions (no higher order quantum corrections), it is ultimately a non-renormalizable theory (meaning we cannot systematically cancel all the ultraviolet (UV) divergences produced by its higher order corrections). In the ST of EW interactions, the so-called vector bosons (VBs) are spin-1 particles which mediate the interactions themselves. In QED there is only 1 massless VB called the photon. Yang-Mills theory aims to generalize this model to allow for the additional VBs found in the weak sector, where they also become non-Abelian fields (which concurrently means they are self-interacting). In such a model, the free VBs have the following Lagrangian:

$$\mathcal{L}_{YM} = -\frac{1}{4}\vec{W}_{\mu\nu}\cdot\vec{W}^{\mu\nu} - \frac{1}{4}B_{\mu\nu}B^{\mu\nu}, \tag{1.3}$$

$$\vec{W}_{\mu\nu} = \partial_\mu\vec{W}_\nu - \partial_\nu\vec{W}_\mu - g\vec{W}_\mu\times\vec{W}_\nu, \tag{1.4}$$

$$B_{\mu\nu} = \partial_\mu B_\nu - \partial_\nu B_\mu, \tag{1.5}$$

where $\vec{W}_\mu = (W_{1\mu}, W_{2\mu}, W_{3\mu})$. It is the cross product in (1.4) which indicates that the $\vec{W}_\mu$ field is self-interacting. The free fermion fields simply obey the standard Dirac Currents of the form $\sim \bar{\psi}i\gamma^\mu\partial_\mu\psi$. However, the gradient of these fields does not transform like the fields themselves under the local

gauge transformations:

$$\psi_L \rightarrow e^{i\alpha^a(x)T_a + i\beta(x)Y}\psi_L, \tag{1.6}$$

$$\psi_R \rightarrow e^{i\beta(x)Y}\psi_R, \tag{1.7}$$

$$T_a \equiv \frac{\tau_a}{2}, \tag{1.8}$$

where τ_a are the standard Pauli spin matrices. We require that the SM is invariant under this transformation, which has two historical roots. The first was motivated by Weyl in the 1920's where it is considered as a generalized "phase measure" analogous to the all-too-familiar coordinate measure. The other naive reason is purely quantum mechanical, as phase plays such a fundamental role in the theory. In order to restore our local (position-dependent phase) gauge invariance, we can introduce the covariant derivatives:

$$D_\mu\{q, l\} = (\partial_\mu + igT^aW_\mu^a + ig'YB_\mu)\{q, l\}, \tag{1.9}$$

$$D_\mu\{\bar{u}, \bar{d}, e\} = (\partial_\mu + ig'YB_\mu)\{\bar{u}, \bar{d}, e\} \tag{1.10}$$

on our fermion fields, which are defined in Table 1.1. The non-derivative terms of (1.9-1.10) represent interactions between the fermions and the gauge fields, and are often called "minimal couplings". In fact, they can be inferred from experiment (e.g. such as in QED), but it is remarkable to see that they naturally arise out of us imposing local gauge-invariance alone. With these

Fermion	Description
$q_f = \begin{pmatrix} u \\ d \end{pmatrix}_f$	LH quarks
$\bar{u}_f$	RH up-type quarks
$\bar{d}_f$	RH down-type quarks
$l_f = \begin{pmatrix} \nu \\ e \end{pmatrix}_f$	LH lepton
$\bar{e}_f$	RH charged lepton

Table 1.1: Fermion fields in the Standard Model.

covariant derivatives defined, the fermion Lagrangian now generalizes to

$$\mathcal{L}_{ferm} = \sum_{\text{generations}} \Big[q^\dagger i\gamma^\mu D_\mu q + \bar{u}^\dagger i\gamma^\mu D_\mu \bar{u} \;+\; \bar{d}^\dagger i\gamma^\mu D_\mu \bar{d} + l^\dagger i\gamma^\mu D_\mu l + \bar{e}^\dagger i\gamma^\mu D_\mu e \Big] \tag{1.11}$$

If one expands the transformation in (1.6-1.7) to linear order in the phase variables (i.e. an infinitesimal gauge transformation), it follows that the gauge fields must transform according to

$$W^a_\mu \;\rightarrow\; W^a_\mu - \frac{1}{g}\partial_\mu \alpha^a(x) - \epsilon^{abc}\alpha^b(x) W^c_\mu, \tag{1.12}$$

$$B_\mu \;\rightarrow\; B_\mu - \frac{1}{g'}\partial_\mu \beta(x). \tag{1.13}$$

At this point, our theory obeys the $SU(2)_L \times U(1)_Y$ gauge symmetry, but all of our physical particles are massless. This is quite unsatisfactory, as for

instance, we have known that the electron possesses a finite mass ever since J.J. Thomson performed the e/m experiment in 1887. It is also the case that our current gauge fields $\vec{W}_\mu$ & B_μ do not correspond to any physical VBs yet.

In order to give our particles a mass, the concept of spontaneous symmetry breaking is used. This is realized by the so-called linear sigma model, defined by the following Lagrangian

$$\mathcal{L}_{Higgs} = (D_\mu H)^\dagger (D^\mu H) - V(H), \tag{1.14}$$

$$V(H) = -\mu^2 H^\dagger H + \lambda (H^\dagger H)^2. \tag{1.15}$$

H is a complex doublet field while L_{Higgs} is symmetric and obeys our gauge groups. However, the potential here is anharmonic, and its ground state minimum is defined by a circle of radius v surrounding $\langle H \rangle = 0$, where v is called the vacuum expectation value (vev). It is for this reason that (1.15) is sometimes called the "Mexican hat potential". Choosing a vev configuration for H is completely arbitrary, and doing so will break our gauge symmetry – hence the aptly named "spontaneous symmetry breaking". There are several employed conventions for the vev configuration. For pedagogical purposes, we will choose the simplest convention. The vev field can simply be chosen as

$$\langle H \rangle = \frac{1}{\sqrt{2}} \begin{pmatrix} 0 \\ v \end{pmatrix}, \tag{1.16}$$

and performing a simple first derivative test on $V(H) = 0$ reveals that $v = \sqrt{\mu^2/\lambda}$. One can then define a small perturbative field to this configuration $h(x)$. Then our new Higgs field is given by

$$H = \frac{1}{\sqrt{2}} \begin{pmatrix} 0 \\ \\ v + h \end{pmatrix}. \tag{1.17}$$

From this definition, the kinetic term in (1.14) becomes

$$(D_\mu H)^\dagger (D^\mu H) = \frac{1}{2} \Bigg\{ \partial^\mu h \partial_\mu h + \Big[\frac{g^2}{4} \Big((W_\mu^1)^2 + (W_\mu^2)^2 \Big) - \frac{g^2}{2} \Big((W_\mu^3)^2 + \frac{g'^2}{g^2} B_\mu^2 - 2 g g' B^\mu W_\mu^3 \Big) \Big] (v + h)^2 \Bigg\}. \tag{1.18}$$

Since $(v + h)^2 = v^2 + 2vh + h^2$, the pure gauge-boson mass terms involve v^2 terms only. This contribution, slightly re-written, is given by

$$\mathcal{L}_{\text{gauge mass}} = \frac{1}{2} \begin{pmatrix} W_1 & W_2 & W_3 & B \end{pmatrix}^\mu \begin{pmatrix} \frac{g^2 v^2}{4} & 0 & 0 & 0 \\ 0 & \frac{g^2 v^2}{4} & 0 & 0 \\ 0 & 0 & \frac{g^2 v^2}{2} & -\frac{g g' v^2}{2} \\ 0 & 0 & -\frac{g g' v^2}{2} & \frac{g'^2 v^2}{2} \end{pmatrix} \times \begin{pmatrix} W_1 \\ W_2 \\ W_3 \\ B \end{pmatrix}_\mu \tag{1.19}$$

Which is clearly not diagonal in the (W_3^μ, B^μ) basis. If the 4×4 matrix in (1.19) were diagonal, it would allow an unambiguous interpretation of the VB masses $\sim m_V^2 V^\mu V_\mu$. This can be attained by the relations

$$W_\mu^\pm = \frac{1}{\sqrt{2}}(W_\mu^1 \mp i W_\mu^2), \tag{1.20}$$

$$Z_\mu = \cos\theta_W - \sin\theta_W B_\mu, \tag{1.21}$$

$$A_\mu = \sin\theta_W W_\mu^3 + \cos\theta_W B_\mu, \tag{1.22}$$

$$\tan\theta_W = \frac{g'}{g}. \tag{1.23}$$

Where the $W_\mu^\pm$ are the charged W boson fields, Z_μ is the neutral Z boson field, and A_μ is the photon field. Now, rather than using the abstract gauge couplings (g, g'), we can replace them with the natural EW couplings $(e, \sin\theta_W)$ via

$$g = \frac{e}{\sin\theta_W}, \tag{1.24}$$

$$g' = \frac{e}{\cos\theta_W}. \tag{1.25}$$

The rotation angle θ_W is known as the Weinberg angle, and it effectively relates the strength of the weak coupling constant to the strength of the EM coupling constant. Another consequence of (1.20-1.23) is the following identity for the quantum numbers of fermions

$$Q = T^3 + Y. \tag{1.26}$$

Before we continue, it is worth mentioning that rather than using (1.17), in the derivation of the EW Feynman rules used in this thesis (see Appendix A), the following alternative choice has been made

$$H = \begin{pmatrix} \phi^+ \\ \frac{1}{\sqrt{2}}(v + h + i\phi^0) \end{pmatrix}. \tag{1.27}$$

Substituting (1.27) into (1.14) leads to new terms involving the unphysical Goldstone bosons $\{\phi^\pm, \phi^0\}$ (informally known as "would-be" Higgs bosons) which can enter calculations as virtual particles. As external particles (or perhaps I should say: on their mass shell), they merely serve as a means to cancel the unphysical longitudinal contribution of their physical VB counterparts $\{W^\pm_\mu, Z_\mu\}$ via the Goldstone Boson equivalence theorem [3]. Our diagonalization exercise also reveals where our VBs get their mass, as one will find

$$m_\gamma = 0, \tag{1.28}$$

$$M_W = \frac{g}{2}v, \tag{1.29}$$

$$M_Z = \frac{\sqrt{g^2 + g'^2}}{2}v, \tag{1.30}$$

$$\frac{M_W}{M_Z} = \cos\theta_W. \tag{1.31}$$

At this point we can also get our physical fermion -VB couplings. This leads to the neutral current (NC) which is part EM and part weak and it also leads

to the purely weak charged current (CC). After some algebra one is left with:

$$\mathcal{L}_{NC} = \sum_{f=\{u,d,e,\nu\}} \bar{f} i\gamma^{\mu}\Big(\partial_{\mu} + ieQ_f A_{\mu} + i\frac{g}{\cos\theta_W}(T_f^3 - Q_f \sin^2\theta_W)Z_{\mu}\Big) f, \tag{1.32}$$

$$\begin{aligned}\mathcal{L}_{CC} = {} & \bar{\nu}(i\gamma^{\mu}\partial_{\mu})\nu + \bar{e}(i\gamma^{\mu}\partial_{\mu})e - \frac{g}{2\sqrt{2}}W_{\mu}^{+}\bar{\nu}\gamma^{\mu}(1-\gamma_5)e \\ & -\frac{g}{2\sqrt{2}}W_{\mu}^{-}\bar{e}\gamma^{\mu}(1-\gamma_5)\nu. \end{aligned} \tag{1.33}$$

Where I have moved to the traditional Dirac spinor notation in which LH & RH fields are acquired by applying the chiral projectors $P_{R,L} = (1 \pm \gamma_5)/2$. I have also specified the flavours of the relevant fermion fields (see Table 1.2). Equations (1.32-1.33) are quite important as they will inevitably enter into any scattering amplitude at the tree level for any EW process. Taking the weak VB propagators into account, which at low q^2 : $M_{tree} \sim g^2/(q^2 - M_W^2) \rightarrow g^2/M_W^2 \sim G_F$, they reconcile nicely with 4-Fermi theory. Next, we still need a way of describing the masses of our SM fermions.

In the SM one cannot construct ordinary mass terms for the fermions such as: $m_e(\bar{e}_L e_R + \bar{e}_R e_L)$ without violating gauge invariance, as the LH and RH components of the different fermion fields have different gauge quantum numbers. Instead, the mechanism of spontaneous symmetry breaking must be invoked. Let's take our scalar Higgs field H with a known vev; then a gauge-invariant coupling linking H to the quarks can be written by [3]:

$$\Delta\mathcal{L}_q = -\lambda_d \bar{Q}_L \cdot H d_R - \lambda_u \epsilon^{ab} \bar{Q}_{La} H_b^{\dagger} u_R + h.c. \,. \tag{1.34}$$

fermion (f):	T_3^f:	Q_f:
$(\nu_l)^L$	$\frac{1}{2}$	0
$(l^-)^L$	$-\frac{1}{2}$	-1
$(u,c,t)^L$	$\frac{1}{2}$	$\frac{2}{3}$
$(d,s,b)^L$	$-\frac{1}{2}$	$-\frac{1}{3}$
$(\nu_l)^R$	0	0
$(l^-)^R$	0	-1
$(u,c,t)^R$	0	$\frac{2}{3}$
$(d,s,b)^R$	0	$-\frac{1}{3}$

Table 1.2: Fermion quantum numbers in the SM. Their hypercharges follow trivially from (1.26). The 3 families of leptons are: $l = e, \mu, \tau$. The 2nd row is the weak isospin partner to the 1st row and the 4th row is the weak isospin partner to the 3rd row.

Since H acquires a vev of the form $\langle H \rangle = \frac{1}{\sqrt{2}}(0, v)$, to LO we can write (1.34) as

$$\Delta\mathcal{L}_q = -\frac{1}{\sqrt{2}}\lambda_d v \bar{d}_L d_R - \frac{1}{\sqrt{2}}\lambda_u v \bar{u}_L u_R + h.c. + \dots \ . \tag{1.35}$$

The λ's are some new dimensionless coupling constants, and we can identify the down and up quark masses as: $m_{d,u} = \lambda_{d,u} v/\sqrt{2}$. Adding additional quark generations allows additional couplings which mixes generations. Now let us define:

$$u_L^i = (u_L, c_L, t_L), \tag{1.36}$$

$$d_L^i = (d_L, s_L, b_L). \tag{1.37}$$

One can always change basis in the quark fields, but this will in turn, complicate their gauge couplings. Let u'^i_L, d'^i_L denote the basis which diagonalizes their Higgs couplings, achieved by the unitary transformation:

$$u^i_L = U^{ij}_u u'^j_L, \tag{1.38}$$

$$d^i_L = U^{ij}_d d'^j_L. \tag{1.39}$$

Then in this new basis the W boson current takes the form:

$$J^{\mu\dagger}_W = \frac{1}{\sqrt{2}}\bar{u}^i_L\gamma^\mu d^i_L = \frac{1}{\sqrt{2}}\bar{u'}^i_L\gamma^\mu(U^\dagger_u U_d)_{ij}d'^j_L = \frac{1}{\sqrt{2}}\bar{u'}^i_L\gamma^\mu V_{ij}d'^j_L, \tag{1.40}$$

while the neutral currents are unaffected as they do not mix flavours. It is this redundancy in the Yukawa couplings, in the form of a residual $U(1)^6$ global symmetry, that has lead to the so-called Cabbibo-Kobayashi-Maskawa (CKM) matrix in (1.40), which we define as:

$$V = U^\dagger_u U_d = \begin{pmatrix} V_{ud} & V_{us} & V_{ub} \\ V_{cd} & V_{cs} & V_{cb} \\ V_{td} & V_{ts} & V_{tb} \end{pmatrix}. \tag{1.41}$$

The CKM matrix is a complex unitary matrix for which a standard parameterization exists, using 3 angles and 1 phase via:

$$V = \begin{pmatrix} 1 & 0 & 0 \\ 0 & \cos\theta_{23} & \sin\theta_{23} \\ 0 & -\sin\theta_{23} & \cos\theta_{23} \end{pmatrix} \begin{pmatrix} \cos\theta_{13} & 0 & \sin\theta_{13}e^{i\delta} \\ 0 & 1 & 0 \\ -\sin\theta_{13}e^{i\delta} & 0 & \cos\theta_{13} \end{pmatrix} \times \begin{pmatrix} \cos\theta_{12} & \sin\theta_{12} & 0 \\ -\sin\theta_{12} & \cos\theta_{12} & 0 \\ 0 & 0 & 1 \end{pmatrix}, \tag{1.42}$$

$$= \begin{pmatrix} c_{12}c_{13} & s_{12}c_{13} & s_{13}e^{-i\delta} \\ -s_{12}c_{23} - c_{12}s_{23}s_{13}ei\delta & c_{12}c_{23} - s_{12}s_{23}s_{13}e^{i\delta} & s_{23}c_{13} \\ s_{12}s_{23} - c_{12}c_{23}s_{13}e^{i\delta} & -c_{12}s_{23} - s_{12}c_{23}s_{13}e^{i\delta} & c_{23}c_{13} \end{pmatrix}, \tag{1.43}$$

where $c_{ij} = \cos\theta_{ij}$ and $s_{ij} = \sin\theta_{ij}$. The CKM matrix is unitary by construction as it plays the role of a basis rotation. It is only through the measurement of its elements that we can determine if it really is unitary. If experiment indicates that (1.41) is non-unitary, one possible explanation for this could be a 4th quark generation, among other possibilities discussed in section 5. Therefore CKM unitarity tests are a new way to look for physics beyond the SM. The general unitarity of V is realized by the condition:

$$\Sigma_i V_{ij} V_{ik}^* = \delta_{jk}. \tag{1.44}$$

One example of (1.44) which will be tested in this thesis is the top row of V:

$$|V_{ud}|^2 + |V_{us}|^2 + |V_{ub}|^2 = 1, \tag{1.45}$$

in which the dominant term is $|V_{ud}|^2$. A precision measurement of the ud matrix element is a strong way to test CKM unitarity as it dominates the LHS of (1.45). However, as we will see, a precision measurement requires an equally precise calculation which will involve a computation of the radiative corrections predicted by perturbative QFT.

There are still actually two ingredients still missing from our EW Lagrangian – and one of those is the need to fix a gauge. To see how this comes about, it is helpful to look at the associated path integral of the photon (the weak VBs are dealt with similarly), which is given by

$$\int DA e^{i\int d^4x \left[-\frac{1}{4}F_{\mu\nu}F^{\mu\nu}\right]}, \tag{1.46}$$

$$F_{\mu\nu} = \partial_\mu A_\nu - \partial_\nu A_\mu. \tag{1.47}$$

And recall that the action in the exponent is invariant under the general gauge transformation:

$$A_\mu(x) \to A_\mu(x) + \frac{1}{e}\partial_\mu \alpha(x) = A'_\mu(x). \tag{1.48}$$

It follows then that the issue is that the path integral is poorly defined as we are integrating over a continuous family of physically redundant equivalent

field configurations. We need a way of performing the path integral which only counts each physical field configuration once. To do this, we start by fixing the gauge via

$$G(A_\mu) = \partial^\mu A_\mu = 0, \tag{1.49}$$

which is called the Lorenz gauge (but others exist as well). We can then take the identity:

$$1 = \int D\alpha(x)\delta(G(A'))det\left(\frac{\delta G(A')}{\delta\alpha}\right), \tag{1.50}$$

and insert it into (1.46). Doing so gives

$$det\left(\frac{\delta G(A')}{\delta\alpha}\right)\int D\alpha \int DA' e^{i\int d^4x\left[-\frac{1}{4}F_{\mu\nu}F^{\mu\nu}\right]}\delta(G(A')). \tag{1.51}$$

We can then make a simple shift in coordinates $A \to A'$ in which $DA = DA'$ and the gauge action $F_{\mu\nu}F^{\mu\nu}$ is also already invariant under this transformation. Meanwhile, from (1.48) we have that

$$det\left(\frac{\delta G(A')}{\delta\alpha}\right) = det\left(\frac{\partial^2}{e}\right). \tag{1.52}$$

The final technique is to generalize (1.49) to $G(A') = \partial^\mu A_\mu(x) - \omega(x)$ then take $\int D\omega(x)e^{-i\int d^4x(\omega^2/2\xi_A)}$ for a properly normalized distribution of functions $\omega(x)$. Performing this $D\omega$ integration with the δ-function and renaming our dummy variable $A' \to A$ gives us [3]:

$$N(\xi_A)det\left(\frac{\partial^2}{e}\right)\left(\int D\alpha\right)\int DA e^{i\int d^4x\left[-\frac{1}{4}F_{\mu\nu}F^{\mu\nu}\right]}e^{-i\int d^4x\frac{1}{2\xi_A}(\partial^\mu A_\mu)^2}. \tag{1.53}$$

The prefactors of (1.53) are unimportant, as they merely wash out in our normalized correlation functions, which are proportional to

$$\langle 0|T\{O(A)\}|0\rangle \sim \frac{\int DAO(A)e^{i\int d^4x\mathcal{L}}}{\int DAe^{i\int d^4x\mathcal{L}}}. \tag{1.54}$$

The effect of (1.53) then, is the addition of the new Lagrangian term

$$\mathcal{L}_{GF} = \frac{1}{2\xi_A}(\partial^\mu A_\mu)^2. \tag{1.55}$$

In fact, we will have the same gauge fixing terms for the other VBs, leaving us with 3 new parameters: $\xi_A, \xi_Z, \xi_W = \xi_\pm$. Choosing a particular value for these parameters amounts to fixing a Lorenz invariant gauge. In ordinary QM, when one imposes mathematical conditions on their wave functions via boundary conditions they arrive at the quantization condition. Analogously, imposing condition (1.49) has lead to the quantization of our photon field. We will be choosing the traditional Feynman gauge in this thesis, where $\xi_i = 1$, which is often the simplest choice, as the gauge boson propagators have now become [3]

$$D_V^{\mu\nu}(q^2) = \frac{ig^{\mu\nu}}{q^2 - M_V^2 + i\epsilon} \to \frac{i}{q^2 - M_V^2 + i\epsilon}\left(g^{\mu\nu} - (1-\xi_V)\frac{q^\mu q^\nu}{q^2 - M_V^2}\right). \tag{1.56}$$

There is however, one subtle complication in the non-Abelian case. The determinant inside (1.51) is A-dependent for the gauge fields in (1.4). In

that situation, one gets a term proportional to

$$det\left(\frac{\delta G(A')}{\delta \alpha}\right) \sim det\left(\frac{1}{g}\partial^{\mu} D_{\mu}\right), \tag{1.57}$$

where g is the non-Abelian coupling constant, and D_{μ} is the covariant derivative. Luckily, this determinant can be expressed as a functional integral over a new set of Grassman fields

$$det(\partial^{\mu} D_{\mu}) = \int DcD\bar{c}e^{i\int d^4x \bar{c}(-\partial^{\mu} D_{\mu})c}. \tag{1.58}$$

The anticommuting fields c, $\bar{c}$ are unphysical (as they do not obey the spin-statistics theorem) and have been named Faddeev-Popov ghosts. They are allowed to enter loop calculations in EW theory as virtual particles, and have their own Feynman rules which originate from (1.58). The interested reader may find more interesting details about how these fields enter loop calculations in [57]. They will also enter the γZ self-energy calculation done in section 4.5.

1.2 Correlation Functions and Perturbation Theory

Most of us have heard of "Feynman diagrams", but some may not know where they come from and how to generate them for a given calculation, so it is worthwhile reviewing their origin. In principle there is no need to define a Feynman diagram in QFT. Formalized by Julian Schwinger (but not unbeknownst to Feynman), there is a rather unique way of doing QFT. It involves introducing an external fictitious field $J(x)$ which acts on your particle field $\phi(x)$ in the form of an interacting Lagrangian density $\mathcal{L}_J = J(x)\phi(x)$. One then varies their quantum amplitude $\int D\phi e^{iS[\phi,J]/\hbar}$ with respect to $J(x)$, and set $J = 0$ afterwards. This "modified quantum amplitude" is a very fundamental object known as the generating functional, which has found a natural home in statistical mechanics, and it also contains all of your theory's physics. For a simple scalar field theory, the generating functional is:

$$Z[J] = (Z[J=0])^{-1} \int D\phi e^{\frac{i}{\hbar}S[\phi]} e^{\frac{i}{\hbar}\int d^4x J(x)\phi(x)}. \tag{1.59}$$

In the path integral formulation of ordinary quantum mechanics, the QM amplitude in going from point 1 to point 2 is:

$$G(1,2) \equiv G(Q_2, Q_1; t_2, t_1) = \int_{q(t_1)=Q_1}^{q(t_2)=Q_2} Dq(\tau) e^{\frac{i}{\hbar}S[q,\dot{q}]}. \tag{1.60}$$

G(2,1) is commonly called the 2-point correlator and if we were to take its modulus square, we effectively find the probability that our particle propagates from point 1 to 2. In QFT, we want the same quantity, as it is a link between our system Lagrangian (residing in $S[\phi]$) and physical observables. At the same time we can generalize G(2,1) to an n-point correlator which represents the QM amplitude of "$(n-j)$ particles going from $(n-j)$ points to j particles at j points". We can find such a significant correlator from the generating functional via appropriate functional derivatives with respect to J:

$$G_n(x_1, \cdots, x_n) = (-i\hbar)^n \frac{\delta^n Z[J]}{\delta J(x_1) \cdots \delta J(x_n)}\bigg|_{J=0}. \tag{1.61}$$

G_n is the so-called n-point time-ordered correlation function, which has the alternate notation:

$$G_n(x_1, \cdots, x_n) = \langle 0|T\{\phi(x_1), \cdots, \phi(x_n)\}|0\rangle. \tag{1.62}$$

Of course, when you substitute $Z[J]$ into G_n, the $\delta/\delta J(x_i)$'s seamlessly pass through the functional integral in (1.59), but after the derivatives have performed their task, one still must integrate over $D\phi$. This is where QFT becomes perturbative. For practical purposes, the only functional integral we confidently know how to do exactly is a Gaussian one:

$$\int D\phi e^{-\frac{i}{\hbar}\int d^4x(\frac{1}{2}\phi Q_0 \phi - J\phi)} = |detQ_0|^{-\frac{1}{2}} e^{\frac{i}{2\hbar}\int d^4x J Q_0^{-1} J}, \tag{1.63}$$

and this is fine if in our system action: $S[\phi] = \int d^4x\mathcal{L}(\phi)$ there exists only linear and quadratic terms in ϕ. For this very reason we have exact solutions for free quantum fields, which merely have quadratic kinetic and mass terms in the particle fields. Any interacting QFT of interest, however, contains cubic or higher order terms in ϕ, rendering the functional integral impossible to do exactly. The solution adopted then is to expand the interaction term into a Taylor series, keeping only the leading terms. This must be done under the assumption that the Taylor series converges, and each consecutive term is smaller than the previous one. i.e.

$$e^{\frac{i}{\hbar}\int d^4x\mathcal{L}_{int}(\phi)} = \sum_{n=0}^{\infty} \frac{1}{n!}\left(\frac{i}{\hbar}\right)^n \mathcal{L}_{int}^n(\phi). \tag{1.64}$$

Each term in $\int D\phi e^{\frac{i}{\hbar}\int d^4x(\mathcal{L}_0(\phi)+\mathcal{L}_{int}(\phi))}$ is then a polynomial in ϕ times a Gaussian function in ϕ, which can be functionally integrated exactly. This constitutes a systematic procedure through which you can find your correlators, which then get substituted into S-matrix elements, which then directly goes into a cross-section (a physically measured quantity in a scattering experiment, for example). As laid out in [2], the procedure is as follows: The scattering matrix S is the matrix which links the initial state to the final state (before and after scattering, respectively) which has a zeroth order identity plus a non-trivial part:

$$S = 1 + iT \tag{1.65}$$

The interesting part is, of course, T, whose matrix element is defined by:

$$\tau \equiv \langle f|iT|i\rangle = (2\pi)^4\delta^4(\sum_{\text{momenta}})i\mathcal{M}(i\to f), \tag{1.66}$$

where $\mathcal{M}(i\to f)$ is the correlator which links the initial state particles to the final state ones and is often called the "Feynman amplitude". The transfer matrix element then gets substituted into the differential cross-section along with a Lorentz-invariant phase space factor. If our initial state was $|i\rangle = |p_1\rangle|p_2\rangle$ and final state $|f\rangle = \prod_j |p_j\rangle$, then the differential cross-section will be:

$$d\sigma = \frac{1}{(2E_1)(2E_2)|\vec{v_1}-\vec{v_2}|}|\mathcal{M}|^2 d\Pi_{\text{LIPS}}, \tag{1.67}$$

where:

$$d\Pi_{\text{LIPS}} = (2\pi)^4\delta^4\Big(\sum_p\Big)\prod_{\text{final states}j}\frac{d^3p_j}{(2\pi)^3}\frac{1}{2E_{p_j}}, \tag{1.68}$$

$$\vec{v_i} = \frac{\vec{p_i}}{p_0}. \tag{1.69}$$

Let's now return to how we get our correlators, but turn our attention to QED, as a transition to EW theory is in mind. In QED, we need to introduce 3 external fields for each of the 3 physical fields: $A_\mu,\ \psi,\ \bar{\psi}$. The resulting generating functional is:

$$Z[j_\mu,\eta,\bar{\eta}] = \frac{\sum_{n=0}^{\infty}\frac{i^n}{n!}\int[dA_\mu d\psi d\bar{\psi}]e^{iS_0[A_\mu,\psi,\bar{\psi}]+i\int dx(A_\mu j^\mu+\bar{\psi}\eta+\bar{\eta}\psi)}(\int d^4x e\bar{\psi}\not{A}\psi)^n}{\sum_{m=0}^{\infty}\frac{i^m}{m!}\int[dA_\mu d\psi d\bar{\psi}]e^{iS_0[A_\mu,\psi,\bar{\psi}]}(\int d^4x e\bar{\psi}\not{A}\psi)^m}, \tag{1.70}$$

which leads to a general time-ordered correlator in the following compact form:

$$\langle 0|T\psi(x_1)\cdots\psi(x_m)\bar{\psi}(y_1)\cdots\bar{\psi}(y_r)A_{\mu_1}(z_1)\cdots A_{\mu_l}(z_l)|0\rangle = \frac{\sum_{n=0}^{\infty}\frac{i^n}{n!}\int[dA_\mu d\psi d\bar{\psi}]e^{iS_0[A_\mu,\psi,\bar{\psi}]}\psi(x_1)\cdots A_{\mu_l}(z_l)(\int d^4x e\bar{\psi}\not{A}\psi)^n}{\sum_{m=0}^{\infty}\frac{i^m}{m!}\int[dA_\mu d\psi d\bar{\psi}]e^{iS_0[A_\mu,\psi,\bar{\psi}]}(\int d^4x e\bar{\psi}\not{A}\psi)^m}. \tag{1.71}$$

In principle, evaluating the RHS of (1.71) for the first few terms is a straightforward exercise, but it is quite tedious. This is where Feynman diagrams come in handy. Richard Feynman realized that there is a diagrammatic representation for all of the terms here. If one can geometrically generate all of the terms diagrammatically, then they could use a prescribed set of "rules" to assign to each diagram its correct mathematical expression. This whole technique, pioneered by Feynman, has proved to shave off calculation times considerably. The diagrams have the added benefit of showing a picture of what the particles are doing physically – something that is very difficult to see by performing the algebra alone. It must also be stressed that one must always establish which correlator they're calculating and to what order in perturbation theory they're working before they commence a calculation.

Of course to get our sought correlators in EW theory we would do exactly the same thing as this QED case, however, due to the very large number of terms in the Electroweak Lagrangian, doing this analytically by hand would be too time-costly to be practical. There are many proposed and

established sets of EW Feynman rules in the literature, each with slightly different conventions. I will employ those of [75] for the calculations in this dissertation, as they are very complete and given in the general R_ξ gauge.

As the number of terms in the Taylor series of (1.71) increases, the field operators form what are called "loops". Correlation functions are customarily calculated in the momentum basis, and these loops form divergent 4 dimensional momentum integrals. The systematic procedure for removing some of these divergences is known as renormalization (see Appendix F). However, even after renormalization, the evaluated momentum loops leads to a small correction to the Lagrangian parameters, which depends on an intrinsic momentum scale (e.g. the momentum transfer between interacting particles). This is what we call a "running" parameter in QFT. For instance, we will see how this comes about to the weak mixing angle in chapter 4.

1.3 Precision SM Tests

It will be useful to review how precision SM tests work in a broader sense before we look at a specific example involving CKM matrix elements. At the Lagrangian level, the SM is defined in terms of a finite number of parameters, including coupling constants and particle masses. Let's denote all these Lagrangian parameters with α_i for $i\epsilon[1, N]$. When one first writes down a model for the SM (or any other particle theory for that matter), these parameters are unknown. To find them, we can choose at least N observables: O_i. Following a well-defined algorithm, each of these observables can be calculated in terms of the theory constants:

$$O_j = O_j(\alpha_i), \tag{1.72}$$

which will become a system of N equations with N unknowns, assuming one chooses N observables. It will then follow that we could measure these N observables and use (1.72) to numerically determine all our α_i. Our theory would then be a predictive one, as we could then calculate any new observable numerically. If the SM was incorrect or incomplete, it could show up as a discrepancy between a predicted observable and the measured value. One way to implement this test is the following:

- Let $O_i, \{i = 1, ..., N\}$ denote the N best-measured observables in the SM.

- Invert the system of equations:

$$O_i = O_i(\alpha_j) \rightarrow \alpha_j = \alpha_j(O_i) \tag{1.73}$$

  it would follow that these N α_j are the most precisely-known Lagrangian parameters, and the O_i used to find them are called the input parameters.

- Now choose any new observable which can also be measured with a high precision, denoted $O^{new}(\alpha_i)$ and substitute (1.73) to get:

$$O^{new} = O^{new}(O_i). \tag{1.74}$$

- One then tests the agreement between the SM prediction of O^{new} in (1.74) and a precision measurement of O^{new}.

As we shall see, for this comparison to be meaningful, one typically needs to consider loop corrections to the SM prediction, a feat which can inherit undesirable challenges in semileptonic processes. Specifically in this thesis, two SM precision tests will be performed.

The weak charge of the proton $Q_w(p)$ corresponds to the strength of the proton's vector coupling to the Z boson, and it is related to the weak mixing angle $\sin^2\theta_W$ via the relation [51]:

$$4s^2_W(0) = 1 - \frac{Q_w(p) - \Box_{WW} - \Box_{ZZ} - \Box_{\gamma Z}(0)}{\rho_{NC} + \Delta_e} + \Delta'_e. \tag{1.75}$$

The test here is to determine how closely the measured quantities on the RHS determines $s^2_W(0)$ as compared to the pure SM prediction of $s^2_W(0)$. $Q_w(p)$ is determined by performing PV asymmetry measurements in $ep \to ep$ via the equation [53]

$$\frac{A_{LR}^{ep,NLO}}{A_{LR}^{ep,Born}} = Q_w(p) + Q^2 B(Q^2, \theta), \tag{1.76}$$

where A_{LR} is defined in section 1.4 and $B(Q^2, \theta)$ is a function which characterizes the structure of the proton. A low Q^2 fit may be performed on the available asymmetry data to get the non-zero intercept $Q_w(p)$. Amongst all terms in the RHS of (1.75), the input parameters of this test are:

$$s^2_W(0) \sim Q_w(p), \rho_{NC}, \hat{\alpha}, \hat{s}_W, m_e, M_Z, M_W \tag{1.77}$$

where $\hat{\alpha}$ and $\hat{s}_W$ are measured at the Z pole mass and ρ_{NC} will be defined in section 4.2. The comparison of $s^2_W|_{SM}$ to $s^2_W|_{exper}$ will be reviewed in section 4.10.

The other SM precision test performed in this dissertation will be the unitarity of the CKM matrix. In this case, the quantity being tested is the LHS of (1.45), for which the SM prediction is 1. $|V_{us}|^2$ and $|V_{ub}|^2$ have PDG experimental averages [70] while $|V_{ud}|^2$ will be updated with the newly calculated radiative corrections of section 3. Just to be clear, the SM doesn't "know" what the individual values of V_{ij} actually are, rather they can be found from experiment. Instead the SM merely predicts that these matrix

elements conform to the unitarity condition. This will be tested in detail in section 5.1.

1.4 Probing the CKM Elements

For the purposes of a precision SM test, there are 2 significant measurements which can directly extract the V_{ud} matrix element: superallowed β decays and neutron lifetime measurements. Both of these processes involves the charged current (CC) interaction between up and down quarks found in (1.33) and can be measured in the lab.

The neutron has been observed to decay into a proton and an electron ever since early experiments at Oak Ridge National Laboratory [4] and Chalk River [5], [6]. Later, Pauli had postulated the emission of a neutrino in the decay products to account for the observed electron energy spectra and out of the need to conserve angular momentum. By the 1960's, the neutron beta decay reaction $n \rightarrow p + e^- + \bar{\nu}_e$ was studied heavily by a still-developing theory of weak interactions.

One way to understand the driving weak interaction responsible for neutron beta decay is to measure either the neutron survival rate or the decay rate through its products. The weak interaction is known to possess a V-A structure $\sim \bar{\psi}(g_V - g_A\gamma^\mu\gamma_5)\psi$. The relative A to V coupling is defined at zero 4-momentum transfer by the parameter:

$$\lambda = \frac{g_A}{g_V}, \tag{1.78}$$

and this term will enter the neutron's lifetime relations later in this section.

On the other hand, superallowed β decays involve the transition between

$J^\pi = 0^+ \to 0^+, I = 1$ nuclei and currently provide the most precise extraction of V_{ud}. There are roughly 20 accessible superallowed transitions which have been measured in the lab for over the last 40 years [7]. The observable quantity which characterizes the β decay is the ft value, which depends on 3 measured quantities: the total transition energy Q_{EC}, the half-life $t_{1/2}$ and the branching ratio R for the specific transition. It is convenient to define a modified ft value which includes nuclear-dependent radiative corrections in it:

$$Ft = ft(1 + \delta'_R)(1 + \delta_{NS} - \delta_C), \tag{1.79}$$

where δ_C is known as the isospin-symmetry breaking correction, while δ'_R and δ_{NS} are transition-dependent corrections. δ'_R depends on the electron's energy E and the Z number of the daughter nucleus, while δ_C and δ_{NS} depend on the details of the nuclear structure at hand. Ft is directly related to the Fermi coupling constant G_v of the nuclear β decay. However, G_v is not by itself, a useful quantity. Rather, by taking its ratio with the Fermi constant for purely leptonic μ decay, G_F, we can access the up-down element of the CKM matrix:

$$|V_{ud}|^2 = \frac{G_v^2}{G_F^2} = \frac{2984.43s}{Ft(1 + \Delta_R^V)}, \tag{1.80}$$

where Δ_R^V contains all the universal inner radiative corrections and will be discussed in some detail in section 2 of this thesis. Equation (1.80) acts like a stringent numerical bridge between experimentally measured Ft values in

superallowed β decays and the resulting SM prediction for $|V_{ud}|^2$.

In the SM, the inverse of the neutron's lifetime comes from an integration of its differential decay rate over final state phase space, and is generally given by [8]:

$$\tau_n^{-1} = \frac{G_V^2 |V_{ud}|^2}{2\pi^3} m_e^5 (1 + 3\lambda^2)(1 + \Delta_R) f, \tag{1.81}$$

where Δ_R are the EW radiative corrections and will be discussed in section 2 and f is a phase space factor. Many of the constants in (1.81) are known experimentally, and the equation may be re-arranged with this information to give a useful V_{ud} testing formula analogous to (1.80):

$$|V_{ud}|^2 = \frac{5099.34s}{\tau_n(1 + 3\lambda^2)(1 + \Delta_R)}. \tag{1.82}$$

Unfortunately neutron lifetime measurements do not provide as precise an extraction of $|V_{ud}|$ as superallowed decays can provide, due to the large experimental uncertainty in λ.

1.5 PVES and the Weak Charge of the Proton

Parity violating electron scattering experiments provide a powerful way of testing the SM. The weak interaction's preference to involve left-handed fermions can be exploited and observed when one takes the difference of cross-sections between LH and RH beam electrons and an unpolarized proton target. The quantity which encapsulates this effect is called the left-right asymmetry, defined as:

$$A_{LR} = \frac{\sigma_L - \sigma_R}{\sigma_L + \sigma_R}, \tag{1.83}$$

where the L(R) refers to left-(right-) handed longitudinally polarized electrons. To leading order (Born level), the interaction which explains the scattering between and electron and proton is the exchange of a single Z-boson or photon(γ) shown in Figure 1.1. The helicity (handedness) of the incident

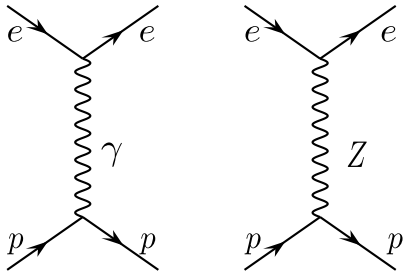

Figure 1.1: Tree level amplitudes M_γ and M_Z which contribute to A_{LR}. Their interference term survives in the numerator of (1.70).

electron is traditionally denoted by $\lambda = \pm 1$. The purely weak exchange amplitude M_Z is highly suppressed with respect to the EM exchange amplitude

M_γ in the SM, simply due to the fact that the Z-boson mass is quite large compared to all other particles present whilst the weak coupling constant is of the same order of magnitude as the EM one.

Despite this smallness, LR asymmetries are sensitive to the γZ interference amplitude, which is on the *ppm* order and can be measured in modern accelerators. Using the EW Feynman rules, we have for the Born amplitudes:

$$M_Z^\lambda = -\frac{2g^2}{(4c_W)^2}\frac{1}{M_Z^2 - q^2} j_{Z\mu}^\lambda J_Z^\mu, \tag{1.84}$$

$$M_\gamma^\lambda = -\frac{e^2}{q^2} j_{\gamma\mu}^\lambda J_\gamma^\mu, \tag{1.85}$$

where $j_{Z\mu}(J_\gamma^\mu)$ are the leptonic(hadronic) neutral currents for Z-exchange and $G_F = \pi\alpha/\sqrt{2}M_Z^2 s_W^2 c_W^2$ is the Fermi constant. The weak leptonic current has both vector (V) and axial-vector (A) terms whereas the EM current is purely vector:

$$j_{Z\mu}^\lambda = \bar{u}_e(k')\gamma_\mu(g_v^e - g_A^e\gamma_5)u_e^\lambda(k), \tag{1.86}$$

$$j_{\gamma\mu}^\lambda = \bar{u}_e(k')\gamma_\mu u_e^\lambda(k). \tag{1.87}$$

At the Born level, the hadronic weak current can be expressed using weak form factors as follows:

$$J^{\mu}_{(Z,\gamma)} = \bar{U}_N(p')\Gamma^{\mu}_{(Z,\gamma)}U_N(p), \tag{1.88}$$

$$\Gamma^{\mu}_{(Z,\gamma)}|_V = \gamma^{\mu}F_1^{(Z,\gamma)N}(Q^2) + \frac{i\sigma^{\mu\nu}q_{\nu}}{2M}F_2^{(Z,\gamma)N}(Q^2), \tag{1.89}$$

$$\Gamma^{\mu}_{Z}|_A = \gamma^{\mu}\gamma_5 G_A^{ZN}(Q^2). \tag{1.90}$$

Alternatively, one can express the Pauli and Dirac form factors in (1.89) in terms of the Sachs EM form factors:

$$G_E^{ZN}(Q^2) = F_1^{ZN}(Q^2) - \tau F_2^{ZN}(Q^2), \tag{1.91}$$

$$G_M^{ZN}(Q^2) = F_1^{ZN}(Q^2) + F_2^{ZN}(Q^2), \tag{1.92}$$

$$\tau = \frac{Q^2}{4M^2}. \tag{1.93}$$

The cross sections in (1.83) are of course the modulus squared of the sum of amplitudes (1.84) + (1.85) which is proportional to:

$$\sigma \sim |M_\gamma + M_Z|^2 = |M_\gamma|^2 + 2Re(M_\gamma^* M_Z) + |M_Z|^2 \tag{1.94}$$

Kinematically, in a typical PVES experiment, $|M_Z|^2$ can be safely neglected while $|M_\gamma|^2$ cancels in the ratio of (1.83). Thus $A_{LR} \approx 2Re(M_\gamma^* M_Z)$. Defining: $Q_W^{LO}(p) = 2g_v^p = 1 - 4\sin^2\theta_W = G_E^{Zp}(0)$ and taking the forward limit in

(1.83) gives the Born prediction:

$$A_{LR}^{LO} = \frac{G_F Q^2}{4\pi\alpha\sqrt{2}} Q_W^{LO}(p) \tag{1.95}$$

which can be used to extract $Q_W(p)$ from a PVES experiment at low Q^2. Unfortunately, the A_{LR} measured in the lab includes all higher-order processes, which as we will see in section 4, amounts to a few percent enhancement of the tree-level prediction. It will suffice to consider just the 1-loop corrections to $e^- p \to e^- p$ to meet the requirements of interpreting the results of such an experiment.

Chapter 2

Radiative Corrections to β Decay

The major contribution of this thesis is an improved calculation of the γW box, which acts as an input towards the extraction of the V_{ud} matrix element. Therefore, it will be worthwhile to give a brief summary of the history of this radiative correction. Doing so will help the reader understand what the status of this radiative correction is before I update the calculation in chapter 3 of this dissertation.

2.1 Historical Survey

After the invent of the Glashow-Salam-Weinberg $SU(2)_L \times U(1)$ Electroweak Standard Theory, a seminal paper was published [9] which attempted to cal-

culate the effects of all 1-loop EW RCs to semileptonic β decays. Since then, some incremental improvements have been made, which will be discussed below. The RCs to semileptonic β decays can be placed into 2 distinct categories:

$$\begin{aligned} \Delta_R^{V/A} &: \text{inner corrections} \\ \delta_R &: \text{outer corrections} \end{aligned}$$

where the former are calculated to a high precision and incorporated into effective couplings, while the latter include energy-dependent terms and carry some nuclear dependence. In keeping with the definitions of equations (1.80) and (1.81), it will be more useful to keep Δ_R^V and define a new radiative correction which is the sum of the inner and outer corrections:

$$\Delta_R = \frac{\alpha}{2\pi}\bar{g}(E_m) + \Delta_R^V, \tag{2.1}$$

while there is no need to consider Δ_R^A as it can be absorbed into the parameter $\lambda = g_A/g_V$. Equation (2.1) is intended for the simplest case where the decay is from a free neutron, but for a superallowed decay, the nuclear structure corrections also come into play. Those nuclear corrections are omitted from this section, as they are conveniently taken into account in the modified Ft value in the denominator of (1.80). The decay rate of β emission from the neutron can generally be expressed from the following correction to the Born

decay rate Γ^0_β:

$$\Gamma_\beta = \Gamma^0_\beta\big[1 + \Delta_R\big], \tag{2.2}$$

where in (2.1) we have [12]:

$$\bar{g}(E_m) \approx 3\ln\left(\frac{M_p}{2E_m}\right) + \frac{81}{10} - \frac{4\pi^2}{3}, \tag{2.3}$$

$$\Delta^V_R = \frac{\alpha}{2\pi}\left[3\ln\left(\frac{M_W}{M_p}\right) - 4\ln c_W\right] + 2\Box^{\gamma W}_A. \tag{2.4}$$

(2.3) is an approximate expression for Sirlin's universal function $g(E, E_m)$ integrated over the electron's final state phase space, where: $E_m = (M_n^2 - M_p^2 + m_e^2)/2/M_n$ is its maximum allowed energy. The last term of (2.4) is a photonic correction to the leading order CC tree exchange in the form of a 1-loop box, which has both long- and short-distance contributions. In [9] it was recognized how to isolate it's hadronic dependence, which resides in the W-boson's axial-vector coupling, where this component was computed to be:

$$\Box^{\gamma W}_A = \frac{\alpha}{4\pi}\Big[\ln\Big(\frac{M_W}{M_A}\Big) + 2C + A_g\Big]. \tag{2.5}$$

$C = .88$ is an elastic contribution to the γW box and $A_g = -.34$ is an estimation of the non-perturbative part of the hadronic QCD corrections which occurs at long-distances. It is thanks to crossing symmetry that we may recast the neutron β decay reaction: $n \to pe^-\nu_e$ to the more tractable $2 \to 2$ process of Figure 2.1. In general, this will not work when it comes time to apply Fermi's golden rule of integrating over final state phase space to de-

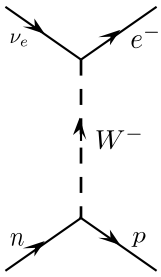

Figure 2.1: The CC tree level amplitude which solely contributes to Γ^0_β.

termine the decay rate, but for the purposes of evaluating inner correction amplitudes, it will be more convenient. In Figure 2.2, the relevant 1-Loop diagrams are listed, and collectively determine our Δ_R.

Of particular interest in this thesis will be the γW boxes as they are unavoidably dependent on the strong interaction. The box and crossed box can be compactly expressed via [9]:

$$M_{\gamma W} = \frac{-ig^2e^2}{2M_W^2}\int \frac{d^4k}{(2\pi)^4}\frac{1}{k^2}\frac{M_W^2}{M_W^2-(k-q)^2}\bar{u}_\nu\gamma_\rho\frac{(1-\gamma_5)}{2}\frac{1}{\not{k}-\not{l}-m_e}\gamma_\lambda v_e \times \int d^x e^{ik\cdot x}\langle p'|T[J^\lambda_\gamma(x)J^\rho_W(0)]|p\rangle, \tag{2.6}$$

of which the 2nd line is just the hadronic current expressed in terms of a time-ordering of the field operators present in the boxes, and it implicitly allows the presence of any QCD corrections. Sirlin showed that the vector coupling of this hadronic current can be combined with other photonic corrections such as those found in Figure 2.1. It is also true that this vector coupling is independent of the details of the strong interaction – a consequence of the conserved vector current (CVC) hypothesis. Furthermore, this

vector part contains an ultraviolet (UV) divergence which is repeated in the corrections to μ decay and is exactly canceled in the V_{ud} ratio [13]. We will return to (2.6) in section 3 explicitly with the goal of calculating the axial-vector component using modern techniques.

The first terms in both equations (2.3) and (2.4) are called "leading logs",

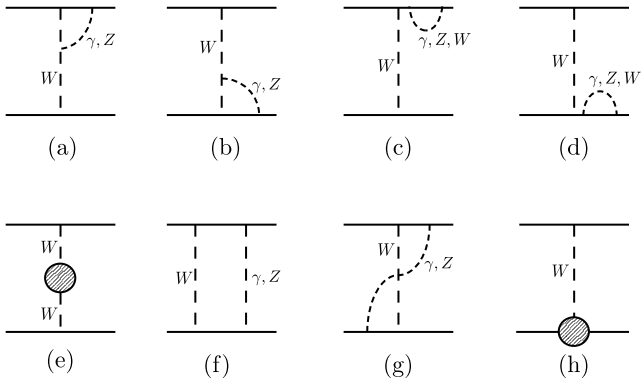

Figure 2.2: 1 Loop radiative corrections to the CC Born amplitude.

which can be re-summed with the aid of renormalization group equation (RGE) analysis. This was done in [10], where the authors suggest the replacement:

$$1 + \tfrac{2\alpha}{\pi}\ln\tfrac{M_Z}{M_p} \to S(M_p, M_Z) = 1.02248, \tag{2.7}$$

$$1 + \tfrac{3\alpha}{2\pi}\ln\tfrac{M_p}{2E_m} \to L(2E_m, M_p) = 1.02094\ . \tag{2.8}$$

Then in 2006, further improvements were made to (2.5), also known as the Gamow-Teller piece, where the authors of [14] re-expressed the axial-vector

part of (2.6) via:

$$M_{\text{Axial}}^{\gamma W} = \frac{\alpha}{8\pi}\int_0^\infty \frac{M_W^2}{Q^2+M_W^2}F(Q^2)dQ^2, \tag{2.9}$$

in which $F(Q^2)$ acted like a form factor that would model the hadronic effects over the full Q^2 range. To do so, the integration domain was phenomenologically separated into 3 distinct regions:

- Short Distance: $1.5\text{GeV}^2 \leq Q^2 < \infty$

  $$F_{SD}(Q^2) = \frac{1}{Q^2}\Big[1 - \frac{\alpha_S(Q^2)}{\pi} - C_2\Big(\frac{\alpha_S(Q^2)}{\pi}\Big)^2 - C_3\Big(\frac{\alpha_S(Q^2)}{\pi}\Big)^3\Big], \tag{2.10}$$

  where the C_i are constants calculated in pQCD and will be discussed in some detail in section 3. This contribution is in the DIS regime where the quarks in the hadron behave independently

- Intermediate Distance: $0.823\text{GeV}^2 \leq Q^2 \leq 1.5\text{GeV}^2$

  $$F_{ID}(Q^2) = \frac{D_1}{Q^2+m_\rho^2} + \frac{D_2}{Q^2+m_A^2} + \frac{D_3}{Q^2+m_{\rho_1}^2}, \tag{2.11}$$

  which acts as an interpolating function between the high and low Q^2 regions and is physically motivated by the exchange of vector mesons.

- Long Distance: $0 \leq Q^2 \leq 0.823\text{GeV}^2$

  $$C_{\text{Born}} = 0.829 \pm 10\%, \tag{2.12}$$

where this constant effectively replaces the C term found in (2.5) and represents the elastic contribution, but integrated over a lower range of Q^2.

The effect of this new treatment reduced the overall error of $\Box_A^{\gamma W}$ by a factor of 2 with very little change to its central value. One of the main goals of this thesis is to use dispersive techniques to re-evaluate (2.6), which will give a more accurate central value to this RC, and may also reduce its hadronic uncertainty. Doing so will, in turn, improve our extraction of V_{ud} through the means of both (1.80) and (1.82). The reason such a calculation technique will be superior to previous attempts is because an equation such as (2.9) is rather phenomenological, and is essentially coarse-graining the explicit loop expression. As we shall see in section 3, dispersive techniques maintain all the details of the loop expression, while forcing experimental input from cross-section data.

Chapter 3

Dispersive Calculation of the γW Box

With introductions aside, is now time to dive into the primary calculations of this dissertation. In chapter 3 I will start by explaining how dispersion relations can be applied to evaluating radiative corrections. This is a modern technique which reduces the hadronic uncertainty in the semileptonic box corrections found in both neutral current and charged current processes. We will then derive an exact expression for the axial part of the γW boxes introduced in chapter 2 using these techniques. This will lead to the need to model a specific structure function $F_3^{\gamma W}$over a 2D kinematical plane from which I will define distinctly chosen regions. After that, the rest of this chapter will model $F_3^{\gamma W}$ in each region and calculate its contribution to the box correction. The results of this work will then be compared to the results

of others at the end of this chapter.

3.1 Dispersion Relations in QFT

Dispersion relations can be a powerful tool for calculating radiative corrections in quantum field theory, and can even be applied to scenarios where perturbation theory is unreliable. The general idea behind them is that they allow one to first calculate the imaginary part of an amplitude. By the optical theorem, this is related to the total cross section for producing the intermediate state, something which can be measured experimentally, as a function of the incident CM energy (s). One well-known example of this is the estimation of the light quark contributions to photon vacuum polarization using experimental data on $\sigma(e^+e^- \to hadrons)$.

The Cauchy-Riemann integral theorem allows us to determine a function $\Box(s)$ at any point on the complex plane if we simply know what this function is everywhere on a closed contour:

$$\Box(s_0) = \frac{1}{2\pi i} \oint \frac{\Box(s)}{s - s_0} ds, \tag{3.1}$$

so long as the function $\Box(s)$ is analytic everywhere inside the contour. Suppose s_0 is somewhere on the real number line, then we could choose the contour of Fig 3.1. Then integrating (3.1) along this contour gives the fol-

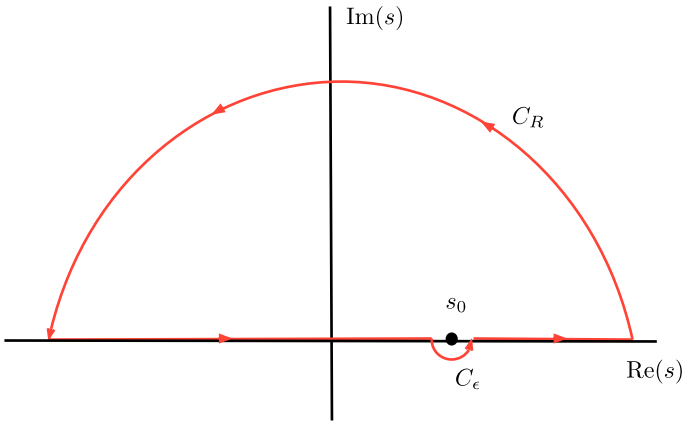

Figure 3.1: Infinite upper semicircle closed contour enclosing a pole on the real number line.

lowing three terms:

$$\begin{aligned}\Box(s_0) &= \frac{1}{2\pi i}P\int_{-\infty}^{\infty}\frac{\Box(s)}{s-s_0}ds + \lim_{\epsilon\to 0}\frac{1}{2\pi i}\int_{C_\epsilon}\frac{\Box(s)}{s-s_0}ds + \lim_{R\to\infty}\frac{1}{2\pi i}\int_{C_R}\frac{\Box(s)}{s-s_0}ds \\ &= \frac{1}{2\pi i}P\int_{-\infty}^{\infty}\frac{\Box(s)}{s-s_0}ds + \frac{1}{2\pi i}(i\pi\Box(s_0)).\end{aligned}$$

Then taking the real part of both sides of this equation gives us:

$$\mathrm{Re}\Box(s_0) = \frac{1}{\pi}P\int_{-\infty}^{\infty}\frac{\mathrm{Im}\Box(s)}{s-s_0}ds, \tag{3.2}$$

and this is our general dispersion relation for our function $\Box(s)$. The $\Box$ function for us will later represent the fractional correction of a 1-loop box

diagram to the Born prediction to an observable:

$$\Box = \frac{\sum\limits_{\text{spins}} M^*_{\text{Born}} M_{\text{Box}}}{\sum\limits_{\text{spins}} |M_{\text{Born}}|^2}, \tag{3.3}$$

whose natural independent kinematical variable is Mandelstam s (Mandelstam u for the crossed box), which flows into the semileptonic reaction of Figure 3.2. Physically, this diagram comes with a threshold condition where $s \geq (m_l + M_h)^2$ must be large enough to produce the intermediate state particles. This threshold condition is realized as a branch cut $s \geq M_h^2$ in the

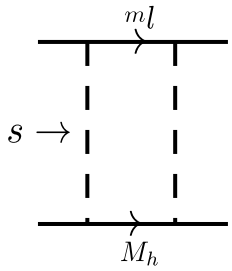

Figure 3.2: Generic box diagram for a semileptonic process wherein the incident CM energy squared is given by Mandelstam s.

function $\Box(s)$. Therefore a new contour must be chosen for its dispersion relation, which is shown in Figure 3.3. Then again employing our trusty

theorem in (3.1) gives:

$$\begin{aligned}\Box(s) &= \frac{1}{2\pi i}\oint \frac{\Box(s')}{s'-s}ds' \\ &= \lim_{R\to\infty}\frac{1}{2\pi i}\int_{C_R}\frac{\Box(s')}{s'-s}ds' + \frac{1}{2\pi i}\int_{\infty}^{M_h^2}\frac{\Box(s'-i\epsilon)}{s'-s}ds' \\ &\quad +\frac{1}{2\pi i}\int_{M_h^2}^{\infty}\frac{\Box(s'+i\epsilon)}{s'-s}ds' \\ &= \frac{1}{2\pi i}\int_{M_h^2}^{\infty}\Big(\frac{\Box(s'+i\epsilon)}{s'-s} - \frac{\Box(s'-i\epsilon)}{s'-s}\Big)ds',\end{aligned}$$

and by Schwarz' reflection principle: $\lim_{\epsilon\to 0}\left[\Box(s'+i\epsilon) - \Box(s'-i\epsilon)\right] = 2i\mathrm{Im}\Box(s')$. This leads to

$$\begin{aligned}\Box(s) = &\frac{1}{2\pi i}\int_{M_h^2}^{\infty}ds'\frac{2i\mathrm{Im}\Box(s')}{s'-s-i\epsilon} \\ = &\frac{1}{\pi}\int_{M_h^2}^{\infty}ds'\frac{\mathrm{Im}\Box(s')}{s'-s-i\epsilon}.\end{aligned} \tag{3.4}$$

Although $s\epsilon\mathbb{C}$ in the derivation of (3.4), physically we will have $s\epsilon\mathbb{R}$ as it is an energy squared. The concept of promoting real variables to complex ones and back again is known as "complexification" (although in the literature it is often improperly deemed as analytic continuation) - and has found many exceptional applications in the physical sciences. (3.4) allows us to calculate a box correction, given we can first determine its imaginary part as a function of Mandelstam s.

There is a systematic procedure for calculating the imaginary part of a Feynman amplitude known as the Cutkosky cutting rules [16] which prescribes

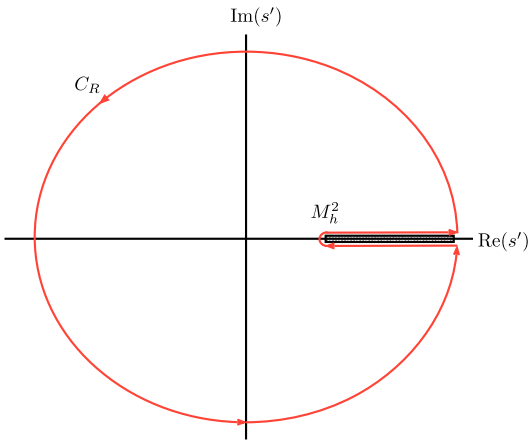

Figure 3.3: Complex contour used for the derivation of (3.4).

one to:

- Cut the diagram in any way such that all the cut propagators can be put on-shell without violating momentum conservation
- For each cut propagator, make the replacement:

$$\frac{1}{p^2 - m^2 + i\epsilon} \to -2\pi i \delta(p^2 - m^2)\Theta(p^0). \tag{3.5}$$

- The result is the discontinuity of the diagram and:

$$\text{Disc}(iM) = -2\text{Im}M. \tag{3.6}$$

(3.6) will then be inserted into the RHS of (3.4), for example, where the $\mathrm{Im}\Box(s')$ is taken from its limit above the branch cut as a matter of convention. Inside the loop integration, the delta function employed in this second step will have the following effect:

$$\int \frac{d^4q}{(2\pi)^4} 2\pi\delta(q^2 - m^2)\Theta(q^0) = \int \frac{d^3q}{(2\pi)^3}\frac{1}{2q^0}. \tag{3.7}$$

The utility of dispersion relations for calculating box diagrams in the SM can therefore be performed via the following algorithm:

- Use the Cutkosky cutting rules to find $\mathrm{Im}M_{\mathrm{box}}(s)$
- Construct $\mathrm{Im}\Box(s)$ from $\mathrm{Im}M_{\mathrm{box}}$ using (3.3)
- Apply the dispersion relation (3.4) to calculate $\Box(s)$.

Before concluding this section, it is worthwhile to connect the dispersive technique to the optical theorem. In any SM process, the scattering matrix is defined as the amplitude in your system going from the initial state to the final state:

$$S = \langle f, t \to \infty | S | i, t \to -\infty \rangle, \tag{3.8}$$

$$S = 1 + iT. \tag{3.9}$$

T is known as the transmission matrix which must encode any interactions present during the scattering event. A strict physical requirement of the S-

matrix is that it be unitary: $S^\dagger S = 1$ and together with (3.9) this implies that

$$-i(T - T^\dagger) = T^\dagger T. \tag{3.10}$$

Taking $\langle f|(3.10)|i\rangle$, inserting a complete set of states $1 = \Sigma_n |n\rangle\langle n|$ between the $T^\dagger T$ and demanding the conservation of overall 4-momentum then gives:

$$\begin{aligned} -i\langle f|(T - T^\dagger)|i\rangle(2\pi)^4\delta^4(P_f - P_i) &= (2\pi)^4\delta^4(P_f - P_i) \\ &\quad \times \sum_n (2\pi)^4\delta^4(P_n - P_i)\langle f|T^\dagger|n\rangle\langle n|T|i\rangle, \\ -i(T_{fi} - T^*_{if}) &= \sum_n (2\pi)^4\delta^4(P_n - P_i)T^*_{nf}T_{ni}, \end{aligned} \tag{3.11}$$

which is the generalized optical theorem. A special case of this is at forward scattering when $i = f$ and

$$2\mathrm{Im}M_{i\to i} = \sum_n (2\pi)^4\delta^4(P_n - P_i)|T_{ni}|^2. \tag{3.12}$$

On the other hand, the cross section for a $1 + 2 \to \{j\}$ process is given by [2]:

$$\sigma_{TOT} = \frac{1}{|\vec{v}_1 - \vec{v}_2|(2E_1)(2E_2)} \int |M|^2(2\pi)^4\delta^4(\Sigma p) \prod_{\text{final states}} \frac{d^3p_j}{(2\pi)^3}\frac{1}{2E_{p_j}}. \tag{3.13}$$

Thus we see that $\mathrm{Im}M \sim \sigma$, and from (3.7) we can also see that the Cutkosky rules will naturally generate the Lorentz invariant phase space integration measure. This is why dispersion relations are so useful: because their cal-

culation input is directly proportional to a total cross section – and cross sections are potentially experimentally accessible.

3.2 Deriving a New Expression for $\Box_A^{\gamma W}$

Now that we have discussed the machinery, it is time to apply it. The amplitude of interest is the γW box below. The inherent challenge to calculating this diagram is that we have one massive and one massless vector boson being exchanged in the loop. This means that all possible momentum scales contributes to this integral. As a result, all possible excited states of the intermediate state hadron can be produced and contribute to this amplitude. Using the EW Feynman rules in Appendix A, this diagram has the following

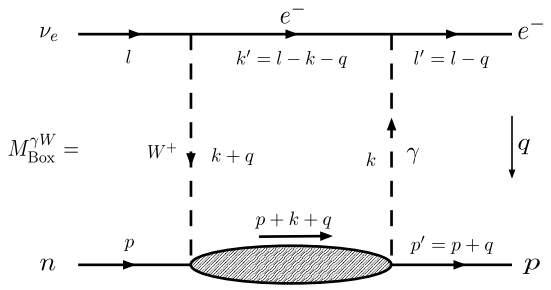

Figure 3.4: Labeled Feynman diagram for the γW box with the loop momentum represented by k.

explicit expression:

$$M^{\gamma W}_{Box} = \frac{-ig^2e^2}{2M_W^2}\int \frac{d^4k}{(2\pi)^4}\frac{1}{k^2}\frac{M_W^2}{M_W^2-(k+q)^2}T^{\lambda\rho}_{(\gamma)}(k)\bar{u}_\nu\gamma_\rho P_L\frac{1}{\not{k}-\not{l}-m_e}\gamma_\lambda v_e, \tag{3.14}$$

where $P_L = (1-\gamma_5)/2$ is the left-handed projector and the hadronic tensor is defined as:

$$T^{\lambda\rho}_{(\gamma)}(k) = \int d^4x e^{ik\cdot x}\langle p|T[J^\lambda_\gamma(x)J^\rho_W(0)]|n\rangle \tag{3.15}$$

As we will be working in the forward limit, we can simplify the integrand of (3.14) somewhat. The W-boson propagator is approximately independent of q:

$$\frac{M_W^2}{M_W^2-(k+q)^2} \approx \frac{M_W^2}{M_W^2-k^2} = \frac{1}{1-k^2/M_W^2}, \tag{3.16}$$

and our forward limit amplitude is:

$$\begin{aligned} M^{\gamma W}_{Box}|_{\rm fwd} &= \frac{-ig^2e^2}{2M_W^2}\int \frac{d^4k}{(2\pi)^4}\frac{1}{k^2(1-k^2/M_W^2)}\bar{u}_e(l)\gamma_\lambda\frac{\not{k}-\not{l}+m_e}{(l-k)^2-m_e^2}\gamma_\rho \\ &\quad \times P_L u_\nu(l)T^{\lambda\rho}_{(\gamma)}(k). \end{aligned} \tag{3.17}$$

From this point on we will simply suppress the fwd subscript. Next we can use the Cutkosky rules to acquire the imaginary part of this amplitude:

$$\begin{aligned} {\rm Im}M^{\gamma W}_{\rm Box} =& (-2i\pi)\frac{(-ig^2e^2)}{2M_W^2}\int \frac{d^4k}{(2\pi)^4}\frac{{\rm Disc}T^{\lambda\rho}_{(\gamma)}(k)}{k^2(1-k^2/M_W^2)} \\ &\times \bar{u}_e(l)\gamma_\lambda(\not{l}-\not{k}+m_e)\delta((l-k)^2-m_e^2)\gamma_\rho P_L u_\nu(l), \end{aligned} \tag{3.18}$$

where it is implicitly understood now that the intermediate state present in ${\rm Disc}T^{\lambda\rho}_{(\gamma)}(k)$ is on its mass shell. Before we proceed, it will be convenient to change our integration variable to the 4-momentum of the intermediate state

electron:

$$k' = l - k. \tag{3.19}$$

We are allowed to do this because 4-momentum integrals are translation-invariant: $d^4k' = d^4k$. Given this choice, let's see what happens to our delta function:

$$\begin{aligned} \delta((l-k)^2 - m_e^2) = & \quad \delta(k'^2 - m_e^2) \\ \approx & \quad \delta(k'^2) \\ \approx & \quad \delta(k'^2_0 - |\vec{k'}|^2) \\ \approx & \quad \delta[(k'_0 + |\vec{k'}|)(k'_0 - |\vec{k'}|)], \end{aligned} \tag{3.20}$$

and since k_0 is the energy of the intermediate electron and it is put on its mass shell, it follows that we should be taking the positive energy root in (3.20). This will leave us with

$$\delta((l-k)^2 - m_e^2) = \frac{\delta(k'_0 - |\vec{k'}|)}{2k'_0}. \tag{3.21}$$

Substituting this back into (3.18) gives

$$\begin{aligned} \mathrm{Im}M^{\gamma W}_{\mathrm{Box}} = (-2i\pi)\frac{(-ig^2e^2)}{2M_W^2}\int \frac{d^3k'dk'_0}{(2\pi)^4}\frac{\mathrm{Disc}T^{\lambda\rho}_{(\gamma)}(k)}{k^2(1-k^2/M_W^2)} \\ \times \bar{u}_e(l)\gamma_\lambda \not{k'}\frac{\delta(k'_0 - |\vec{k'}|)}{2k'_0}\gamma_\rho P_L u_\nu(l) \\ = \frac{g^2e^2}{2M_W^2}\int \frac{d^3k'}{(2\pi)^3 2k'_0}\frac{\mathrm{Disc}T^{\lambda\rho}_{(\gamma)}(k)}{k^2(1-k^2/M_W^2)}\bar{u}_e(l)\gamma_\lambda \not{k'}\gamma_\rho P_L u_\nu(l). \end{aligned} \tag{3.22}$$

It is customary to express a 1 Loop CC correction in terms of αG_F, and we will follow suit to acquire:

$$\mathrm{Im}M^{\gamma W}_{\mathrm{Box}} = -8\sqrt{2}G_F\pi\alpha \int \frac{d^3k'}{(2\pi)^3 2k'_0} \frac{\mathrm{Disc}T^{\lambda\rho}_{(\gamma)}(k)}{k^2(1-k^2/M_W^2)} \bar{u}_e(l)\gamma_\lambda \not{k}'\gamma_\rho P_L u_\nu(l). \tag{3.23}$$

Before we continue performing operations with this expression, at some point we will need the Born amplitude to acquire an expression for $\Box^{\gamma W}_A$. So let's take the time to now get an expression for M_{Born}. The diagram is exactly that found in Figure 2.1. Upon applying the EW Feynman rules, it is simply given by

$$M_{Born} = \frac{g^2}{2M_W^2}\bar{u}_e(l)\gamma_\mu P_L u_\nu(l)\bar{u}_p(p)\gamma^\mu P_L u_n(p), \tag{3.24}$$

where we've made the somewhat harsh simplification of treating the nucleon like a simple fermion. This won't affect our final $\Box^{\gamma W}_A$ correction because the leading-order cross section $\sigma^{LO}_{CC} \sim |M_{Born}|^2$ will have a proper treatment of the nucleon in it, while what we're eventually after will be of the form:

$$\sigma^{NLO}_{CC} \sim \sigma^{LO}_{CC}(1 + \Box^{\gamma W}_A + \text{other corrections}). \tag{3.25}$$

At this point one would normally substitute (3.23) and (3.24) into (3.3) to get an expression for $\mathrm{Im}\Box^{\gamma W}$ and finally use (3.4). However, since we are working in the forward limit, it will suffice to simply take a ratio of the amplitudes. A nice demonstration of this trick can be found in [15]. With this in mind we can take traces to put our two amplitudes into a useable

form without spinors, starting with the Born amplitude:

$$\begin{aligned} M_{Born} &= 2\sqrt{2}G_F \sum_{spins} u_\nu(l)\bar{u}_e(l)\gamma_\mu P_L \sum_{spins} u_n(p)\bar{u}_p(p)\gamma^\mu P_L \\ &= 2\sqrt{2}G_F \sum_{spins} \not{l}\gamma_\mu P_L \sum_{spins} \not{p}\gamma^\mu P_L \\ &= 2\sqrt{2}G_F \mathrm{Tr}[\not{l}\gamma_\mu P_L]\mathrm{Tr}[\not{p}\gamma^\mu P_L] \\ &= 2\sqrt{2}G_F(2l_\mu)(2p^\mu) \\ &= 8\sqrt{2}G_F(l\cdot p) \\ &= 8\sqrt{2}G_F ME, \end{aligned} \tag{3.26}$$

which is a rather compact expression. Next we'll need to apply this trace technology to (3.23). Traditionally, box diagrams such as this are expressed as a product contraction between a leptonic and a hadronic tensor – which we will also do here. Defining:

$$L^{\gamma W}_{\mu\nu} = \bar{u}_e\gamma_\mu \not{k}'\gamma_\nu P_L u_\nu(l), \tag{3.27}$$

$$H^{\mu\nu}_{\gamma W} = \int d^4x e^{ik\cdot x}\langle p|T[J^\mu_\gamma(x)J^\nu_W(0)]|n\rangle, \tag{3.28}$$

then (3.23) can be written as:

$$\mathrm{Im}M^{\gamma W}_{\mathrm{Box}} = -8\sqrt{2}G_F\pi\alpha \int \frac{d^3k'}{(2\pi)^3 2k'_0}\frac{L^{\gamma W}_{\mu\nu}\mathrm{Disc}H^{\mu\nu}_{\gamma W}}{k^2(1-k^2/M_W^2)}. \tag{3.29}$$

Now let's perform the trace algebra to the leptonic tensor:

$$\begin{aligned} L^{\gamma W}_{\mu\nu} &= \sum_{spins} u_\nu(l)\bar{u}_e(l)\gamma_\mu \not{k}'\gamma_\nu P_L \\ &= \frac{1}{2}\mathrm{Tr}[\not{l}\gamma_\mu \not{k}'\gamma_\nu(1-\gamma^5)] \\ &= 2(l_\mu k'_\nu - l\cdot k' g_{\mu\nu} + l_\nu k'_\mu) + 2il^\alpha k'^\beta \epsilon_{\alpha\beta\mu\nu}, \end{aligned} \tag{3.30}$$

where the antisymmetric levi-civita tensor term originates from the γ_5 term inside the trace. Had we taken a difference between a LH neutrino and a RH one, it is the same levi-civita term which survives and thus it is responsible for parity-violation. The hadronic tensor in (3.28) cannot receive the same explicit manipulation, but instead can be expressed in terms of 3 general structure functions as follows:

$$\mathrm{Disc}H^{\mu\nu}_{\gamma W} = 4\pi W^{\mu\nu}_{\gamma W}, \tag{3.31}$$

$$W^{\mu\nu}_{\gamma W} = \Big(-g^{\mu\nu} + \frac{k^\mu k^\nu}{k^2}\Big)F_1^{\gamma W} + \frac{p^\mu p^\nu}{p\cdot k}F_2^{\gamma W} + \frac{i\epsilon^{\mu\nu\alpha\beta}p_\alpha k_\beta}{2p\cdot k}F_3^{\gamma W}. \tag{3.32}$$

The $F_1^{\gamma W}$ and $F_2^{\gamma W}$ terms are associated with the total vector coupling of W to the hadron while the $F_3^{\gamma W}$ term is associated with the axial-vector coupling. Since we are only interested in doing a dispersive calculation to the axial part, we'll only insert the axial part of (3.32) into (3.29). With that decision, we can contract our leptonic and hadronic tensors. As $\epsilon^{\mu\nu\alpha\beta}$ is completely antisymmetric in its indices, it follows that contracting the first

3 terms of (3.30) with it will give zero. Therefore our contraction reduces to the single term:

$$L^{\gamma W}_{\mu\nu} H^{\mu\nu}_{\gamma W} = 2il^{\alpha} k'^{\beta} \epsilon_{\alpha\beta\mu\nu} i \frac{\epsilon^{\mu\nu\lambda\rho} p_{\lambda} k_{\rho}}{2p \cdot k} F_3^{\gamma W}(k), \tag{3.33}$$

where select Lorenz indices were renamed to avoid miss-using the Einstein summation notation. We can then use the identity: $\epsilon^{\mu\nu\lambda\rho}\epsilon_{\alpha\beta\mu\nu} = -2(g^{\lambda}_{\alpha} g^{\rho}_{\beta} - g^{\lambda}_{\beta} g^{\rho}_{\alpha})$ to get

$$\begin{aligned} L^{\gamma W}_{\mu\nu} H^{\mu\nu}_{\gamma W} &= 4 \frac{l^{\alpha} k'^{\beta}}{2p \cdot k} (g^{\lambda}_{\alpha} g^{\rho}_{\beta} - g^{\lambda}_{\beta} g^{\rho}_{\alpha}) F_3^{\gamma W} p_{\lambda} k_{\rho} \\ &= \frac{2}{p \cdot k} (l^{\lambda} k'_{\rho} - k'^{\lambda} l^{\rho}) F_3^{\gamma W} p_{\lambda} k_{\rho} \\ &= \frac{2}{p \cdot k} [(l \cdot p)(k' \cdot k) - (k' \cdot p)(l \cdot k)] F_3^{\gamma W}. \end{aligned} \tag{3.34}$$

We can simplify the term in the square brackets into a more useful form:

$$\begin{aligned} (l \cdot p)(k' \cdot k) - (k' \cdot p)(l \cdot k) &= (l \cdot p)(l - k') \cdot k' - l \cdot (l - k')(p \cdot k') \\ &\approx (l \cdot p)(l \cdot k') + (l \cdot k')(p \cdot k') \\ &\approx (l \cdot k')(l \cdot p + p \cdot k'). \end{aligned} \tag{3.35}$$

Also:

$$k^2 = (l - k')^2 = l^2 - 2l \cdot k' + k'^2 \approx -2l \cdot k', \tag{3.36}$$

and therefore (3.29) is:

$$\mathrm{Im}M_{\mathrm{Box}}^{\gamma W} = (4\pi)8\sqrt{2}G_F\pi\alpha \int \frac{d^3k'}{(2\pi)^3 2k'_0} \frac{p\cdot(l+k')F_3^{\gamma W}}{(p\cdot k)(1-k^2/M_W^2)}. \tag{3.37}$$

We are getting close to a final form for $\mathrm{Im}M_{\mathrm{Box}}^{\gamma W}$, but we're not quite there yet. The integration measure d^3k' is unfortunately not a useful one for our structure function, whose conventional variables includes the 4-momentum transfer squared to the hadron $Q^2 = -k^2$ and the invariant mass squared of the intermediate state hadron: W^2. So let's change to this new set of variables. If $\theta_{k'}$ is the scattered angle of the intermediate electron w.r.t. the direction of the incident neutrino, chosen along the $+\hat{z}$ axis, then

$$\begin{aligned} d^3k' &= 2\pi|\vec{k'}|^2 d(\cos\theta_{k'}) d|\vec{k'}| \\ &\approx 2\pi k'^2_0 d(\cos\theta_{k'}) dk'_0. \end{aligned} \tag{3.38}$$

Meanwhile in the CM frame, this intermediate electron energy is

$$k'^{CM}_0 = \frac{s-W^2}{2\sqrt{s}} \Rightarrow dk'^{CM}_0 = -\frac{dW^2}{2\sqrt{s}}, \tag{3.39}$$

where $s = (l+p)^2$ is the incident CM energy squared. Also in this frame we have:

$$Q^2 = 2l\cdot k' = 2l_0 k'_0(1-\cos\theta_{k'}) \Rightarrow d(\cos\theta_{k'}) = -\frac{dQ^2}{2l_0 k'_0}. \tag{3.40}$$

Putting this all together means that:

$$\begin{aligned} d^3k' &= \frac{\pi {k'}_0}{2\sqrt{s}l_0} dQ^2 dW^2, \\ \Rightarrow \frac{d^3k'}{(2\pi)^3 2{k'}_0} &= \frac{dW^2 dQ^2}{32\pi^2 p\cdot l}. \end{aligned} \tag{3.41}$$

We will also need everything in the integrand of $\mathrm{Im}M_{\mathrm{Box}}^{\gamma W}$ to be expressed in terms of our new integration measure. In the rest frame of the initial neutron we have:

$$p\cdot l = ME, \tag{3.42}$$

$$p\cdot k = M\nu, \tag{3.43}$$

$$p\cdot k' = M(E-\nu), \tag{3.44}$$

where ν is the energy transfer from the lepton to the hadron. The above relations substituted into our (3.37) gives us:

$$\mathrm{Im}M_{\mathrm{Box},A}^{\gamma W} = \frac{\sqrt{2}G_F\alpha}{ME}\int dW^2 dQ^2 \Big(\frac{2ME}{W^2-M^2+Q^2} - \frac{1}{2}\Big)\frac{F_3^{\gamma W}}{1+Q^2/M_W^2}, \tag{3.45}$$

where the A subscript is thrown in to remind us that this is purely the axial-vector part. Finally, we can divide (3.45) by (3.26) for the imaginary part of the box correction, but must multiply the ratio by an additional factor of 1/2, as the we are taking 2 spin sum averages in the box amplitude but only

one in the Born amplitude. The simplified result is:

$$\mathrm{Im}\Box^{\gamma W}_{\mathrm{Box,A}} = \frac{\alpha}{8(ME)^2}\int_{W_\pi^2}^{s} dW^2 \int_0^{Q^2_{max}} dQ^2 \Big(\frac{2ME}{W^2-M^2+Q^2} - \frac{1}{2}\Big)\frac{F_3^{\gamma W}}{1+Q^2/M_W^2}, \tag{3.46}$$

where $Q^2_{max} = (s-M^2)(s-W^2)/s$ is associated with the extreme case of $\cos\theta_{k'} = 1$ and W_π^2 is the single pion threshold, as that is the minimum mass allowed above the elastic case. Although it is difficult to tell by looking at (3.46), $\mathrm{Im}\Box^{\gamma W}_{\mathrm{Box,A}}$ is an odd function of the incident neutrino's energy E – a well known fact about the γZ box as well [61]. This has consequences on the dispersion relation (3.4). In fact we're better off taking a step back and starting with the general relation of (3.2) with this knowledge about $\mathrm{Im}\Box^{\gamma W}_{\mathrm{Box,A}}$. We can simply replace Mandelstam s with E in these dispersion relations. Starting with the statement

$$\mathrm{Im}\Box^{\gamma W}_{A}(-E) = -\mathrm{Im}\Box^{\gamma W}_{A}(E). \tag{3.47}$$

From (3.2) alone, it follows that

$$\begin{aligned}\mathrm{Re}\Box^{\gamma W}_{A}(E) &= \frac{1}{\pi}P\int_{-\infty}^{\infty} dE' \frac{\mathrm{Im}\Box^{\gamma W}_{A}(E')}{E'-E} \\ &= \frac{1}{\pi}P\int_{-\infty}^{0} dE' \frac{\mathrm{Im}\Box^{\gamma W}_{A}(E')}{E'-E} + \frac{1}{\pi}P\int_{0}^{\infty} dE' \frac{\mathrm{Im}\Box^{\gamma W}_{A}(E')}{E'-E}.\end{aligned} \tag{3.48}$$

Introducing a new dummy variable for the 1st integral: $E'' = -E'$ gives

$$\begin{aligned}\mathrm{Re}\Box_A^{\gamma W}(E) &= -\frac{1}{\pi}P\int_0^\infty dE''\frac{\mathrm{Im}\Box_A^{\gamma W}(-E'')}{E''+E} + \frac{1}{\pi}P\int_0^\infty dE'\frac{\mathrm{Im}\Box_A^{\gamma W}(E')}{E'-E} \\ &= \frac{1}{\pi}\int_0^\infty dE'\Big(\frac{\mathrm{Im}\Box_A^{\gamma W}(E')}{E'-E} - \frac{\mathrm{Im}\Box_A^{\gamma W}(-E')}{E'+E}\Big),\end{aligned} \tag{3.49}$$

and now we can substitute (3.47) into the 2nd term of (3.49) to finally conclude:

$$\mathrm{Re}\Box_A^{\gamma W}(E) = \frac{2}{\pi}\int_0^\infty dE'\frac{E'}{E'^2-E^2}\mathrm{Im}\Box_A^{\gamma W}(E'). \tag{3.50}$$

This is our dispersion relation applicable to the axial γW box. The utility of (3.50) is twofold: not only does it calculate the real part of the box, but by analytically continuing to the negative energy axis, we are implicitly adding the crossed box! The uncrossed box does not allow negative energy. However, the crossed box can be thought of crossing the external lepton lines between initial and final states - which by crossing symmetry is related to their antiparticles which are effectively representing the particle with negative energy. See Figure 3.5. Next we need to substitute (3.46) into (3.50). Once we do this it will be possible to slide the energy integral through the Q^2 and W^2 integrals by using [17]:

$$\int_{\nu_\pi}^\infty dE'\int_{W_\pi^2}^s dW^2\int_0^{Q^2_{max}} dQ^2 = \int_{W_\pi^2}^\infty dW^2\int_0^\infty dQ^2\int_{E_{min}}^\infty dE', \tag{3.51}$$

$$E_{min} = \frac{W^2-M^2+Q^2}{4M} + \frac{1}{4M}\sqrt{(W^2-M^2+Q^2)^2+4M^2Q^2}. \tag{3.52}$$

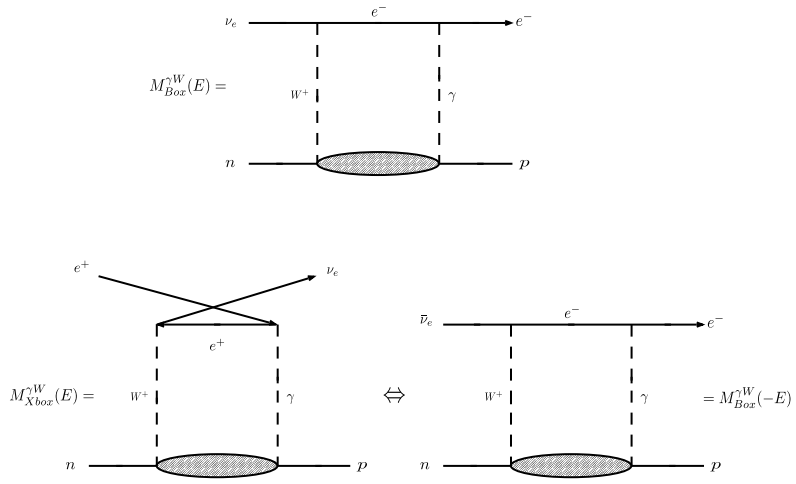

Figure 3.5: One way to represent a crossed box is by crossing the lepton lines. Due to crossing symmetry, this can be thought of as the box at negative energy.

Substituting this into (3.46) then leads to:

$$\begin{aligned} \mathrm{Re}\Box^{\gamma W}_A(E) = \frac{\alpha}{8\pi}\int_{W_\pi^2}^{\infty} dW^2 \int_0^{\infty} dQ^2 \frac{F_3^{\gamma W}}{1+Q^2/M_W^2} \\ \times \left[\frac{1}{M^2}\int_{E_{min}}^{\infty} dE' \frac{1}{E'(E'^2-E^2)}\Big(\frac{2ME'}{W^2-M^2+Q^2}-\frac{1}{2}\Big)\right], \end{aligned} \tag{3.53}$$

and now the integral inside the square brackets can be evaluated analytically. Letting $\chi = W^2 - M^2 + Q^2$, it is:

$$\begin{aligned}&\frac{1}{M^2}\int_{E_{min}}^{\infty} dE' \frac{1}{E'(E'^2 - E^2)}\Big(\frac{2ME'}{\chi} - \frac{1}{2}\Big) \\ &= \frac{2}{M\chi}\frac{1}{E}\tanh^{-1}\Big(\frac{E}{E_{min}}\Big) + \frac{1}{4M^2E^2}\ln\Big(1 - \frac{E^2}{E_{min}^2}\Big).\end{aligned} \tag{3.54}$$

Using this expression would allow us to truly know the energy-dependence of $\mathrm{Re}\Box_A^{\gamma W}(E)$, were we to properly integrate over W^2 and Q^2 in the remaining expression of (3.53). However, for the purposes of β decay in the processes discussed in section 1.2 we can take the $E \to 0$ limit where we find:

$$\begin{aligned}\lim_{E\to 0}\frac{1}{M^2}\int_{E_{min}}^{\infty} dE' \frac{1}{E'(E'^2 - E^2)}\Big(\frac{2ME'}{\chi} - \frac{1}{2}\Big) &= \frac{2}{M\chi E_{min}} + \frac{1}{4M^2}\lim_{E\to 0}\frac{1}{E^2} \\ &\quad \times\ln\Big(1 - \frac{E^2}{E_{min}^2}\Big), \\ \lim_{E\to 0}\frac{1}{E^2}\ln\Big(1 - \frac{E^2}{E_{min}^2}\Big) &= -\frac{1}{E_{min}^2}, \\ \Rightarrow \lim_{E\to 0}\frac{1}{M^2}\int_{E_{min}}^{\infty} dE' \frac{1}{E'(E'^2 - E^2)}\Big(\frac{2ME'}{\chi} - \frac{1}{2}\Big) &= \frac{1}{ME_{min}}\Big(\frac{2}{\chi} - \frac{1}{4ME_{min}}\Big).\end{aligned} \tag{3.55}$$

At last, substituting (3.55) into (3.53) gives us our final result of this section:

$$\begin{aligned}
\mathrm{Re}\Box_A^{\gamma W}(0) &= \frac{\alpha}{8\pi}\int_{W_\pi^2}^{\infty} dW^2 \int_0^{\infty} dQ^2 \frac{F_3^{\gamma W}(Q^2,W^2)}{1+Q^2/M_W^2}\frac{1}{ME_{min}}\Big(\frac{2}{\chi}-\frac{1}{4ME_{min}}\Big),\\
\chi &= W^2 - M^2 + Q^2,\\
E_{min} &= \frac{\chi+\sqrt{\chi^2+4M^2Q^2}}{4M}.
\end{aligned} \tag{3.56}$$

This is our "master formula" for evaluating the fractional correction of the axial part of the γW boxes to the Born cross section. It is an exact expression whose remaining physics input resides in the $F_3^{\gamma W}$ interference structure function. Knowledge of this function over the positive $\{W^2, Q^2\}$ quadrant is necessary to now reliably calculate this radiative correction.

3.3 Kinematical Regions of $F_3^{\gamma W}$

We will next need to model our $F_3^{\gamma W}$ over the integration domain of (3.56). Since Q^2 is the 4-momentum transfer of one vector boson (γ or W), it can physically assume any value. Low $Q^2 \lessapprox (1-2)\text{GeV}^2$ corresponds to the long-distance limit, where the vector bosons see a non-trivial hadron structure. On the other hand, at high $Q^2 \gtrapprox 2\text{GeV}^2$, very short distances are probed and here the vector bosons begin to see individual quarks/partons. This latter region is known as the deep inelastic scattering (DIS) region, and allows one to use the parton model to describe $F_3^{\gamma W}$. It is also valid to treat any QCD interactions perturbatively (pQCD) for this high Q^2, where the strong coupling constant is sufficiently small.

The other integration variable W^2 is the invariant mass squared of the intermediate state hadron. A special case of the $\nu_e n \to e^- p$ process is when the nucleon stays a ground state nucleon depicted in Figure 3.6. This is called

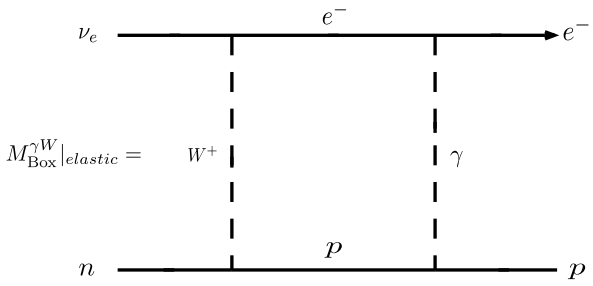

Figure 3.6: The elastic γW box wherein the W-boson changes neutron to proton.

the elastic contribution which corresponds to $W^2 = M^2$ where M is the mass

of the proton for the box or the neutron in the crossed box. This elastic process corresponds to adding a discrete pole to the contour of Figure 3.3 at the nucleon mass, and rather than re-implement a new contour, its contribution to the box correction will be isolated. In general the intermediate hadron can assume various nucleonic resonances: $W^2 = m_R^2 > (M+m_\pi)^2$. For very large $W^2 \geq 4\text{GeV}^2$ and low $Q^2 \leq 2\text{GeV}^2$, $F_3^{\gamma W}$ enters the so-called Regge region where QCD becomes non-perturbative due to asymptotic freedom and some other effective picture of the hadron constituents must be adopted. All of the details of each region will be discussed in detail in the sections following this one. For visual aid purposes, the shaded colours in Figure 3.7 will be

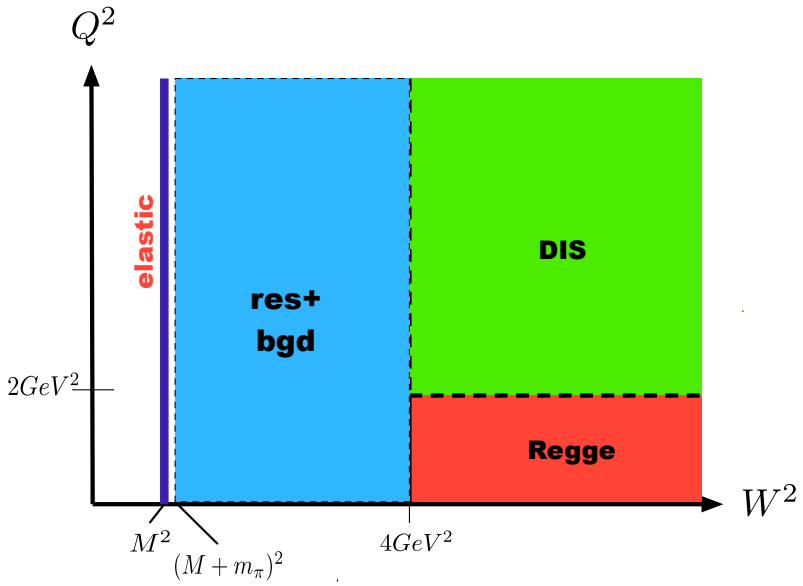

Figure 3.7: The kinematical regions by which $F_3^{\gamma W}$ will be modeled from. The dashed lines represent the fact that the boundaries are not unique, and that the total radiative correction should not depend on their choice.

maintained throughout the thesis to represent that particular region. In the calculation of (3.56) in the following sections, $F_3^{\gamma W}$ is modeled differently in the 4 shown regions. Namely:

- $F_{3,el}^{\gamma W}$: $W^2 = M^2, 0 \leq Q^2 < \infty$,
- $F_{3,res+bgd}^{\gamma W}$: $W_\pi^2 \leq W^2 \leq 4\text{GeV}^2, 0 \leq Q^2 < \infty$,
- $F_{3,Reg}^{\gamma W}$: $4\text{GeV}^2 \leq W^2 < \infty, Q^2 \leq 2\text{GeV}^2$,
- $F_{3,DIS}^{\gamma W}$: $4\text{GeV}^2 \leq W^2 < \infty, Q^2 \geq 2\text{GeV}^2$.

Although the structure function will have a different functional form in each region, the rest of the integrand in (3.56) is fixed, and can tell us how the box correction is weighted across the plane. To see this, look at Figure 3.8 which gives a 2D surface plot of the weighting function:

$$\omega(Q^2, W^2) = \frac{1}{1 + Q^2/M_W^2} \frac{1}{ME_{min}(Q^2, W^2)} \left(\frac{2}{\chi(Q^2, W^2)} - \frac{1}{4ME_{min}(Q^2, W^2)} \right). \tag{3.57}$$

This function ω of course gets multiplied by $F_3^{\gamma W}(Q^2, W^2)$ which has the general behaviour:

$$F_3^{\gamma W} \to const,\ Q^2 \to 0\ , \tag{3.58}$$

$$F_3^{\gamma W} \to 0,\ Q^2 \to \infty\ , \tag{3.59}$$

$$F_3^{\gamma W} \to \infty,\ W^2 \to \infty\ , \tag{3.60}$$

$$F_3^{\gamma W} \to 0,\ W^2 \to W_\pi^2\ . \tag{3.61}$$

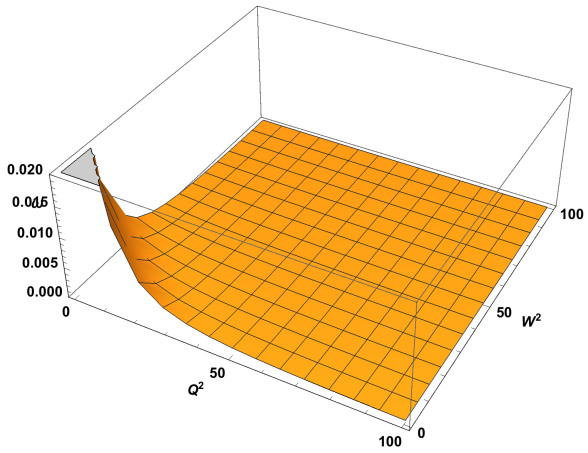

Figure 3.8: The weighting function $\omega(Q^2, W^2)$ plotted over the plane. It essentially approaches zero as either of its variables gets above the scale of the W boson mass.

3.4 Elastic Contribution

To calculate the elastic contribution to $\Box_A^{\gamma W}$, we simply need to derive the expression for $F_{3,el}^{\gamma W}$. This means we can just focus on the hadronic tensor. In the elastic limit, the vertex couplings for the Wnp and γpp of Figure 3.6 are simply written in terms of form factors defined as follows:

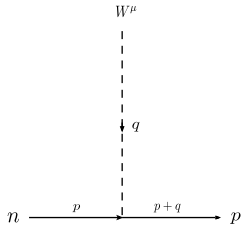

$$= \Gamma^\mu_{CC}(q) = \gamma^\mu F_1^V + \tfrac{i}{2M}\sigma^{\nu\beta}q_\beta F_2^V - \gamma^\mu\gamma_5 G_A, \quad (3.62)$$

$$F_1^V = \tfrac{1}{2}(F_i^p - F_i^n), \quad (3.63)$$

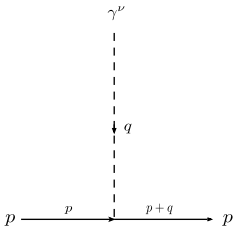

$$= \Gamma^\nu_\gamma(q) = F_1^p\gamma^\nu + \tfrac{i}{2M}\sigma^{\nu\alpha}q_\alpha F_2^p, \quad (3.64)$$

$$\sigma^{\nu\beta} = \tfrac{i}{2}[\gamma^\nu, \gamma^\beta], \quad (3.65)$$

where F_1 and F_2 are called the Dirac and Pauli form factors respectively. With the above definitions we can now construct the hadronic trace as fol-

lows:

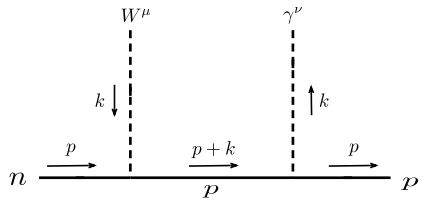

$$= \frac{1}{2}\mathrm{Tr}[\Gamma^\mu_{CC}(k)(\not{p}+\not{k}+M)\Gamma^\nu_\gamma(k)(\not{p}+M)]. \tag{3.66}$$

Since we are interested in the axial-vector part of the hadronic tensor, we can just take all the terms proportional to $\epsilon^{\mu\nu\{pk\}}$. Substituting (3.62)-(3.69) into (3.66) generates one such term, and it is:

$$H^{\mu\nu}_{\gamma W,A}(\mathrm{Box}) = 2iG_A(k)[F_1^p(k) + F_2^p(k)]\epsilon^{\mu\nu\{kp\}}. \tag{3.67}$$

Furthermore, we may express this in terms of the EM Sachs form factors which were defined in (1.28-1.29). Doing so reveals that the electric form factor drops out, and we are left with an isoscalar combination of magnetic form factors:

$$H^{\mu\nu}_{\gamma W,A}(\mathrm{Box}) = 2iG_A(k)[G_M^n(k)]\epsilon^{\mu\nu\{kp\}}. \tag{3.68}$$

It is in fact the sum of Box + Xbox that we would like to represent in the F_3 structure function, and so we simply get:

$$H^{\mu\nu}_{\gamma W,A}(\mathrm{Box}+\mathrm{Xbox}) = 2iG_A(k)[G_M^n(k) + G_M^p(k)]\epsilon^{\mu\nu\{kp\}}. \tag{3.69}$$

Then looking back at (3.31) and (3.32) we can equate levi-cevita terms with the understanding that we must multiply (3.69) by $2\pi\delta(W^2 - M^2)$ as we need

the discontinuity:

$$\begin{aligned} 4\pi\frac{i\epsilon^{\mu\nu\alpha\beta}k_\alpha p_\beta}{2(p\cdot k)}F_{3,el}^{\gamma W} &= 2iG_A(GM^n+G_M^p)\epsilon^{\mu\nu\alpha\beta}p_\alpha k_\beta 2\pi\delta(W^2-M^2), \\ \Rightarrow F_{3,el}^{(0)} &= -2M\nu G_A G_M^S\delta(W^2-M^2), \end{aligned} \tag{3.70}$$

where we have replaced the superscript of our structure function with a (0) which means it is the isoscalar ($S=p+n$) component of the EM current. As the reader should be convinced by the end of section 3, this is always the case for the γW boxes, and so we will be using that notation for all the regions as well. Q^2 and W^2 are independent variables, but the variable Bjorken $x=Q^2/2M\nu$ is constructed from both. Nonetheless, we can replace the factor in (3.70) with $2M\nu=Q^2/x$ and put the elastic structure function into (3.56) to get

$$\Box_{A,el}^{\gamma W}=\frac{\alpha}{8\pi}\int dW^2\int dQ^2\frac{Q^2G_AG_M^S\delta(W^2-M^2)}{x(1+Q^2/M_W^2)}\frac{1}{ME_{min}}\left(\frac{2}{\chi}-\frac{1}{4ME_{min}}\right). \tag{3.71}$$

We can then apply the delta function to perform the W^2 integral at which $x=1$ and after simplifying completely, one obtains the expression:

$$\Box_{A,el}^{\gamma W}=\frac{\alpha}{2\pi}\int_0^\infty dQ^2\frac{G_A(Q^2)[G_M^p(Q^2)+G_M^n(Q^2)]}{Q^2(1+Q^2/M_W^2)}\frac{1+2\sqrt{1+4M^2/Q^2}}{(1+\sqrt{1+4M^2/Q^2})^2}, \tag{3.72}$$

and this is our elastic formula for the correction we seek expressed in terms of EM form factors. Notice that the photon coupling is a purely isoscalar combination, a fact we will return to throughout this dissertation. The axial form

factor can be empirically represented by a simple dipole parameterization:

$$G_A(Q^2) = \frac{g_A}{\left(1 + \frac{Q^2}{m_A^2}\right)^2}, \tag{3.73}$$

which is a choice which is supported by data spanning both electroproduction and neutrino experiments alike. We use the PDG 2018 values for both g_A and m_A given in Appendix C. Although the axial coupling is well-constrained, the axial mass parameter spans quite a range in the literature: $\sim 0.85 - 1.35\text{GeV}^2$ [18],[19]. The magnetic form factors are not well-described by a simple monopole or dipole, so instead we use the explicit data for them appended to reference [20]. Substituting these form factors as well as the experimental uncertainties they carry yields the following result for our elastic contribution:

$$\Box^{\gamma W}_{A,el} = (0.8967 \pm .0607)\frac{\alpha}{2\pi} = (1.04 \pm .07) \times 10^{-3} \tag{3.74}$$

Which is roughly a 2% increase to Sirlin's .88 result for C_{Born}. It should be remarked that the dispersive analysis of (3.56) does nothing to improve the elastic contribution computation, as this is a special case where the full loop calculation can be done exactly in terms of form factors. Rather it perhaps just makes the numerical computation of the raw data of $G_M^S(Q^2)$ a more straightforward exercise. A nice demonstration of the loop calculation of $\Box^{\gamma W}_{A,el}$ can be found in [12]. As a last comment on the elastic contribution, I

have observed that this correction is somewhat sensitive to the m_A parameter, and this has been plotted in Figure 3.9.

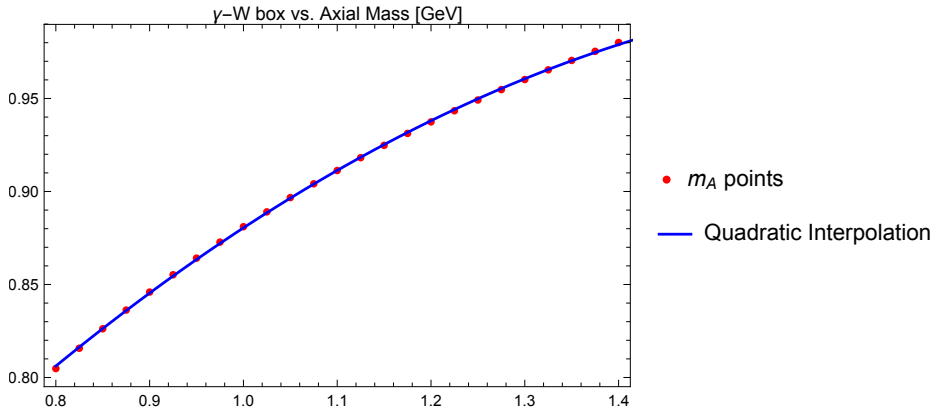

Figure 3.9: The dependence of the box correction on the axial mass parameter in units of $\alpha/2\pi$ for the broad range of m_A found in the literature.

3.5 Resonance Region

Above the pion threshold $W^2 \geq (M + m_\pi)^2$ the exchanged vector bosons in the γW box can excite the initial state neutron into a resonance particle. There are many 1/2-integer spin N and Δ resonances which have been studied using πN and γN scattering experiments. The tabulated resonance states range in mass from $1.232 - 2.95$GeV, each with known J^P numbers [21]. However, only the first few low-mass resonances in this range have accurate vector and axial form factors or helicity amplitudes [22]-[25].

Since the exchanged photon here is isoscalar, it cannot change the isospin of the hadron it interacts with. On the other hand, the W-boson is purely isovector and must cause an isospin I_3 change of 1 quanta to the hadron. The QM rules of the addition of angular momenta then forces the isospin of the resonance to be $I = 1/2$. This then excludes the Δ resonances with $I = 3/2$ from our $F_{3,res}^{(0)}$ model. As a consequence, the only resonances we may insert into our structure function are: $P_{11}(1440)$, $D_{13}(1520)$ and $S_{11}(1535)$.

According to [23], the isoscalar combination of EM form factors for the P_{11} and S_{11} resonances is zero. On the other hand, we can potentially expect a non-negligible resonance contribution to $\Box_A^{\gamma W}$ from the D_{13} resonance. Taking conventional differences into account, I find that:

$$F_{3,res}^{(0)} = -\nu \mathcal{W}_3^{\text{Lal.}}, \tag{3.75}$$

where $\mathcal{W}_3^{\text{Lal.}}$ is the axial structure function used by Lalakulich for neutrino scattering. With this established all that is left is to take the isoscalar combination of EM form factors – doing so for the D_{13} contribution gives us:

$$F_{3,D_{13}}^{(0)}|_{\text{Lal.}} = -\frac{4\nu}{3M}\Gamma_{D_{13}}(W)\Big[-C_4^S(Q^2)(Q^2-\nu M)+C_5^S(Q^2)\nu M \\ +C_3^S(Q^2)\frac{M}{m_{D_{13}}}(2m_{D_{13}}^2-2Mm_{D_{13}}+Q^2-\nu M)\Big]C_5^A(Q^2), \tag{3.76}$$

which has been plotted in Figure 3.10 and the Breit-Wigner resonance function is defined as:

$$\Gamma_{D_{13}}(W) = \frac{m_{D_{13}}\Gamma_{D_{13}}}{\pi}\frac{1}{(W^2-m_{D_{13}})^2+m_{D_{13}}^2\Gamma_{D_{13}}^2}. \tag{3.77}$$

All of the parameters of (3.76) and (3.77) are given in Appendix C, including

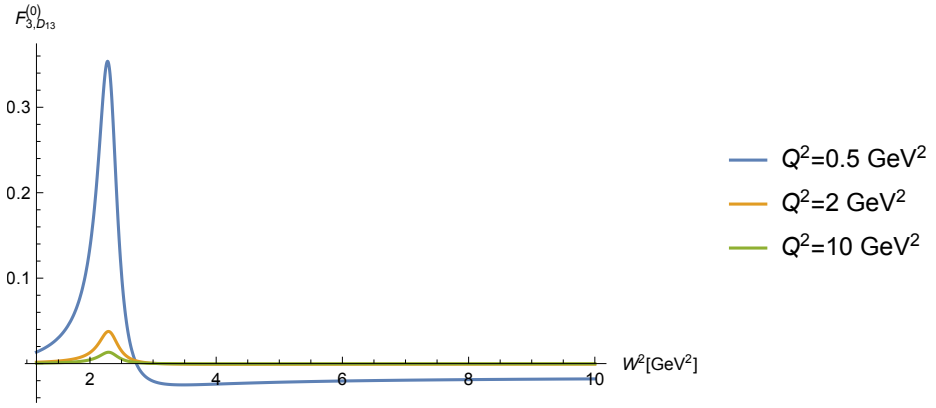

Figure 3.10: Lalakulich plots of $F_3^{(0)}$ vs W^2 for the D_{13} resonance at several Q^2 values.

the form factors. Inserting (3.76) into (3.56) gives the numerical contribution

of this single resonance to the box correction:

$$\Box^{\gamma W}_{A,D_{13}}|_{\text{Lal.}} = .08 \times 10^{-3}. \tag{3.78}$$

An alternative to (3.75) is to strictly work in the helicity amplitude formalism. The benefits of this are that these amplitudes have a rich library of parameterizations amongst several major collaborations [25], [26]. We will be using the MAID amplitudes from [25] and find that there is actually a non-zero contribution from the other 2 resonances. In this model the amplitudes take the form:

$$\bar{A}_\alpha(Q^2) = \bar{A}_\alpha(0)\big(1 + a_1 Q^2 + a_2 Q^4 + a_3 Q^8\big)e^{-b_1 Q^2} \tag{3.79}$$

Again, after taking conventional differences into account, the results of the MAID parameterization are shown in Table 3.1. which will form a preferred result, as they are more recent and they do not assume the other resonances are zero. This is a significant difference from (3.78) as the new

Resonance	$\Box^{\gamma W}_{A,res}(\times 10^{-3})$
D_{13}	0.054
P_{11}	-0.009
S_{11}	-0.002
total	.04

Table 3.1: γW box corrections from 3 resonances using the MAID helicity amplitudes

total resonance contribution has effectively been reduced by 1/2. We can then use the difference between the MAID prediction and the Lalakulich prediction to assign a rough error estimate to this resonance correction via $\delta\Box^{\gamma W}_{A,res} \sim |\Box^{\gamma W}_{A,D_{13}}(Lal.) - \Box^{\gamma W}_{A,D_{13}}(MAID)| \approx .02 \times 10^{-3}$. Then our final resonance contribution will stand as:

$$\Box^{\gamma W}_{A,res} = (.04 \pm .02) \times 10^{-3}. \tag{3.80}$$

Physically, in the region $W_\pi^2 \leq W^2 \leq 4\text{GeV}^2$, $F^{(0)}_{3,res}$ is not the only contribution to the full structure function however. There is also a non-resonant background which we will denote by $F^{(0)}_{3,\text{bgd}}$. To estimate this contribution, we can relate it to the purely EM structure function $F_1^{\gamma\gamma}$ which is known from inelastic $e^- p$ cross sections. In order to find this subtle relationship, it is very helpful to consider these structure functions in the parton model, where:

$$F_3^{(0)} = \frac{u_\text{v} - d_\text{v}}{3}, \tag{3.81}$$

$$F^{\gamma Z}_{3,p+n} = u_\text{v} + d_\text{v}. \tag{3.82}$$

The kinematical region of the nonresonant background we need to consider is approximately $.4 \leq x \leq .88$, and the valence distribution normalizations are: $\int dx u_\text{v} = 2\int dx d_\text{v} = 2$. Consequently, one finds that in the resonance

region we have:

$$F_3^{(0)} \approx \frac{F_{3,d}^{\gamma Z}}{9}, \tag{3.83}$$

where we've simply replaced $p + n \to d$ for the deuteron on the RHS. We next need to estimate the nonresonant background for $F_{3,d}^{\gamma Z}$. To do this, we can start by considering the following general parton expressions:

$$F_1^{\gamma\gamma} = \frac{1}{2}\Sigma_q e_q^2 (q + \bar{q}), \tag{3.84}$$

$$F_3^{\gamma Z} = 2\Sigma_q e_q g_A^q (q - \bar{q}). \tag{3.85}$$

In the resonance region the quark PDFs dominate over the antiquark ones, while as hinted before: $u(x) \approx 2d(x)$. With these crude assumptions one can use (3.84) and (3.85) to show that:

$$\frac{F_{3,d}^{\gamma Z}}{F_{1,d}^{\gamma\gamma}} \approx \frac{18}{5}. \tag{3.86}$$

In the low x limit, the ratio in (3.86) goes to zero and one could imagine replacing the RHS with some sort of average over all x. However, we only need to know this ratio for high x and so we shall assume the ratio of 18/5 and apply it to our sought background structure function. Combining (3.83) and (3.86) reveals the simple re-scaling result:

$$F_{3,\mathrm{bgd}}^{(0)} \approx \frac{2}{5} F_{1,p}^{\gamma\gamma}, \tag{3.87}$$

where we have use the known fact that $F_{1,n}^{\gamma\gamma}$ is only marginally different than zero. Although it is not guaranteed to describe our background, (3.87) can offer an educated first guess. The non-resonant background for $F_1^{\gamma\gamma}$ is related to the nonresonant cross section for $e^- p$ scattering which has been parameterized in [27]. Let us assume this same parameterization can apply to $F_{3,\mathrm{bgd}}^{(0)}$ and rather than use (3.87) explicitly, we can relax the proportionality constant to a free parameter η_S:

$$F_{3,\mathrm{bgd}}^{(0)}(Q^2,W^2) = \eta_S \frac{W^2-M^2}{8\pi^2\alpha}\frac{1}{f_c}\left(1+\frac{W^2-(M+m_\pi)^2}{Q^2+Q_0^2}\right)^{-1} \times \sum_{i=1}^{2} \frac{\sigma_T^{NR,i}(0)[W-(M+m_\pi)]^{(i+1/2)}}{(Q^2+a_i^T)^{(b_i^T+c_i^T Q^2+d_i^T Q^4)}}, \tag{3.88}$$

and all of the parameters contained in (3.88) are provided in Appendix C while $f_c = 389.39$ is the conversion factor for $\mu b \rightarrow \mathrm{GeV}^{-2}$. We are left now with the task of determining a value of η_S. Although the parton model expression of (3.81) isn't well-trusted below $W^2 = 4\mathrm{GeV}^2$, it IS well-trusted above that boundary. Therefore we may impose the boundary condition that the background of (3.88) nicely match (3.81) there. Doing so for a large range of Q^2 values consistently indicates that:

$$\eta_S \approx \frac{9}{10},\ Q^2 \geq 2\mathrm{GeV}^2. \tag{3.89}$$

For $Q^2 \leq \mathrm{GeV}^2$, (3.88) needs to be matched to the Regge model of $F_3^{(0)}$, which we will not arrive at until section 3.7. At this lower Q^2 range I find

that $\eta_S \approx 18/25$. It is then the sum of (3.88) and say, (3.76) which represents the full $F_3^{(0)}$ structure function in the region $W_\pi^2 \leq W^2 \leq 4\text{GeV}^2$. Since we have already computed the pure resonance part which considered the area under it's high W^2 tail, we simply need to compute the sole contribution of (3.88) for $W^2 \leq 4\text{GeV}^2$ to find:

$$\Box^{\gamma W}_{A,bgd} = 0.16 \times 10^{-3}. \tag{3.90}$$

As can be seen in Figure 3.11, the rescaled Christy-Bosted background agrees

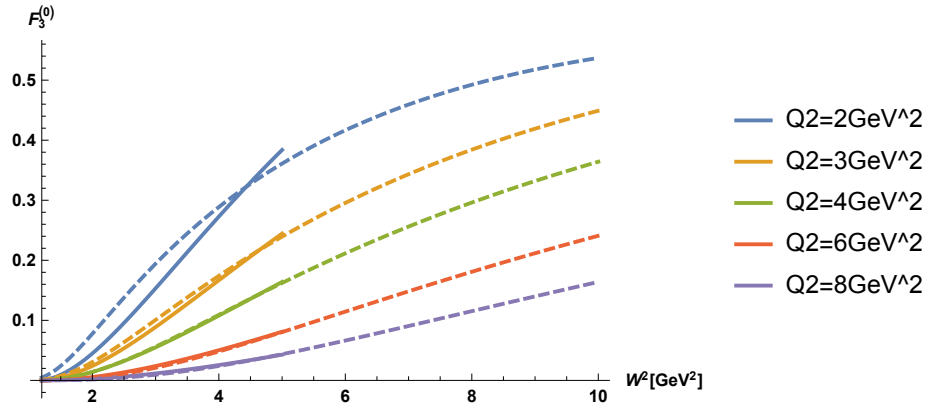

Figure 3.11: Comparing plots of $F^{(0)}_{3,bgd}$ between the prediction from (3.88-3.89) and the DIS prediction of (3.81) at several Q^2 values.

rather well with the extrapolated parton model. We cannot use the parton model below this boundary, but we can compare it's prediction towards $\Box^{\gamma W}_A$ with that of (3.88) for $Q^2 \geq 2\text{GeV}^2$ and $W^2 \leq 4\text{GeV}^2$. We will call this contribution the high Q^2, low W^2 background contribution, and the difference

is:

$$\Box^{\gamma W}_{A,CB}|_{\text{high}Q^2} = .017 \times 10^{-3}, \tag{3.91}$$

$$\Box^{\gamma W}_{A,DIS}|_{\text{high}Q^2} = .019 \times 10^{-3}. \tag{3.92}$$

Since we only need the correction to the 10^{-5} level, the difference between (3.91) and (3.92) is negligible and is graphically represented in Figure 3.11. The last thing we should try to do is assign a reasonable uncertainty estimate to the background prediction in (3.90). This can be deduced from quantifying the inexactness of η_S. Doing so reveals a 10% uncertainty. We can combine this with (3.80) to get the total resonance + background contribution:

$$\Box^{\gamma W}_{A,\text{res+bgd}} = (.20 \pm .03) \times 10^{-3}. \tag{3.93}$$

The DIS model of (3.81) has a very small uncertainty $< 1\%$ and is plotted along with our total background plus resonance structure function around the boundary $W^2 = 4GeV^2$ in Figure 3.12. From the figure, one can see that we have some flexibility to change the boundary somewhat without appreciably changing the net area under $F_3^{(0)}$.

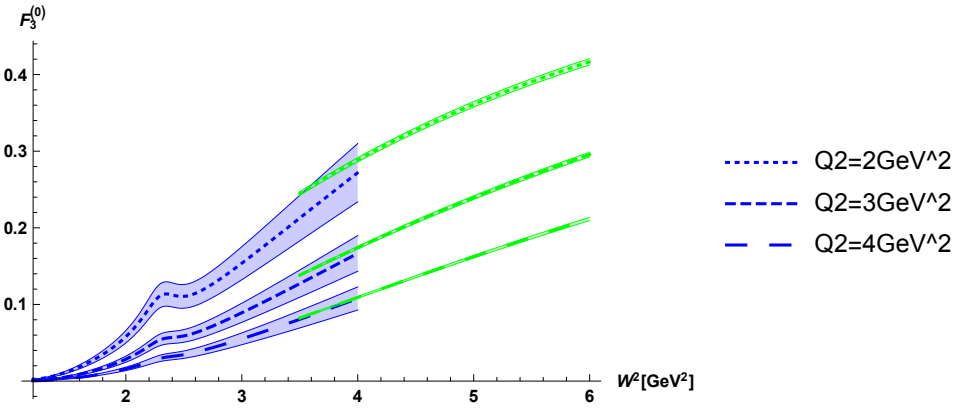

Figure 3.12: Lot W^2 plot of $F_3^{(0)}$ at several high Q^2 values. Blue curves are from the rescaled Bosted-Christy background plus Lalakulich resonance contribution while green curves are from the parton model.

3.6 DIS Contribution

When Q^2 is high the vector bosons probe very short distances in the hadron. To leading order in the strong interaction, the quarks are considered as just free particles, but one can systematically introduce higher orders of quark-quark interactions via pQCD. This is because the strong coupling constant g_s is small in the DIS region where perturbation theory is valid. We will deal with the non-perturbative situation in section 3.7.

In the DIS region $F_3^{(0)}$ can be modeled in terms of partons (quarks, gluons, etc.), which each carry a certain fraction x of the hadron's total momentum. In this model, each parton, such as a quark $q = q(x, Q)$ is considered a function of Bjorken x and the 4-momentum transfer Q and is called a parton distribution function (PDF). PDFs are not observables, but rather, observables can be constructed from them. Using DIS data, the PDFs can be

constrained and computed/estimated. This has been done by many research groups around the globe, and for instance, the LHA PDF sets are publicly available [28] at the time of writing this thesis.

To pursue the goal of calculating our observable $\Box^{\gamma W}_{A,DIS}$, we need to first find an expression for $F^{(0)}_{3,DIS}$ in terms of PDFs. This was actually given in (3.81) of the previous section when it was needed for less lofty reasons, so now a proof of that expression will be given here. I must note that one must be cautious in deriving an expression for $F^{(0)}_{3,DIS}$ in the parton model as it is unique. So far every other structure function found in the other semileptonic boxes has been flavour-diagonal, whereas this one is not. This poses a challenge, as it means a different quark is leaving the process as the one which had entered (temporally). Being an interference structure function, that makes it somewhat difficult to book-keep the differences between the various quark diagrams which are to represent $\langle p|T[J^{\lambda}_{\gamma}(x)J^{\rho}_{W}(0)]|n\rangle$.

One possible solution to sort this out is to use the machinery of isospin rotations described in [77]. There the authors defined the timelike quark-quark operator:

$$\hat{O}^{qq'} = \bar{\psi}_q \hat{n}[0,z]\psi_{q'}|_{z^2=0}. \tag{3.94}$$

We will also need to know some of the quantum numbers of the quarks we will be considering, and these are given in Table 3.2. The isospin rotations in general isospin space allow us to write non-diagonal matrix elements of

the operator in (3.94) in terms of diagonal ones and are [77]:

$$\langle +|\hat{O}^{+-}|-\rangle = \langle +|\hat{O}^{++}|+\rangle - \langle +|\hat{O}^{--}|+\rangle \tag{3.95}$$

$$\langle +|\hat{O}^{+-}|-\rangle = \langle -|\hat{O}^{--}|-\rangle - \langle -|\hat{O}^{++}|-\rangle \tag{3.96}$$

$$\langle -|\hat{O}^{-+}|+\rangle = \langle +|\hat{O}^{++}|+\rangle - \langle +|\hat{O}^{--}|+\rangle \tag{3.97}$$

$$\langle -|\hat{O}^{-+}|+\rangle = \langle -|\hat{O}^{--}|-\rangle - \langle -|\hat{O}^{++}|-\rangle \tag{3.98}$$

where $\pm$ refers to $I_3 = \pm\frac{1}{2}$ in the above relations. Next we need to consider the quark diagrams of the γW boxes and crossed boxes. Starting with the boxes we can have:

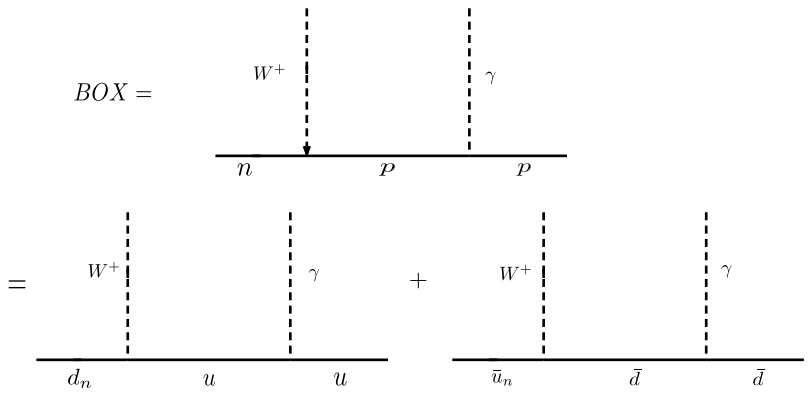

Figure 3.13: Allowed quark diagrams which can participate in the $n\nu \to pe^-$ γW box, neglecting strange and charm flavours.

$$\Rightarrow BOX = e_u \langle p|\hat{O}^{ud_n}|n\rangle - e_{\bar{d}} \langle p|\hat{O}^{\bar{d}\bar{u}_n}|n\rangle. \tag{3.99}$$

This expression makes the assumption that the process is elastic, which it in general is not forced to be. So now we may generalize this to isospin space and write:

$$\Rightarrow BOX = e_u\langle +|\hat{O}^{+-}|-\rangle - e_{\bar{d}}\langle +|\hat{O}^{+-}|-\rangle. \tag{3.100}$$

Now the goal here is to express this in terms of diagonal matrix elements in isospin(flavour) space. In that regard it's the flavour of the 'q' in e_q for each term. Applying (3.95) reveals that:

$$\begin{aligned} BOX &= e_u(\langle +|\hat{O}^{++}|+\rangle - \langle +|\hat{O}^{--}|+\rangle) - e_{\bar{d}}(\langle +|\hat{O}^{++}|+\rangle - \langle +|\hat{O}^{--}|+\rangle) \\ &= e_u(\langle p|\hat{O}^{uu}|p\rangle - \langle p|\hat{O}^{dd}|p\rangle) - e_{\bar{d}}(\langle p|\hat{O}^{\bar{d}\bar{d}}|p\rangle - \langle p|\hat{O}^{\bar{u}\bar{u}}|p\rangle) \\ &= e_u(u-d) - e_{\bar{d}}(\bar{d}-\bar{u}) \\ &= e_u(u-d) + e_d(\bar{d}-\bar{u}). \end{aligned} \tag{3.101}$$

For reference, see Table 3.2 which gives us the relevant quantum numbers of the quarks considered here. We can repeat this same process for the crossed box as well, starting with Figure 3.14.

q	e_q	I_3^q
u	$+\frac{2}{3}$	$+\frac{1}{2}$
$\bar{u}$	$-\frac{2}{3}$	$-\frac{1}{2}$
d	$-\frac{1}{3}$	$-\frac{1}{2}$
$\bar{d}$	$+\frac{1}{3}$	$+\frac{1}{2}$

Table 3.2: Quark charge numbers and isospin projections in the SM.

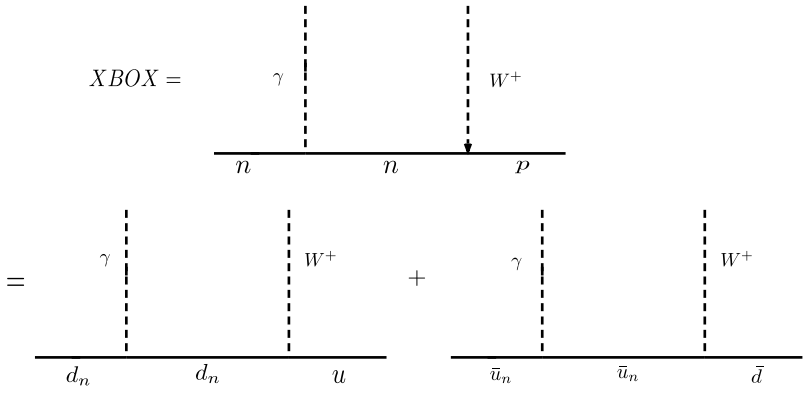

Figure 3.14: Allowed quark diagrams which can participate in the $n\nu \to pe^-$ γW crossed box, neglecting strange and charm flavours.

$$
\begin{aligned}
\Rightarrow XBOX &= e_d\langle p|\hat{O}^{ud}|n\rangle - e_{\bar{u}}\langle p|\hat{O}^{d\bar{u}}|n\rangle \\
&= e_d\langle +|\hat{O}^{+-}|-\rangle - e_{\bar{u}}\langle +|\hat{O}^{+-}|-\rangle \\
&= e_d(\langle -|\hat{O}^{--}|-\rangle - \langle -|\hat{O}^{++}|-\rangle) - e_{\bar{u}}(\langle -|\hat{O}^{--}|-\rangle - \langle -|\hat{O}^{++}|-\rangle) \\
&= e_d(\langle n|\hat{O}^{dd}|n\rangle - \langle n|\hat{O}^{uu}|n\rangle) - e_{\bar{u}}(\langle n|\hat{O}^{\bar{u}\bar{u}}|n\rangle - \langle n|\hat{O}^{\bar{d}\bar{d}}|n\rangle) \\
&= e_d(d_n - u_n) - e_{\bar{u}}(\bar{n}_n - \bar{d}_n) \\
&= e_d(u - d) + e_u(\bar{d} - \bar{u}),
\end{aligned}
\tag{3.102}
$$

as we want the PDFs in the proton as a matter of convention. Finally we can take the sum of (3.101) and (3.102) for the total structure function:

$$\begin{aligned} F_{3,DIS}^{(0),LO} &= BOX + XBOX \\ &= e_u(u-d) + e_d(\bar{d}-\bar{u}) + e_d(u-d) + e_u(\bar{d}-\bar{u}) \\ &= e_u(u-\bar{u}-d+\bar{d}) + e_d(u-\bar{u}-d+\bar{d}) \\ &= (e_u+e_d)[u_{\rm v}-d_{\rm v}] \\ &= \frac{u_{\rm v}^{LO}-d_{\rm v}^{LO}}{3}. \end{aligned} \tag{3.103}$$

I have attached the "leading order" superscript here as this expression strictly assumes that there is no strong interaction present – in which case we need the LO PDFs on the RHS of (3.103). Now the natural variables of our structure function are (x, Q^2) where $x = Q^2/2M\nu$, and it will be convenient to stick with these natural DIS variables so let us re-express (3.56) with the appropriate integration measure [61]:

$$\Box_{A,DIS}^{\gamma W} = \frac{\alpha}{2\pi}\int_{Q_0^2}^{\infty} dQ^2 \frac{1}{Q^2(1+Q^2/M_W^2)} \int_0^{x_{max}} dx \frac{(2r-1)}{r^2} F_{3,DIS}^{(0)}, \tag{3.104}$$

$$r = 1 + \sqrt{1+4M^2x^2/Q^2}, \tag{3.105}$$

$$x_{max} = Q^2/(W_{min}^2 - M^2 + Q^2). \tag{3.106}$$

Our nominal choice of boundaries shown in Figure 3.7 means that $Q_0^2 = 2\text{GeV}^2$ and $W_{min}^2 = 4\text{GeV}^2$. As we will see later, (3.104) is the largest contribution to $\Box_A^{\gamma W}$, and since it is so important we should really be replacing

$F_{3,DIS}^{(0),LO}$ with at least its $\mathcal{O}(\alpha_S)$ correction. One observation made by the authors of [29] is that in the high Q^2 limit: $(M^2/Q^2 \ll 1)$:

$$\Box_{A,DIS}^{\gamma W} \approx \frac{3\alpha}{8\pi}\int_{Q_0^2}^{\infty} dQ^2 \frac{1}{Q^2(1+Q^2/M_W^2)}\int_0^1 dx F_{3,DIS}^{(0)}. \tag{3.107}$$

This expression applies to the case of using the parton model over the full interval $0 \leq x \leq 1$. The major benefit however, is that since our $F_{3,DIS}^{(0)}$ is exclusively constructed from valence quark distributions, the x-integration can simply use the following exact sum rules [32]:

$$\int_0^1 dx u_{\rm v}(x,Q^2) = 2, \tag{3.108}$$

$$\int_0^1 dx d_{\rm v}(x,Q^2) = 1, \tag{3.109}$$

$$\Rightarrow \int_0^1 dx F_{3,DIS}^{(0),LO} = \frac{1}{3}. \tag{3.110}$$

The remaining Q^2 integration then simply generates a leading logarithm and we get:

$$\Box_{A,DIS}^{\gamma W,LO} = \frac{\alpha}{4\pi}\ln\frac{M_W}{Q_0} \tag{3.111}$$

The pQCD corrections to the GLS sum rule have been computed in [31] and for the RHS of (3.107) they can be included to give:

$$\Box_{A,DIS}^{\gamma W,N^3LO} = \frac{\alpha}{8\pi}\int_{Q_0^2}^{\infty} dQ^2 \frac{1}{Q^2(1+Q^2/M_W^2)}\Bigg[1 - \frac{\alpha_S(Q^2)}{\pi} - C_2\Big(\frac{\alpha_S(Q^2)}{\pi}\Big)^2 - C_3\Big(\frac{\alpha_S(Q^2)}{\pi}\Big)^3\Bigg], \tag{3.112}$$

where $C_2 = 4.583 - .333N_F$, $C_3 = 41.440 - 7.607N_F + 0.177N_F^2$ and N_F is the effective number of quark flavours at Q^2. Following this prescription and choosing α at the Thomson limit $Q^2 = 0$ gives: $\Box_{A,DIS}^{\gamma W,N^3LO} = 2.17 \times 10^{-3}$ just as quoted in [29].

One advantage of using (3.112) is that since it uses sum rules, there are no PDF uncertainties to be found. Furthermore, since the higher order pQCD corrections are completely negligible to the box correction, the expression can essentially be considered "exact". The alternative is to return to (3.104) and to only integrate up to x_{max} which forces us to include the α_S corrections in a different way. A concise way of doing this is outlined in [32], which states that the NLO structure function can be computed from the convolution of the PDFs with the $\mathcal{O}(\alpha_S)$ Wilson coefficient in function space. Applying this technique to our particular structure function gives:

$$F_{3,DIS}^{(0),NLO}(x,Q^2) = \int_x^1 \frac{dz}{z} C_3^{(1)}(z) \frac{[u_{\rm v}^{NLO}(x/z,Q^2) - d_{\rm v}^{NLO}(x/z,Q^2)]}{3}, \tag{3.113}$$

and now we must insert the NLO PDFs (i.e. PDFs calculated to $O(\alpha_S)$). $C_3^{(1)}(z)$ is the NLO Wilson coefficient, given by [33]:

$$\begin{aligned} C_3^{(1)}(z) = \delta(1-z) + \frac{\alpha_s}{4\pi}\Bigg[& 2(1+z)\ln\left(\frac{z}{1-z}\right) - 4\frac{\ln z}{1-z} \\ & + 2(z+2) - \left(\frac{2\pi^2}{3}+9\right)\delta(1-z) \\ & + 4\left(\frac{\ln(1-z)}{1-z}\right)_+ - \frac{3}{(1-z)_+}\Bigg], \end{aligned} \tag{3.114}$$

which is often represented in moment space in the literature. The terms in (3.114) with a '+' subscript are distributions defined in Appendix D and are designed to be finite inside $\int^1 dx$. We will be using (3.113) as the input to (3.104) whilst isolating its small differences from using (3.107). To help accomplish this, the 2nd integral in (3.104) can be exactly replaced by:

$$\int_0^{x_{max}} dx F_3^{(0)} = \frac{3}{4}\int_0^1 dx F_3^{(0)} + \int_0^1 dx F_3^{(0)}\left(\frac{2r-1}{r^2} - \frac{3}{4}\right) - \int_{x_{max}}^1 dx F_3^{(0)} \frac{2r-1}{r^2}. \tag{3.115}$$

The first term of (3.115) gives precisely (3.107). The 2nd term considers the effect of finite Q^2, and the 3rd term quantifies the difference between taking $x_{max} \to 1$ versus any value below 1. We have actually already calculated the LO effect of this 3rd term on $\Box_A^{\gamma W}$ in (3.92); in fact it's presence here represents our will not to double-count this piece. Let us declare the sum of these last 2 terms as the "higher power" corrections, while we truly expect the 1st term to be the dominant contribution.

One convenience here is that (3.115) can be equally applied to LO or NLO in

the strong interaction, which is simply facilitated by inserting either (3.103) or (3.113) respectively. It was found that the 2 terms of the higher power contribution secretly conspire to largely cancel each other out and their sum is $\sim 10^{-6}$ which is negligible and we will indeed recover (3.107).

There is a convolution theorem stated in [34] which allows one to decouple the Wilson coefficient from the PDF distribution when the RHS of (3.113) is integrated over all x as will be our case in (3.107). For any quark valence distribution, it states that:

$$\begin{aligned}\int_0^1 dx q_{\rm v}^{NLO}(x) &= \int_0^1 dx \int_x^1 \frac{dz}{z} C_3^{(1)}(z) q_{\rm v}(x/z) \\ &= \int_0^1 dx C_3^{(1)}(x) \int_0^1 dx q_{\rm v}(x).\end{aligned} \tag{3.116}$$

The Wilson coefficients have the nice property that they can be analytically integrated over all x to a simple number. In the case of (3.114) we get:

$$\int_0^1 C_3^{(1)}(x) dx = 1 - \frac{\alpha_S}{\pi}. \tag{3.117}$$

This of course leads to the first 2 terms in (3.112). Unfortunately (3.116) cannot be used to evaluate the higher power terms, and the general convolution integration must be performed numerically with the NLO PDFs. This has been done and the results are indeed negligible. The LHA sets used for PDF input in the DIS correction includes those of [28]: CJ15 [35], MMHT14 [36], HERA20 [38], CT14 [37] and ABKM09 [39]. Each set has multiple PDFs

for each light quark flavour, from which the central set is used to calculate the central value. The uncertainty of the higher power correction can be calculated using a prescription suggested in [35]. It involves considering a quadrature sum of differences between neighbouring PDF sets via:

$$\delta\sigma = \frac{T}{2}\sqrt{\sum_{i=1}^{i_{max}}[\sigma_{2i-1} - \sigma_{2i}]^2}, \tag{3.118}$$

where σ is the observable of interest we have constructed from the PDFs. The uncertainty of the higher power correction has been computed via this means and is found negligible. This is not surprising as the central value is already 10^{-6} while the valence quark distributions are very well constrained to begin with. The dominant sum rule contribution does not require this uncertainty analysis for reasons discussed earlier. The numerical stability of the normalizations in (3.108-3.109) were tested for all the LHA sets and deviations from those sum rules were found negligible and independent of Q^2. Another necessity in computing the DIS correction is to input the running strong constant $\alpha_S(Q^2)$, which is also provided by the LHA sets. On one "edge" of the DIS region we have $\alpha_S \approx .366$, while at the Z-pole we have $\alpha_S \approx .118$. The weighted average is determined from integrating (3.112) over $2\text{GeV}^2 \leq Q^2 < \infty$. It is insightful to know the average value of this constant which yields the same box correction as the explicit running would. It is found to be:

$$\bar{\alpha}_S = 0.1927, \tag{3.119}$$

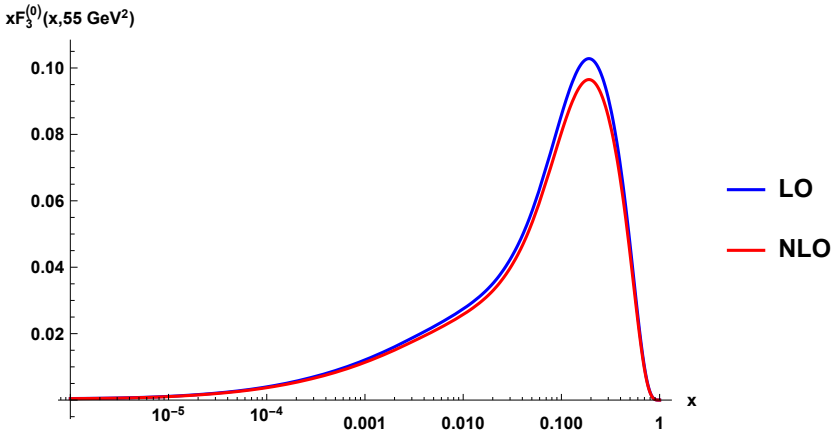

Figure 3.15: CJ15 plot of the LO and NLO $F^{(0)}_{3,DIS}$ structure functions. Traditionally they are multiplied by x to tame their large behaviour at low x.

which corresponds to $Q^2 \approx 55\text{GeV}^2$. It is found that the NLO correction in the strong constant leads to a roughly 6.1% suppression to the LO value of $\Box^{\gamma W}_{A,DIS}$. The last effect we need to consider to the DIS contribution is the

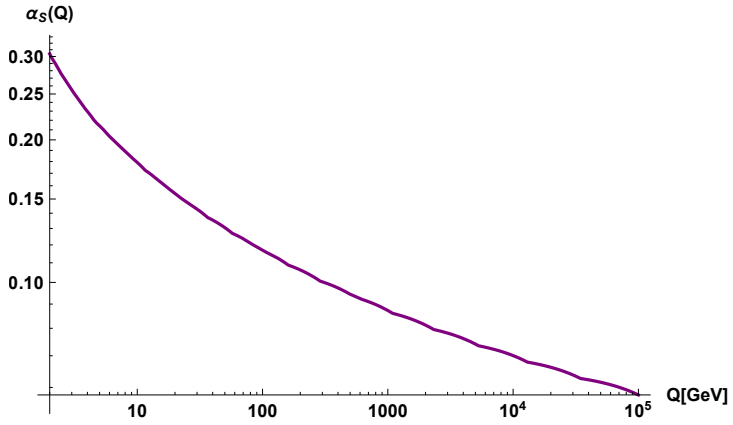

Figure 3.16: The CJ15 running of the strong fine structure constant.

running of the EM fine structure constant $\alpha = \alpha_{EM}(Q^2)$ inside the integral of (3.104). We can also confine ourselves to the NLO version as the higher

order corrections beyond that are negligible to $\Box^{\gamma W}_{A,DIS}$:

$$\Box^{\gamma W,NLO}_{A,DIS} = \frac{1}{8\pi}\int_{Q_0^2}^{\infty} dQ^2 \frac{\alpha_{EM}(Q^2)}{Q^2(1+Q^2/M_W^2)}\left[1-\frac{\alpha_S(Q^2)}{\pi}\right]. \tag{3.120}$$

The function $\alpha = \alpha_{EM}(Q^2)$ comes from evaluating the photon's 1 loop corrected self energy (SE) via:

$$\alpha_{EM}(Q^2) = \frac{\alpha_{EM}(0)}{1-\frac{\Pi_T^{\gamma\gamma}(Q^2)}{Q^2}}, \tag{3.121}$$

where:

$\Pi^{\gamma\gamma}_{\mu\nu}(Q^2) =$ 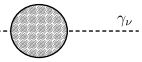 $= \Pi_T^{\gamma\gamma}(Q^2)\Big(g_{\mu\nu} - \frac{q_\mu q_\nu}{q^2}\Big) + \Pi_L^{\gamma\gamma}(Q^2)\frac{q_\mu q_\nu}{q^2}.$ (3.122)

$\Pi_T^{\gamma\gamma}(Q^2)$ is considered the transverse component of the photon's self energy and the 1-loop corrections that goes into (3.122) can be split into fermionic and bosonic loops. The fermionic loops are of the form:

$\Pi^{\gamma\gamma}_{T,fer}(Q^2) =$ 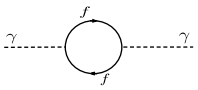

$$= \frac{e^2Q_f^2}{16\pi^2}\frac{4}{3}\Big[2m_f^2 - \frac{q^2}{3} + 2A_0(m_f) + (q^2+2m_f^2)B_0(q^2;m_f,m_f)\Big], \tag{3.123}$$

which is expressed in terms of Passarino Veltman functions which are defined in Appendix F. In the case where f is a lepton, (3.123) is sufficient to use as their masses are well-known. On the other hand if f is a quark then this result must be applied with caution as the true free quark masses are not

exactly known, but rather, their "effective" masses inside the hadron would be the input. For the contribution from the quark loops we can instead use the same dispersive techniques discussed in section 3.1 to calculate $\Pi^{\gamma\gamma}_{T,had}$ by relating it to a total cross section (see Figure 3.17). Formally, we can split

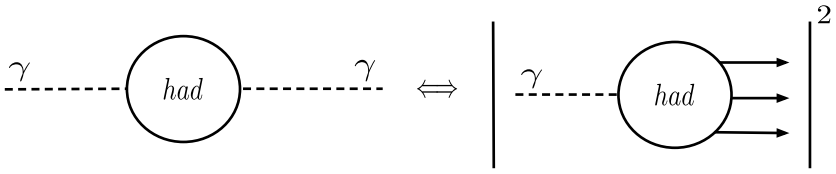

Figure 3.17: The hadronic loop contribution to the photonic SE can be delegated to the total cross section for the process $\sigma(e^+e^- \to \gamma^* \to hadrons)$

the total photon corrections into the following parts:

$$\Pi^{\gamma\gamma}_T = \Pi^{\gamma\gamma}_{T,lep} + \Pi^{\gamma\gamma(5)}_{T,had} + \Pi^{\gamma\gamma}_{T,top} + \Pi^{\gamma\gamma}_{T,Bos}. \tag{3.124}$$

The bosonic contributions only set in for $q^2 \geq M_W^2$, and so they will not be necessary to consider in our $\alpha_{EM}(Q^2)$ in the box correction, whose integrand quickly goes to zero above the W-boson scale anyways. In [40], the following definitions are made:

$$\Delta\alpha^{(5)}_{had}(s) = -\frac{\Pi^{\gamma\gamma(5)}_{T,had}(s) - \Pi^{\gamma\gamma(5)}_{T,had}(0)}{s}, \tag{3.125}$$

$$R_\gamma(s) = \frac{\sigma^{(0)}(e^+e^- \to \gamma^* \to \text{hadrons})}{4\pi\alpha^2/3s}. \tag{3.126}$$

Then using the optical theorem, the author claims that:

$$\Delta\alpha^{(5)}_{had}(s) = -\frac{\alpha s}{3\pi}\left(P\int_{m_\pi^2}^{E^2_{cut}} ds' \frac{R^{data}_\gamma(s')}{s'(s'-s)} + P\int_{E^2_{cut}}^{\infty} \frac{R^{pQCD}_\gamma(s')}{s'(s'-s)} \right), \quad (3.127)$$

and this equation allows one to systematically (albeit numerically) compute the light quark contribution to the photon vacuum polarization from available cross section data. As the top quark is quite massive (~ 173GeV), we cannot use the light fermion mass approximation. Nonetheless, it's contribution has been computed to leading order in M_Z^2/m_t^2 [40] and it is:

$$\Delta\alpha_{top} \approx -\frac{\alpha}{3\pi}\frac{4}{15}\frac{M_Z^2}{m_t^2} \rightarrow \text{“negligible”}. \quad (3.128)$$

The results of the above expressions (3.121-3.128) has been nicely summarized into data files by F. Jegerlehner and is publicly available [41]. This data was used directly to evaluate $\alpha_{EM}(Q^2)$ inside (3.120). The net effect of the running EM constant leads to a 4% enhancement to $\Box^{\gamma W}_{A,DIS}$ from the Thomson limit prediction. Thus the average value of α_{EM} in the DIS region weighted by the $\Box^{\gamma W}_A$ integrand is:

$$\bar{\alpha}_{EM} = \frac{1}{131.75}. \quad (3.129)$$

With all of the aforementioned techniques and input choices outlined in this section, the final DIS contribution using (3.120) was found to be:

$$\Box_{A,DIS}^{\gamma W} = 2.27 \times 10^{-3} \tag{3.130}$$

Should the precision requirements of the V_{ud} tighten in the future, a robust calculation of this contribution to NNLO in the strong interaction using even (157) is well understood, and can be systematically achieved. For the time-being (3.130) will aptly apply to our situation. An important remark is that the $F_3^{(0)}$ structure function generally increases as x goes to zero via:

$$F_3^{(0)} \sim x^{-0.5}, \;\; x \to 0, \tag{3.131}$$

which is known from both the DIS and Regge models. This means that the observable $\Box_A^{\gamma W}$ depends on the PDFs at low x to some extent. The divergent behaviour of (3.131) is nonetheless integrable in (3.104), rendering our correction finite as it should be.

3.7 Regge Region

At large W^2 and low Q^2, we can no longer describe our $F_3^{(0)}$ structure function with the parton model. This region also enters the deep continuum of unknown possible resonance states. Regge theory aims to explain: the hadron spectrum, the forces between these particles, and the high energy behaviour of scattering amplitudes [42]. The Regge phenomenology states that cross sections at high energy are given in the form:

$$\sigma_{tot} = As^{\epsilon} - Bs^{-\eta}, \tag{3.132}$$

where s =CM energy squared and A, B, ϵ, η are all found from fitting σ_{tot} to data. The first term originates from pomeron exchange which goes to zero for a valence-like distribution as we have. The second term is called the Reggeon term, which for our case has $s \sim \nu$, and η corresponds to the ρ trajectory intercept: $-\eta \to \alpha_0^{\rho} = .477$ [45], giving:

$$F_{3,Reg}^{(0)} \sim \left(\frac{\nu}{\nu_0}\right)^{\alpha_0^{\rho}}. \tag{3.133}$$

To finish constructing our structure function, we will follow a very similar model used by Seng et al. in [29], which combines VMD theory [46] with a phenomenological background function of order unity which smoothly goes to zero at the pion threshold. In this model, the physical process which describes $F_{3,Reg}^{(0)}$ is one in which the vector bosons (γ, W) fluctuate into appropriate

vector mesons. In particular, as shown in Figure 3.18(a), the W-boson must fluctuate into a charged axial a_1 meson while the isoscalar photon fluctuates into a neutral ω meson. The a_1 & ω mesons then connect via an isovector ρ meson exchange with the hadron. This amplitude in fact, ensures we end up with a purely axial-vector coupling to the hadron. Pure VMD theory is

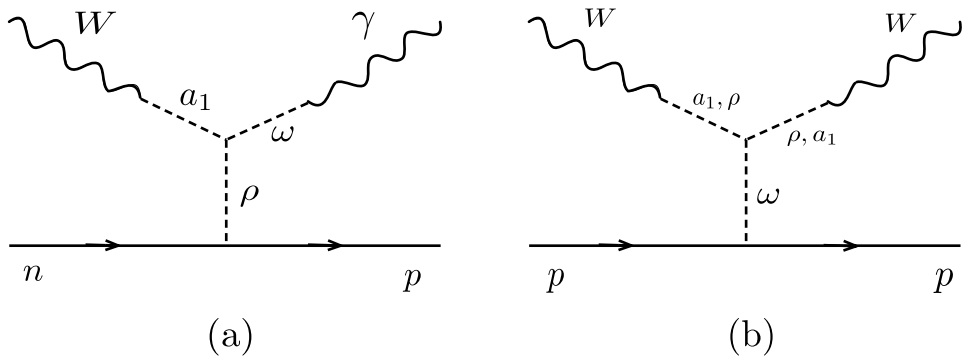

Figure 3.18: Vector meson exchange diagrams for (a) $F_3^{(0)}$ and (b) $F_3^{\nu p(\bar{\nu}p)}$ which can occur in the Regge region. The two possible combinations in (b) are topologically equivalent, resulting in a symmetry factor of 2 while the process in (a) is unique.

known to miss a fraction of the full cross section it aims to model, and so one can then consider extensions to it, such as the generalized vector dominance (GVDM) model [47]-[48]. The difference between VDM and GVDM structure

functions is:

$$F_i^{VMD}(Q^2) \sim \sum_V r_V \Big(\frac{m_V^2}{Q^2+m_V^2}\Big)^2, \tag{3.134}$$

$$F_i^{GVMD}(Q^2) \sim \sum_V r_V \Big(\frac{m_V^2}{Q^2+m_V^2}\Big)^2 \Big(1+\xi_V \frac{Q^2}{m_V^2}\Big) + r_C\Big[(1-\xi_C)\frac{m_0^2}{Q^2+m_0^2} + \xi_C \frac{m_0^2}{Q^2}\ln\Big(1+\frac{Q^2}{m_0^2}\Big)\Big], \tag{3.135}$$

$$r_C = 1 - \sum_V r_V. \tag{3.136}$$

The generalized model introduces 3 more fitting parameters beyond the VMD model. As we will see later, the full parameter space of GVDM applied to $F_{3,Reg}^{(0)}$ will be much more than necessary to fit to the available data. As the data which constrains this structure function is rather poor, we will choose only a slight extension to the VMD model by simply setting $r_C = 0$, while letting (r_V, ξ_V) remain free parameters to finalize our model:

$$F_{3,Reg}^{(0)}(W^2,Q^2) = \frac{f(1+gQ^2)\Theta(W^2-W_{th}^2)}{(1+Q^2/m_\rho^2)(1+Q^2/m_{a_1}^2)}\big[1-e^{\frac{W_{th}^2-W^2}{\Lambda_{th}^2}}\big]\Big(\frac{\nu}{\nu_0}\Big)^{\alpha_0^\rho}, \tag{3.137}$$

$$W_{th}^2 = (M+m_\pi)^2. \tag{3.138}$$

One of the key differences between the above model and that used in [29] is that Seng's W-threshold is at 2 pions while his single pion production amplitude is calculated separately using heavy-baryon chiral perturbation theory (χPT) – a small contribution $\sim 10^{-4}$ to $\Box_A^{\gamma W}$. One immediate issue with using (3.137) is that there is no direct data which constrains $F_{3,Reg}^{(0)}$.

In order to find the free parameters (f, g), we can relate the $F_3^{(0)}$ structure function to another one which does have data: $F_3^{\nu p+\bar{\nu}p}$. It is defined as the average of the PDG's $(F_3^{W^-} + F_3^{W^+})/2$ which are depicted in Figure 3.19. Next, note that in the parton model we have:

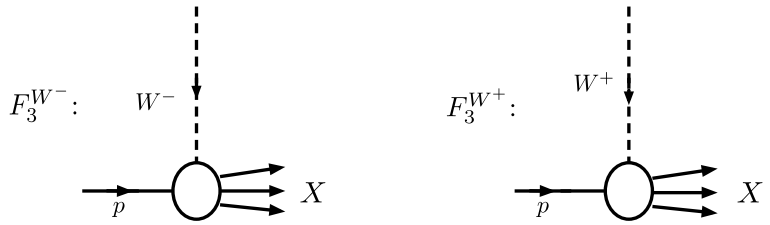

Figure 3.19: Neutrino and antineutrino structure function diagrams. The lepton current (not shown) involves the interaction between a lepton and its neutrino partner.

$$F_3^{(0)} = \frac{u_{\rm v} - d_{\rm v}}{3}, \tag{3.139}$$

$$F_3^{\nu p+\bar{\nu}p} = u_{\rm v} + d_{\rm v}. \tag{3.140}$$

If we make the rough assumption then that $u_{\rm v} \approx 2d_{\rm v}$ we find the simple relationship in the DIS region:

$$\frac{F_3^{\nu p+\bar{\nu}p}}{F_3^{(0)}} \approx 9. \tag{3.141}$$

In fact, it was found by the authors of [29] that this ratio is approximately satisfied in the VMD framework as well (except that rather than a 9, their factor is 36 due to a different normalization convention of $F_3^{(0)}$). Hence we can use (3.141) as a link between our sought $F_3^{(0)}$ and available data on $F_3^{\nu p+\bar{\nu}p}$ at

low Q^2 to determine our free parameters (f, g). This data will come from the 1st Nachtmann moment of the neutrino(+antineutrino) structure function, which is defined as:

$$M_3^{\nu p+\bar{\nu}p}(1,Q^2) = \frac{2}{3}\int_0^1 dx \frac{\xi}{x^2}\Big(2x - \frac{\xi}{2}\Big)F_3^{\nu p+\bar{\nu}p}(x,Q^2), \tag{3.142}$$

$$\xi = \frac{2x}{1+\sqrt{1+4M^2x^2/Q^2}}. \tag{3.143}$$

Note that as $M^2/Q^2 \to 0$ we have $\xi \to x$ and the 1st Nachtmann moment just reduces to the traditional Cornwall-Norton moment: $\int_0^1 dx F_3(x,Q^2)$. The most recent data on $M_3^{\nu p+\bar{\nu}p}(1,Q^2)$ at low Q^2 can be found in [50]; which we will use to constrain the moment. Utilizing (3.142) at low Q^2 forces one to know $F_3^{\nu p+\bar{\nu}p}$ for all x and for our purposes we will decompose this structure function into 3 distinct parts:

$$F_3^{\nu p+\bar{\nu}p}(f,g,x,Q^2)|_{\text{low}Q^2} = F_{3,el}^{\nu p+\bar{\nu}p}(x,Q^2)+F_{3,res}^{\nu p+\bar{\nu}p}(x,Q^2)+9F_{3,Reg}^{(0)}(f,g,x,Q^2), \tag{3.144}$$

where (3.141) has been deliberately applied to give the last term. The elastic structure function can be derived in terms of nucleon form factors just as $F_{3,el}^{(0)}$ was to get:

$$F_{3,el}^{\nu p+\bar{\nu}p}(x,Q^2) = \frac{1}{2}[G_M^p(Q^2) - G_M^n(Q^2)]G_A(Q^2)x\delta(1-x), \tag{3.145}$$

where we will use the same form factor parameterizations as those which entered the $\Box^{\gamma W}_{A,el}$ calculation, only with an isovector combination this time. The dominant resonance which enters $F_{3,res}^{\nu p+\bar{\nu}p}$ is the $\Delta(1232)$. We use the form factor parameterization of Lalakulich [22] once again to model this new structure function. Considering addition of isospin within the subprocesses: $\bar{\nu} : pW^- \to \Delta^0$ and $\nu : pW^+ \to \Delta^{++}$ one can show that the latter is an example of a stretched state $|I, m_I\rangle = |\frac{3}{2}, +\frac{3}{2}\rangle$, while the former has final state $|\frac{3}{2}, -\frac{1}{2}\rangle$. Since the Clebsch-Gordon coefficient $C(\frac{3}{2}, 1, \frac{1}{2}; -\frac{1}{2}, 1, \frac{1}{2}) = 1/\sqrt{3}$ we have that:

$$F_{3,\Delta}^{\bar{\nu}p} = \frac{1}{3} F_{3,\Delta}^{\nu p}, \tag{3.146}$$

and we find that $F_{3,res}^{\nu p+\bar{\nu}p} = \frac{2}{3} F_{3,\Delta}^{\nu p}$, as the two structure functions differ by a minus sign. We have also assumed that the other higher mass resonances are negligible compared to the Δ. Since we have kept agreement with PDG convention, we can once again use (3.75), which is even more obvious now as both sides of the equation are applied to neutrino scattering. This allows us to find our sought structure function, which is:

$$\begin{aligned} F_{3,res}^{\nu p+\bar{\nu}p} = &-\frac{2\nu}{M}\frac{m_\Delta \Gamma_\Delta}{\pi}\frac{4}{3}\frac{1}{(W^2 - m_\Delta^2)^2 + m_\Delta^2 \Gamma_\Delta^2} \\ &\times \left\{ \frac{1}{m_\Delta}\Big[-\frac{C_3^V C_4^A}{M}(m\nu - Q^2) - C_3^V C_5^A M \Big](2m_\Delta^2 + 2M m_\Delta + Q^2 - M\nu) \right. \\ &\left. + (M\nu - Q^2)\Big[-\frac{C_4^V C_4^A}{M^2}(M\nu - Q^2) - C_4^V C_5^A \Big] \right\}. \end{aligned} \tag{3.147}$$

With this now, (3.144) can then be inserted into (3.142) and a least-squares fit can be performed on the 2 parameters (f, g). At very high Q^2, the Nachtmann moment in (3.142) is dominated by the GLS sum rule where:

$$\begin{aligned} M_3^{\nu p+\bar{\nu}p}(1,Q^2)|_{\text{high}Q^2} &= \int_0^1 dx F_3^{\nu p+\bar{\nu}p}(x,Q^2) \\ &\approx 3\Big(1-\tfrac{\alpha_S(Q^2)}{\pi}\Big), \end{aligned} \tag{3.148}$$

to NLO in α_S. As $Q^2 \to 2\text{GeV}^2$, (3.148) no longer accurately predicts the moment and it must be computed explicitly via (3.142). At $Q^2 = 2\text{GeV}^2$, this moment is:

$$M_3^{\nu p+\bar{\nu}p}(1,2\text{GeV}^2) = \frac{2}{3}\int_0^1 dx \frac{\xi}{x^2}\Big(2x-\frac{\xi}{2}\Big)(u_{\text{v}}^{NLO}+d_{\text{v}}^{NLO})|_{Q^2=2\text{GeV}^2} = 2.49\pm.01, \tag{3.149}$$

where we have used the CJ15 PDFs. Since the valence distributions are globally well-constrained by DIS data, there is no need to compute this moment with other PDF sets. (3.149) is chosen as another data point with which the $M_3^{\nu p+\bar{\nu}p}(1,Q^2,f,g)$ fit should include as this moment is well-described by PDFs for $Q^2 \geq 2\text{GeV}^2$. The fit itself is plotted along with its uncertainty band in Figure 3.20. The result of that fit is:

$$f = 0.80 \pm .03, \tag{3.150}$$

$$g = 0.63 \pm .10\text{GeV}^{-2}. \tag{3.151}$$

Finally, one can then insert these fit parameters and integrate $F^{(0)}_{3,Reg}$ over the whole Regge region to find the contribution to the γW box. Doing so yields:

$$\Box^{\gamma W}_{A,Reg} = (.37 \pm .10) \times 10^{-3} \tag{3.152}$$

A few remarks worth mentioning here are the following:

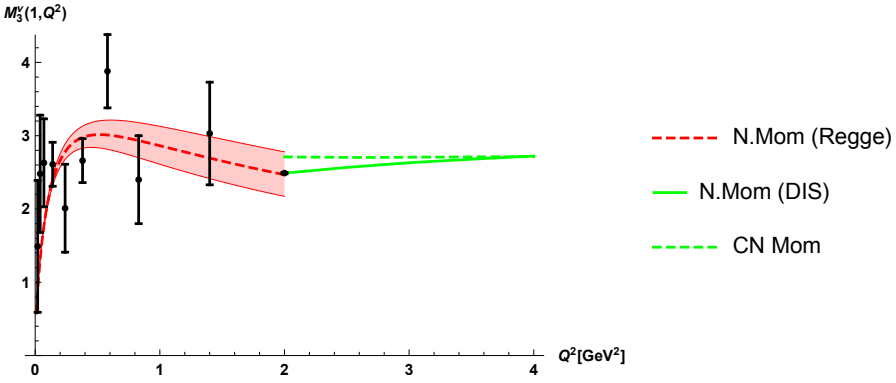

Figure 3.20: Fitting the Regge model (red) of (3.137) to the data (black) provided in [50] for the neutrino scattering Nachtmann moment $M_3^{\nu p+\bar{\nu}p}$, which has been matched to the DIS moment (green) at the boundary. At high Q^2 both the CN and Nachtmann moments are compared.

- Although the DIS prediction of $M_3^{\nu p+\bar{\nu}p}(1, 2\text{GeV}^2)$ has a very large weight, it cannot decrease the large uncertainty of the fit ($f \pm \Delta f, g \pm \Delta g$). This is because the poor low Q^2 data (in both statistics and weights) limits the certainty of the 2-parameter fit.

- Secondly, the Cornwall-Norton moment clearly over predicts $M_3^{\nu p+\bar{\nu}p}(1, Q^2)$ around $2\text{GeV}^2 \leq Q^2 \leq 3\text{GeV}^2$. This difference may indicate the presence of higher-twist effects which have not been considered.

Also, shown in Figures 3.21 & 3.22 is the $F_{3,Reg}^{(0)}$ structure function at the boundaries of the Regge Region as compared to the neighbouring models. The matching to the DIS model has "washed" out a precise matching at every W^2 value, as only the Nachtmann moments have been equated at the boundary, rather than the structure functions themselves.

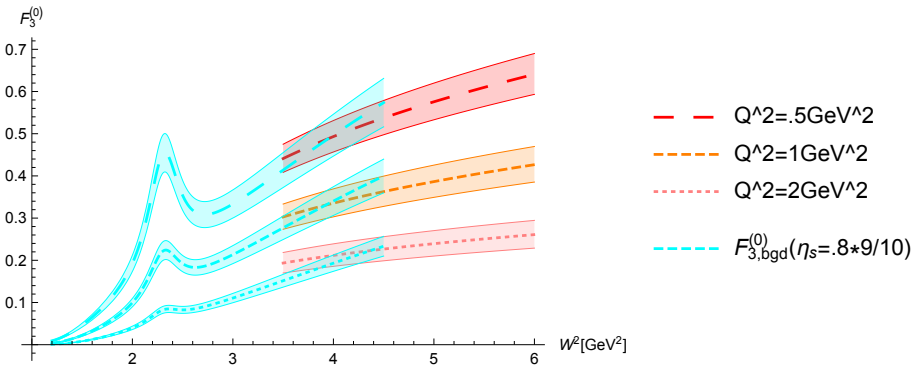

Figure 3.21: Comparison of the Regge and background + resonance $F_3^{(0)}$ structure functions at $W^2 = 4\text{GeV}^2$.

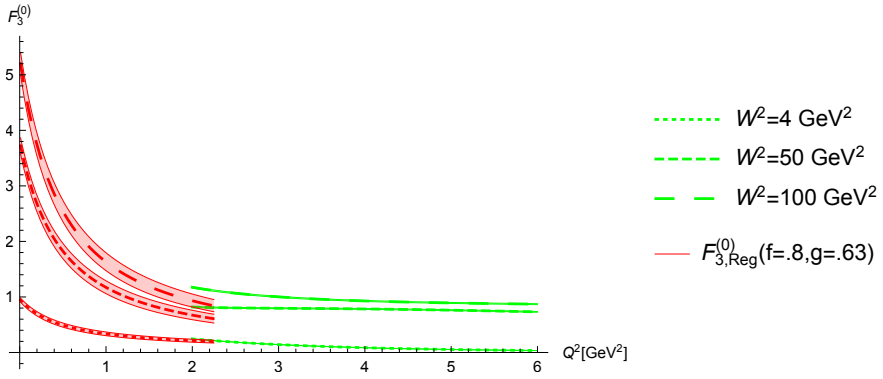

Figure 3.22: Comparison of the Regge and DIS $F_3^{(0)}$ structure functions at $Q^2 = 2\text{GeV}^2$.

3.8 Total $\Box_A^{\gamma W}$

The sum of all the $\Box_A^{\gamma W}$ contributions computed in section 3 (SBM) is summarized into Table 3.8.1 where it is also compared to the results of Seng *et al.* (SGRM). It is this total box correction which will then effectively replace (2.5).

$\Box_A^{\gamma W}(\times 10^{-3})$	SBM	SGRM	MS
elastic	1.04(7)	1.06(6)	–
resonance	0.04(2)	0.00(0)	–
DIS + high-Q^2 bgd	2.27(0)	*2.17(0)	–
πN	0.00	0.12	–
Regge	0.37(10)	0.31(8)	–
low-Q^2 bgd	0.16(2)	0.13	–
total	3.88(13)	3.79(10)	3.26(19)

Table 3.3: γW box corrections from 3 separate groups. SBM represents this work, SGRM is taken from [29]-[30], and MS is from [14]. *The SGRM DIS contribution has been calculated at α_{EM} fixed at the Thomson limit.

As can be seen from the table, the consequence of applying these "state-of-the-art" dispersive techniques to the semileptonic γW box tends to increase the central value of this radiative correction by at least 16%. The consequences of this jump in value will be discussed in detail in section 5. It's also interesting to note that the absolute uncertainty of $\Box_A^{\gamma W}$ has improved by nearly a factor of 2. Scanning through the various contributions of Table 3.3, I make the following comments:

- The elastic contributions are highly complementary as this portion is highly unambiguous. What differences are present are essentially due to a particular choice of slightly different calculation input.

- The resonance region is small, but not completely negligible. We put our number in to the nearest 10^{-5} for the record.

- Both authors essentially agree for the DIS contribution, as once one inserts the running EM fine structure constant into the SGRM prediction, the result is a 4% enhancement – recovering our number.

- The π_N contribution is absent from our model, however, the sum (π_N + Regge + $\text{bgd}_{\text{low}Q^2}$) should ideally agree, which they essentially do:

$$(\pi_N + \text{Regge} + \text{bgd}_{\text{low}Q^2})|_{SBM} = .53(10) \times 10^{-3} \tag{3.153}$$

$$(\pi_N + \text{Regge} + \text{bgd}_{\text{low}Q^2})|_{SGRM} = .56(8) \times 10^{-3} \tag{3.154}$$

Taking the differences into account, the two separate computations do agree with each other within their uncertainties. Together, they provide strong support for replacing the Marciano and Sirlin Result from 2006.

Chapter 4

Radiative Corrections to $Q_W(p)$

Let us now turn our attention to the other observable of interest in this dissertation: the weak charge of the proton. The process and its Born level treatment was discussed in chapter 1.4 and now we will be looking at its 1 loop corrections. Once all of the Feynman diagrams are defined, we will proceed and calculate each one's effect on $Q_W(p)$. Much of this work has already been done, but we will be re-evaluating all of these corrections in two limits: the Thomson limit ($Q^2 = 0$) and the scattering limit ($Q^2 \gg m_e^2$). I have also decided to use a process-independent and gauge-invariant definition of the weak mixing angle, which will be computed in explicit detail. The results of this work will be compared to a recent measurement of the proton's weak charge [53] at the end of the chapter.

4.1 The 1 Loop Formula

At the tree level, $e^- p \to e^- p$ scattering is mediated by the exchange of a single photon or Z-boson as shown in Figure 1.1 and leads to the relation (1.32), where the LO prediction of the proton's weak charge is:

$$Q_W^{LO}(p) = 1 - 4\sin^2\theta_W = 0.0688, \tag{4.1}$$

which is customarily taken in the Thomson limit $Q^2 \to 0$. Our goal now is to modify (4.1) to include all 1 loop RCs. This was done in [51] (EKR), which has since become the standard parameterization adopted:

$$Q_W^{NLO}(p)|_{\text{EKR}} = [\rho_{NC} + \Delta_e][1 - 4\sin^2\theta_W(0) + \Delta_e'] + \Box_{WW} + \Box_{ZZ} + \Box_{\gamma Z}, \tag{4.2}$$

where Δ_e, Δ_e' denote lepton vertex corrections, $\sin^2\theta_W$ originates from SE corrections to the mixed $\gamma - Z$ boson, ρ_{NC} contains SE corrections to the Z & $W-$bosons, and the $\Box$'s denote their respective box corrections. The classes of diagrams for all of these corrections are summarized in Figure 4.1. In the pages that follow, we will be taking a close re-examination of all the corrections in (4.2) and in doing so, we will resort to modifying the EKR expression slightly.

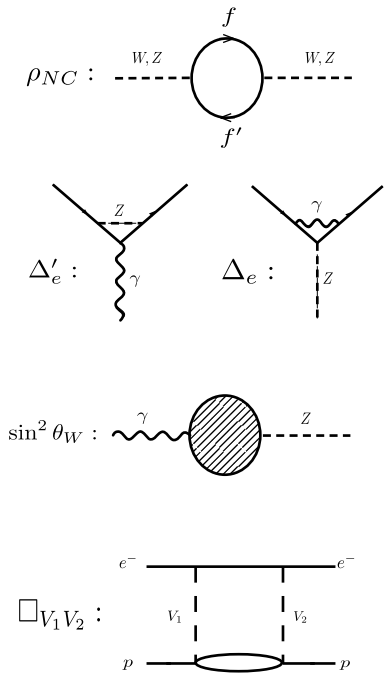

Figure 4.1: 1 Loop Feynman diagrams which correct the LO prediction to $Q_W(p)$ in the $e^-p \to e^-p$ process.

4.2 ρ_{NC} Correction

At the tree level, the ratio of the neutral to charged current is $\rho_{NC}^{LO} = M_W^2/(M_Z^2 \cos^2\theta_W) = 1$. However, at the 1 loop level the masses of the heavy vector bosons get corrected by the SE diagrams in Figure 4.1. For the

W-boson, the dominant fermion loop is from the top and bottom quarks:

$$\Pi^{\mu\nu}_{WW}(q^2) \quad = \quad \mu \; \overset{W}{\overset{q}{\longrightarrow}} \; \overset{t,b}{\underset{b,t}{\overset{k+q}{\bigcirc}{}^{k}}} \; W \; \nu$$

$$= \left(\frac{-ig}{2\sqrt{2}}\right)(-1)\int \frac{d^4k}{(2\pi)^4}\frac{i}{(q+k)^2-m_t^2}\frac{i}{k^2-m_b^2}\times$$

$$\mathrm{Tr}[\gamma^\mu(1-\gamma_5)(\not{k}+\not{q}+m_t)\gamma^\nu(1-\gamma_5)(\not{k}+m_b)]$$

$$= \Pi^T_{WW}\left(g^{\mu\nu}-\frac{q^\mu q^\nu}{q^2}\right)+\Pi^L_{WW}\frac{q^\mu q^\nu}{q^2}, \tag{4.3}$$

$$\Rightarrow \Pi^T_{WW}(q^2) = \frac{\sqrt{2}G_F M_W^2}{16\pi^2}\frac{4}{3}\Bigg\{m_t^2+m_b^2-\frac{q^2}{3}+A_0(m_b)+A_0(m_t)$$

$$-\frac{m_t^2-m_b^2}{2q^2}[A_0(m_t)-A_0(m_b)]+\frac{2q^4-q^2(m_t^2-m_b^2)-(m_t^2-m_b^2)^2}{2q^2}B_0(q^2;m_t,m_b)\Bigg\}. \tag{4.4}$$

We would actually like to know our correction at $q^2 = 0$, thus we can take that limit here to find:

$$\Pi^T_{WW}(0) = \frac{\sqrt{2}G_F M_W^2}{16\pi^2}\frac{2\left(m_t^4\ln\frac{m_t^2}{\mu^2}-m_b^4\ln\frac{m_b^2}{\mu^2}\right)}{m_t^2-m_b^2}-(m_t^2+m_b^2). \tag{4.5}$$

Repeating this analysis for the Z-boson case, we get:

$$\Pi^T_{ZZ}(0) = \frac{\sqrt{2}G_F M_Z^2}{16\pi^2\cos^2\theta_W}\left(2m_t^2\ln\frac{m_t^2}{\mu^2}+2m_b^2\ln\frac{m_b^2}{\mu^2}\right). \tag{4.6}$$

Since (4.5) and (4.6) corrects the masses of their respective vector bosons, their effect on ρ_{NC} is exactly:

$$\rho_{NC}^{NLO} = \frac{M_W^2\left(1+\frac{\Pi_{WW}^T(0)}{M_W^2}\right)}{M_Z^2\cos^2\theta_W\left(1+\frac{\Pi_{ZZ}^T(0)}{M_Z^2}\right)} \approx \rho_{NC}^{LO}\left(1+\frac{\Pi_{WW}^T(0)}{M_W^2}-\frac{\Pi_{ZZ}^T(0)}{M_Z^2}\right), \quad (4.7)$$

$$= \rho_{NC}^{LO}(1+\Delta\rho_{NC}), \quad (4.8)$$

and the $\mathcal{O}(G_F)$ correction can be simplified to:

$$\Delta\rho_{NC} = \frac{\Pi_{WW}^T(0)}{M_W^2} - \frac{\Pi_{ZZ}^T(0)}{M_Z^2} = \frac{\sqrt{2}G_F}{16\pi^2}\left(m_t^2+m_b^2-\frac{2m_t^2m_b^2}{m_t^2-m_b^2}\ln\frac{m_t^2}{m_b^2}\right). \quad (4.9)$$

ρ_{NC} is the ratio of neutral to charged currents in EW theory and it is a gauge-invariant quantity. The RHS of (4.9) is zero if $m_t = m_b$, and the term inside the round brackets is sensitive to the mass splitting $m_t^2 - m_b^2 \approx m_t^2$, thus the contribution from the other quark doublets is highly suppressed.

4.3 Δ_e Correction

The bare eeZ vertex is given in Appendix A in terms of the standard neutral current $V-A$ coupling $\sim \gamma^\mu(g_V^e - g_A^e\gamma_5)$. Δ_e is the correction to this vertex when a massless photon is exchanged between the electron lines. To begin calculating this effect, we start by applying the same Feynman rules with this virtual photon added in:

Λ_μ^{Zee} =

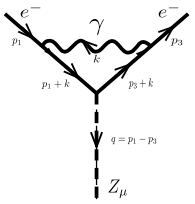

$$= \frac{i^5 e^2 g}{2\cos\theta_W}\int \frac{d^4k}{(2\pi)^4}\frac{\bar{u}(p_3)\gamma_\alpha(\not{p}_3+\not{k}+m)(g_V^e\gamma_\mu - g_A^e\gamma_\mu\gamma_5)(\not{p}_1+\not{k}+m)\gamma_\alpha u(p_1)}{[(p_1+k)^2-m^2](k^2-\lambda^2)[(p_3+k)^2-m^2]}. \quad (4.10)$$

Let's first look at the vector coupling $\sim g_V^e$. We will also suppress the prefactor $ig/2\cos\theta_W$ in front of the integral sign, as this will be common to the bare vertex. Then one will find that:

$$\begin{aligned}\Lambda_\mu^{Zee}|_V = \frac{\alpha}{4\pi}\bar{u}(p_3)\Big\{&\gamma_\mu[(4m^2-2q^2)C_0(m^2,m^2,q^2;m,\lambda,m)\\ &+4B_0(m^2;m,\lambda)-3B_0(q^2;m,m)-1]\\ &+2m(p_1^\mu+p_3^\mu)[B_0(0;m,\lambda)-2B_0(m^2;m,\lambda)\\ &+B_0(q^2;m,m)+1]\Big\}g_V^e.\end{aligned} \quad (4.11)$$

This vertex is traditionally decomposed into the following form:

$$\Lambda_\mu^{Zee}|_V = \bar{u}(p_3)\left[\gamma_\mu F_1(q^2) + \frac{i\sigma_{\mu\nu}}{2m}q^\nu F_2(q^2)\right]u(p_1), \tag{4.12}$$

whilst our expression in (4.11) is of the form $\bar{u}[\gamma_\mu G(q^2) + (p_1 + p_3)_\mu H(q^2)]u$. To help us get something resembling (4.12) we can use the Gordon identity, which states that:

$$\bar{u}(p)(p' + p)_\mu u(p) = \bar{u}(p')[2m\gamma_\mu - i\sigma_{\mu\nu}q^\nu]u(p), \tag{4.13}$$

and apply it to the 2nd term in (4.11). This reveals that we really do have (4.12), where:

$$F_1(q^2) = G(q^2) + 2mH(q^2), \tag{4.14}$$

$$F_2(q^2) = -2mH(q^2). \tag{4.15}$$

Let's look first at our F_2 term which is the origin of the so-called anomalous magnetic moment. From (4.11), it is predicted to be:

$$
\begin{aligned}
F_2(q^2) &= -2m\Big(\frac{\alpha}{4\pi}\Big)\Big(\frac{2m}{4m^2-q^2}\Big)[B_0(0;m,\lambda)-2B_0(m^2;m,\lambda) \\
&\quad +B_0(q^2;m,m)+1]g_V^e \\
&= -\frac{\alpha}{4\pi}\Big(\frac{4m^2}{4m^2-q^2}\Big)[B_0(0;m,0)-2B_0(m^2;m,0) \\
&\quad +B_0(q^2;m,m)+1]g_V^e \\
&\approx -\frac{\alpha}{4\pi}\Big(\frac{4m^2}{4m^2-q^2}\Big)\Bigg[2\Delta_\epsilon-2\Big(\Delta_\epsilon-\ln\frac{m^2}{\mu^2}+2\Big)-2\ln\frac{m^2}{\mu^2} \\
&\quad +\frac{t}{6m^2}+2\Bigg]g_V^e \\
&= -\frac{\alpha}{4\pi}\Big(\frac{24m^2-2q^2}{12m^2-3q^2}\Big)g_V^e, \\
&\Rightarrow \quad F_2(0) = -\frac{\alpha}{2\pi}g_V^e, \qquad (4.16)
\end{aligned}
$$

which is nothing more than the famous Schwinger moment which is found in an analogous correction in pure QED [43]. As it stands, $F_1(q^2)$ is UV and IR divergent, and we must renormalize the Zee vertex in order to attain a physical result for it. We can use the results of Appendix G on renormalized perturbation theory to rid ourselves of this UV divergence. Doing so leads to our renormalized vertex:

$$\hat{\Lambda}_\mu^{Zee}|_V = \bar{u}(p_3)\left[\gamma_\mu \hat{F}_1(q^2) + \frac{i\sigma_{\mu\nu}}{2m}q^\nu F_2(q^2)\right]u(p_1), \tag{4.17}$$

$$\hat{F}_1(q^2) = G(q^2) + 2mH(q^2) + \delta Z_\psi, \tag{4.18}$$

$$Z_\psi = 1 - \frac{A_0(m)}{m^2} + 4m^2 B_0'(m^2; m, \lambda), \tag{4.19}$$

and F_2 is unaffected in the renormalization process. Next, we should take the $q^2 \to 0$ limit and confirm that $\hat{F}_1(0) = 0$. We've already evaluated the middle term in (4.18) – putting the other 2 terms in gives us:

$$\begin{aligned}
\hat{F}_1(0) = \tfrac{\alpha}{4\pi}\{&4m^2[B_0'(m^2; m, \lambda) - C_0(m^2, m^2, 0; m, \lambda, m)] \\
&-3B_0(0; m, m) + 2B_0(m^2, m, 0) + B_0(0; m, 0) - 1\}g_V^e \\
= \tfrac{\alpha}{4\pi}\Big\{ &-4 - 3\Big(\Delta_\epsilon - \ln\tfrac{m^2}{\mu^2}\Big) + 2\Big(\Delta_\epsilon + 2 - \ln\tfrac{m^2}{\mu^2}\Big) + \Delta_\epsilon + 1 - \ln\tfrac{m^2}{\mu^2} - 1\Big\}g_V^e \\
&= 0,
\end{aligned} \tag{4.20}$$

as expected by the renormalization procedure. Next let's turn our attention to the axial part of (4.10) which is:

$$\begin{aligned}\Lambda_\mu^{Zee}|_A = \frac{\alpha}{4\pi}\bar{u}_e\gamma_\mu\gamma_5 u_e\Bigg\{&(4m^2-q^2)C_0(m^2,m^2,q^2;m,\lambda,m)-2\\ &+4\frac{(2m^2-q^2)}{4m^2-q^2}B_0(m^2;m,\lambda)+\frac{(3q^2-4m^2)}{4m^2-q^2}B_0(q^2;m,m)\Bigg\}g_A^e\\ +\frac{\alpha}{4\pi}\bar{u}_e\gamma_5(p_1-p_3)_\mu u_e\Bigg\{&\frac{1}{q^2}B_0(0;m,\lambda)-\frac{2}{4m^2-q^2}B_0(m^2;m,\lambda)\\ &+\frac{(3q^2-4m^2)}{q^2(4m^2-q^2)}B_0(q^2;m,m)-\frac{1}{q^2}\Bigg\}g_A^e.\end{aligned} \tag{4.21}$$

The $\bar{u}_e\gamma_5 u_e$ correction which is proportional to $(p_1-p_3)_\mu$ is inconsequential to us as this current disappears in the PV amplitude. Now let's look at the $\gamma_\mu\gamma_5$ term at $q^2\to 0$, where it reduces to:

$$\begin{aligned}\Lambda_\mu^{Zee}|_A(\gamma_\mu\gamma_5\text{ term}) \to \frac{\alpha}{4\pi}\bar{u}_e\gamma_\mu\gamma_5 u_e[&4m^2C_0(m^2,m^2,0;m,\lambda,m)-2\\ &+2B_0(m^2;m,\lambda)-B_0(0;m,m)]g_A^e.\end{aligned} \tag{4.22}$$

Just like the γ_μ term in $\Lambda_\mu^{Zee}|_V$ required the addition of the counterterm $+Z_\psi\gamma_\mu$, so too will this term, as it is the net $(g_V^e\gamma_\mu + g_A^e\gamma_\mu\gamma_5)$ vertex which is getting renormalized. Thus, after renormalization we will get:

$$\begin{aligned}
\Lambda_\mu^{Zee}|_A(\gamma_\mu\gamma_5 \text{ term})|_{q^2=0} &= \frac{\alpha}{4\pi}\bar{u}_e\gamma_\mu\gamma_5 u_e[4m^2C_0(m^2,m^2,0;m,\lambda,m) - 2 \\
&\quad +2B_0(m^2;m,\lambda) - B_0(0;m,m) - B_0(0;m,m) \\
&\quad +4m^2B_0'(m^2;m,\lambda)]g_A^e \\
&= \frac{\alpha}{4\pi}[4m^2(C_0 + B_0') + 2B_0(m^2;m,0) \\
&\quad -2B_0(0;m,m) - 2]g_A^e \\
&= -\frac{\alpha}{2\pi}g_A^e, \qquad (4.23)
\end{aligned}$$

which is exactly equal and opposite to the correction to the vector correction in (4.16). This is actually no coincidence, as the CVC hypothesis states that the $V-A$ structure of the vertex must be preserved, even after the inclusion of radiative corrections. (4.23) will actually change sign in the PV correction A_{LR} as follows:

$$\begin{aligned}
\delta Q_W(p) &\sim \delta A_{LR} \sim \frac{M^{PV}_{Z,\gamma-loop}}{M^{PV}_Z}, && (4.24)\\
M^{PV}_{Z,\gamma-loop} &\sim g^e_A\left[\bar{u}_e\gamma_\mu\gamma_5\Big(-\frac{\alpha}{2\pi}\Big)P_L u_e - \bar{u}_e\gamma_\mu\gamma_5\Big(-\frac{\alpha}{2\pi}\Big)P_R u_e\right]\\
&= -g^e_A\Big(\frac{\alpha}{2\pi}\Big)[\bar{u}_e\gamma_\mu\gamma_5 P_L u_e - \bar{u}_e\gamma_\mu\gamma_5 P_R u_e]\\
&= -g^e_A\Big(\frac{\alpha}{2\pi}\Big)\left[\mathrm{Tr}\Big(\not{p}\gamma_\mu\gamma_5\frac{(1-\gamma_5)}{2}\Big) - \mathrm{Tr}\Big(\not{p}\gamma_\mu\gamma_5\frac{(1+\gamma_5)}{2}\Big)\right]\\
&= -\frac{g^e_A}{2}\Big(\frac{\alpha}{2\pi}\Big)[-\mathrm{Tr}(\not{p}\gamma_\mu 1) - \mathrm{Tr}(\not{p}\gamma_\mu 1)]\\
&= g^e_A\Big(\frac{\alpha}{2\pi}\Big)(4p_\mu), && (4.25)\\
M^{PV}_Z &\sim g^e_A(4p_\mu). && (4.26)
\end{aligned}$$

Therefore, our correction to the proton's weak charge in the Thomson limit is:

$$\delta Q_W(p) = \frac{\alpha}{2\pi} \equiv \Delta_e. \tag{4.27}$$

This expression was first calculated by Marciano & Sirlin [78] as an atomic parity violation correction - valid in the Thomson limit. However, it will be important to look at all of these corrections in the scattering limit at which $q^2 \gg m_e^2$. This is technically the limit in which experiments such as Qweak [54] are done, where $\langle Q^2\rangle \approx 0.025\mathrm{GeV}^2$. Recall that

$$F_2(q^2) = \frac{\alpha}{4\pi}\left(\frac{4m^2}{4m^2-q^2}\right)[B_0(0;m,0) - 2B_0(m^2;m,\lambda) + B_0(q^2;m,m) + 1], \tag{4.28}$$

and from this general expression, we can take the scattering limit:

$$\begin{aligned} F_2(q^2) &\rightarrow \frac{\alpha}{4\pi}\left(\frac{4m^2}{4m^2-q^2}\right)\left[\Delta_\epsilon + 1 - \ln\frac{m^2}{\mu^2} - 2\left(\Delta_\epsilon + 2 - \ln\frac{m^2}{\mu^2}\right)\right. \\ &\quad \left. +\Delta_\epsilon - \ln\frac{m^2}{\mu^2} + 2 + \ln\Big(\frac{-m^2}{q^2}\Big) + 1\right] \\ &= \frac{\alpha}{4\pi}\left(\frac{4m^2}{4m^2-q^2}\right)\ln\Big(\frac{-m^2}{q^2}\Big) \\ &= 4m^2\frac{\alpha}{4\pi}\lim_{t\to\infty}\frac{\ln(-m^2/t)}{4m^2-t} \\ &= 0. \end{aligned} \tag{4.29}$$

Next, recall the $\gamma_\mu g_V^e$ correction which was:

$$\begin{aligned} \hat{F}_1(q^2) = \frac{\alpha}{4\pi}[&-(2q^2-4m^2)C_0(m^2,m^2,q^2;m,\lambda,m) + 4B_0(m^2;m,\lambda) \\ &-3B_0(q^2;m,m) - 2 - B_0(0;m,m) + 4m^2B_0'(m^2;m,\lambda)]g_V^e. \end{aligned} \tag{4.30}$$

This expression is somewhat complicated in the scattering limit, and the details are not terribly illuminating. Unlike the Thomson limit, its IR divergence is quite present now, and is of the form:

$$\hat{F}_1(q^2 \gg m^2) \sim \frac{\alpha}{4\pi} g_V^e \ln\frac{Q^2}{m^2} \ln\frac{\lambda^2}{m^2}. \tag{4.31}$$

This IR divergence gets canceled when combined with the other IR-divergent amplitudes and the result is simply:

$$\hat{F}_1(q^2 \gg m^2) \to 0. \tag{4.32}$$

Finally, let's compare this to the $\gamma_\mu\gamma_5$ correction in the axial vertex. Earlier we had:

$$\begin{aligned}
\hat{G}_1(q^2) &= (4m^2 - q^2)C_0 - 2 + 4\frac{2m^2 - q^2}{4m^2 - q^2} B_0(m^2; m, 0) \\
&\quad + \frac{(3q^2 - 4m^2)}{4m^2 - q^2} B_0(q^2; m, m) - B_0(0; m, m) + 4m^2 B_0'(m^2; m, \lambda), \\
&\to q^2 C_0 - 2 + 4B_0(m^2; m, 0) - 3B_0(q^2; m, m) - B_0(0; m, m) \\
&\quad + 4m^2 B_0'(m^2; m, \lambda) \\
&= \hat{F}_1(q^2 \gg m^2) \to 0.
\end{aligned} \tag{4.33}$$

Just as in the Thomson limit, we see that the $V-A$ vertex gets a common correction, which in this case, gets canceled by other diagrams. We can always count on the cancellation of IR divergences such as those in (4.31) as is guaranteed by the Bloch-Nordsieck theorem [44], which states that all IR divergences get cancelled in any observable in QED. To summarize our findings, the net effect of the vertex diagram shown in (4.10) leads to the

following correction to $Q_W(p)$:

$$\Delta_e = \begin{cases} \frac{\alpha}{2\pi}, & q^2 = 0 \\ 0, & q^2 \gg m_e^2 \end{cases} . \tag{4.34}$$

Technically this is quite a difference between the scattering and atomic limits, but in practice, the quantity $\frac{\alpha}{2\pi} \approx .00116$ is a 0.1% correction to the already small $Q_W(p) \approx .0708$. Hence it is hardly worth putting the finite Thomson limit into (4.2), and one can simply take this correction to be negligible:

$$\Delta_e \approx 0. \tag{4.35}$$

4.4 Δ'_e Correction

There is another leptonic vertex correction wherein the γee vertex has a Z-boson loop formed across the electron lines. The associated amplitude is given by:

$\Lambda_\mu^{\gamma ee} =$ 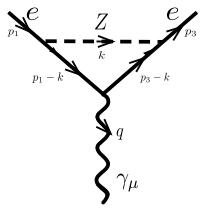

. (4.36)

In this case the photon only has a pure vector coupling. As we know, this bare vertex cannot form a PV amplitude alone. However, due to the axial-vector couplings between the Z-boson and electron, which occurs twice here, a PV effect is possible, and as we shall see this indeed happens. Employing the EW Feynman rules gives us:

$$\Lambda_\mu^{\gamma ee} = \frac{g^2}{4c_W^2}\int \frac{d^4k}{(2\pi)^4}\frac{1}{[(p_3-k)^2-m^2][(p_1-k)^2-m^2](k^2-M_Z^2)} \times \bar{u}_e(p_3)\gamma^\beta(g_V^e - g_A^e\gamma_5)(\not{p}_3 - \not{k} + m)\gamma_\mu(\not{p}_1 - \not{k} + m)\gamma_\beta(g_V^e - g_A^e\gamma_5)u(p_1). \quad (4.37)$$

After expanding the numerator via the contraction of the β's one will get 3 types of terms: ${g_V^e}^2, g_V^e g_A^e, {g_A^e}^2$. It is only the $V \times A$ terms which can generate a PV amplitude. This part of the numerator is given by:

$$\Lambda^{\gamma ee}_{\mu,PV} = -\frac{4g^2}{4c_W^2}\int \frac{d^4k}{(2\pi)^4}\frac{1}{[(p_3-k)^2-m^2][(p_1-k)^2-m^2](k^2-M_Z^2)} \times\bar{u}_e(p_3)[-2k_\mu \not{k}\gamma_5 + \gamma_\mu\gamma_5(k^2-m^2) + \not{p}_1\gamma_\mu\not{k}\gamma_5 + \not{k}\gamma_\mu\not{p}_3\gamma_5 - \not{p}_1\gamma_\mu\not{p}_3\gamma_5]u_e(p_1)g_V^e g_A^e. \quad (4.38)$$

We can then perform the loop integration explicitly followed by the PaVe reduction to obtain the somewhat lengthy expression:

$$\begin{aligned}\Lambda^{\gamma ee}_{\mu,PV} &= -\frac{g^2}{c_W^2}g_V^e g_A^e \bar{u}_e(p_1-p_3)_\mu\gamma_5 u_e \frac{1}{mq^2(4m^2-q^2)} \\ &\quad \big\{[q^2(2m^2+M_Z^2)-2m^2M_Z^2]B_0(m^2;m,M_Z) \\ &\quad +m^2(4-3q^2-2M_Z^2)B_0(q^2;m,m)+(q^2-4m^2)A_0(m) \\ &\quad +(4m^2-q^2)A_0(M_Z) \\ &\quad +2m^2(q^2+M_Z^2)(4m^2-M_Z^2-q^2)C_0(m^2,m^2,q^2;m,M_Z,m)\big\} \\ &\quad -\frac{g^2}{2c_W^2}g_V^e g_A^e \bar{u}_e\gamma_\mu\gamma_5 u_e \frac{1}{4m^2-q^2}\big\{(4q^2-8m^2+2M_Z^2)B_0(m^2;m,M_Z) \\ &\quad +(4m^2-3q^2-2M_Z^2)B_0(q^2;m,m) \\ &\quad +2(q^2+M_Z^2)(4m^2-M_Z^2-q^2)C_0\big\}. \end{aligned} \quad (4.39)$$

As we know, the matrix element $\bar{u}_e(p_1-p_3)_\mu\gamma_5 u_e$ cannot lead to a PV effect, and so we may neglect that term from now on. The $\gamma_\mu\gamma_5$ term does indeed lead to a $Q_W(p)$ correction, and our goal is to evaluate it in both the Thomson and scattering limits. In doing so, we must be careful not to forget the additional factor of $D(q^2)=\frac{1}{q^2}$ which comes from the photon propagator, as

it will be a crucial ingredient to attain the correct final limit. Continuing then, the $\gamma_\mu\gamma_5$ term in (4.39) is:

$$\Lambda^{\gamma ee}_{\mu,PV} = -\frac{g^2}{2c_W^2} g_V^e g_A^e \bar{u}_e \gamma_\mu \gamma_5 u_e \frac{1}{4m^2 - t}\big\{(-8m^2 + 2M_Z^2 + 4t)B_0(m^2; m, M_Z) \\ +(4m^2 - 2M_Z^2 - 3t)B_0(t; m, m) + 2(M_Z^2 + t)(4m^2 - M_Z^2 - t)C_0\big\}, \tag{4.40}$$

where $t \equiv q^2$. We can then use the results of Appendix G and take the Thomson limit $t \to 0$. In a somewhat pragmatic fashion, we can impose the renormalization condition $\Lambda^{\gamma ee}_\mu(t = 0) = 0$ by simply subtracting it at the $t = 0$ limit:

$$\hat{\Lambda}^{\gamma ee}_\mu = \Lambda^{\gamma ee}_\mu(t) - \Lambda^{\gamma ee}_\mu(0), \tag{4.41}$$

and from (4.40) we have:

$$\Lambda^{\gamma ee}_{\mu,PV}(0) = 2\left(4 + \Delta_e + \ln\frac{\mu^2}{m^2} - \frac{M_Z^2}{m^2}\right) + \left(\frac{4M_Z^2}{m^2} - \frac{M_Z^4}{m^4}\right)\ln\frac{m^2}{M_Z^2} \\ +2\left(2 - \frac{M_Z^2}{m^2}\right)\frac{M_Z^2}{m^2}\sqrt{1 - \frac{4m^2}{M_Z^2}}\ln\left(\frac{M_Z^2(1 + \sqrt{1 - 4m^2/M_Z^2})}{2mM_Z}\right). \tag{4.42}$$

While for small t, a Taylor series reveals that:

$$\begin{aligned}\Lambda^{\gamma ee}_{\mu,PV}(t) &\approx \Lambda^{\gamma ee}_{\mu,PV}(0) + \frac{t}{3(4m^8 - m^6M_Z^2)}\Bigg\{ -28m^6 - m^4M_Z^2 + 2m^2M_Z^2 \\ &+ 2(M_Z^4 - 12m^4)\sqrt{M_Z^4 - 4m^2M_Z^2}\ln\left(\frac{\sqrt{M_Z^4 - 4m^2M_Z^2} + M_Z^4}{2mM_Z}\right) \\ &+ (24m^6 - 14m^4M_Z^2 - 2m^2M_Z^4 + M_Z^6)\ln\left(\frac{m^2}{M_Z^2}\right)\Bigg\}. \qquad (4.43)\end{aligned}$$

It's here now that the photon propagator saves us after invoking (4.41), allowing us to get a non-zero result in the Thomson limit. Then taking the ratio with the Born amplitude gives us:

$$\begin{aligned}\Delta'_e &= -\frac{M_Z^2\alpha}{4\pi}D(t)\hat{\Lambda}^{\gamma ee}_{\mu}(t)|_{t\to 0} \\ &= \frac{\alpha}{4\pi}\frac{1}{3z^3(4z-1)}\Bigg\{(4z-1)[(6z^2 - 2z - 1)\ln z - z(7z+2)] \\ &\quad +2(1-12z^2)\sqrt{1-4z}\ln\left(\frac{\sqrt{1-4z}+1}{2\sqrt{z}}\right)\Bigg\}, \qquad (4.44)\end{aligned}$$

where we have defined the dimensionless quantity $z \equiv m^2/M_Z^2$. Since $z \ll 1$ we can then take a Taylor series around $z = 0$ to find:

$$\begin{aligned}\Delta'_e &\approx -\frac{\alpha}{18\pi}(1 - 6\ln z)(2)\Big(\frac{1}{2} - 2s_W^2\Big), \\ \Rightarrow\ \Delta'_e &= -\frac{\alpha}{3\pi}\left(\frac{1}{6} + \ln\frac{M_Z^2}{m^2}\right)(1 - 4s_W^2). \qquad (4.45)\end{aligned}$$

This is our official Thomson limit result, and it is the same result used by

EKR. Next, let's evaluate this correction in the scattering limit. To do so, we can start with the general expressions for the PV functions inside (4.40) and apply our renormalization condition to find:

$$\begin{aligned}
\hat{\Lambda}^{\gamma ee}_{\mu,PV}(t) &= -\frac{1}{3m^4 t(4m^2-t)}\Bigg\{6m^2 t(2m^2-M_Z^2)(4m^2-t) \\
&- 6M_Z t\sqrt{M_Z^2-4m^2}\Big[2m^2(M_Z^2-t)-M_Z^2 t\Big] \\
&\quad \times\ln\left(\frac{\sqrt{M_Z^2-4m^2}+M_Z}{2m}\right)+2m^4(M_Z^2+t)(4m^2-M_Z^2-t) \\
&\quad \times\left(6\mathrm{Li}_2(1+M_Z^2/t)+3\ln^2\Big(\frac{-M_Z^2}{t}\Big)+\pi^2\right)+6m^4\sqrt{t(t-4m^2)} \\
&\quad \times(4m^2-2M_Z^2-3t)\ln\left(\frac{\sqrt{t(t-4m^2)}+2m^2-t}{2m^2}\right) \\
&+ 3M_Z^2 t(8m^4-2m^2M_Z^2+M_Z^2 t)\ln\frac{m^2}{M_Z^2}\Bigg\}. \qquad (4.46)
\end{aligned}$$

To help us systematically proceed with the scattering limit, it will be very helpful to express this in terms of the 2 dimensionless quantities:

$$x \equiv -\frac{t}{M_Z^2}, \qquad (4.47)$$

$$z \equiv \frac{m^2}{M_Z^2}. \qquad (4.48)$$

This leaves us with the equivalent expression:

$$\begin{aligned}\hat{\Lambda}^{\gamma ee}_{\mu,PV}(t) &= \frac{1}{3xz^2(x+4z)}\Bigg\{-2(x-1)z^2(x+4z-1)\Big[6\mathrm{Li}_2(1-1/x) \\ &\quad +3\ln^2 x+\pi^2\Big]+6z^2\sqrt{x(x+4z)}(3x+4z-2) \\ &\quad \times\ln\left(\frac{\sqrt{x(x+4z)}+x+2z}{2z}\right)-6x(2z-1)z(x+4z) \\ &\quad +6x\sqrt{1-4z}(2xz+x+2z)\ln\left(\frac{\sqrt{1-4z}+1}{2\sqrt{z}}\right) \\ &\quad +3x[x+2(1-4z)z]\ln z\Bigg\}. \end{aligned} \tag{4.49}$$

From here, we can perform a Taylor series about $z=0$, which to LO evaluates to:

$$\begin{aligned}\hat{\Lambda}^{\gamma ee}_{\mu,PV}(t) \approx -\frac{1}{3x^2}\Bigg[&12(x-1)^2\mathrm{Li}(1-1/x)+2\pi^2x^2+21x^2-4\pi^2x \\ &-12x+6(x-1)^2\ln^2 x-6x(3x-2)\ln x+2\pi^2\Bigg]. \end{aligned} \tag{4.50}$$

Finally, we can take the Taylor series (again) about $x=0$ up to $\mathcal{O}(x)$, multiply by $D(t)$, then take the limit $x\to 0$ to find:

$$\Delta'_e=-\frac{\alpha}{3\pi}(1-4s^2_W)\left(\ln\frac{M^2_Z}{Q^2}+\frac{11}{6}\right), \tag{4.51}$$

which is a distinctly different expression than the Thomson limit in (4.45).

However, the two are related via:

$$\Delta'_e(Q^2) = \Delta'_e(0) + \frac{\alpha}{3\pi}(1 - 4s^2_W)\left(\ln\frac{Q^2}{m^2} - \frac{5}{3}\right). \tag{4.52}$$

This relation has a rather interesting connection to the running of the weak mixing angle. As we shall see in the following section, the difference $\Delta'_e(Q^2) - \Delta'_e(0)$ is equal to the electron's contribution to the running of $\sin^2\theta_W$. The numerical difference between the scattering and Thomson limits evaluates to:

$$\Delta'_e(.025\text{GeV}^2) - \Delta'_e(0) = +.0006, \tag{4.53}$$

which is a $+0.8\%$ increase to the Thomson limit correction, and a -1.9% correction to $Q_W(p)$. One noteable difference between Δ_e and Δ'_e is that Δ'_e is suppressed by $(1 - 4s^2_W)$ while Δ_e is not. Despite this, Δ_e is negligible, while the large logarithm in (4.51) makes Δ'_e a more dominant correction to the proton's weak charge. This concludes our vertex corrections for now. It should be remarked that vertex corrections are generally process-dependent, and mathematically they may contain both IR and UV divergences – both of which must be systematically removed for a physical result to ensue.

4.5 The Weak Mixing Angle

At low Q^2, A_{LR} receives contributions from amplitudes which involve a single Z-boson coupling to the electron together with a single photon coupling to the proton. These two neutral vector bosons can interact through the loops depicted in Figure 4.1. There are a number of fermionic and bosonic SE corrections which correct the $\gamma - Z$ propagator and they are shown in Figure 4.2. In addition to these traditional SE diagrams, there is also a subtle contribution which comes from the "pinch" part of the two vertex diagrams at the end of Figure 4.2. Before continuing forth and calculating all of these

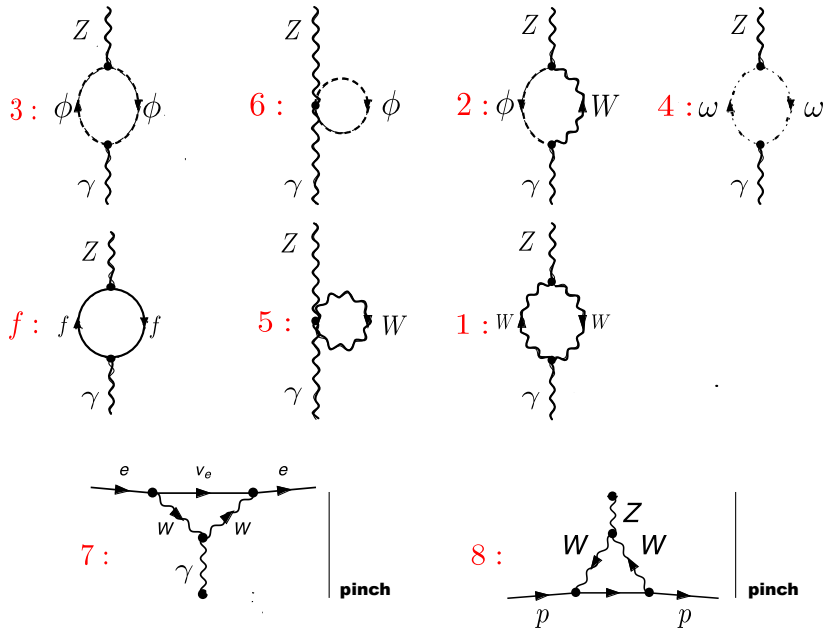

Figure 4.2: 1 Loop Feynman diagrams which contribute to the running of $\sin^2\theta_W(q^2)$

diagrams, let's take the time to clearly relate them to $\sin^2\theta_W$. We use a form factor approach suggested by Sirlin and Ferroglia [55], in which:

$$\sin^2\theta_W(q^2) = \kappa(q^2)\sin^2\theta_W(M_Z^2), \tag{4.54}$$

where the form factor $\kappa(q^2)$ is related to the $\gamma - Z$ self energy correction via:

$$\kappa(q^2) = 1 - \frac{c_W}{s_W}\frac{\hat{\Pi}^{\gamma Z}(q^2)}{q^2}, \tag{4.55}$$

and $\hat{\Pi}^{\gamma Z}$ here denotes the $\bar{\text{MS}}$ renormalized SE evaluated at the t'Hooft scale $\mu = M_Z$. In our goal to acquire the total γZ SE, we will start by finding the lone fermion (f) contribution in Figure 4.2, which is customarily separated from all the bosonic contributions. In terms of PaVe functions, it is given by:

$$\begin{aligned}\Pi_f^{\gamma Z}(q^2) = \quad & \tfrac{1}{3}\tfrac{\alpha}{2c_W s_W \pi}\sum_{f\neq t} Q_f N_c^f (T_f^3 - 2s_W^2 Q_f) \times \\ & \Big[-(q^2 + 2m_f^2)B_0(q^2; m_f, m_f) + 2m_f^2 B_0(0; m_f, m_f) + \tfrac{q^2}{3}\Big].\end{aligned} \tag{4.56}$$

This fermion sum, which excludes the heavy top quark, contains all leptons and quarks which possess an EM charge. Although the lepton masses are well-known, the quark masses are not. Therefore, rather than use the above formula for $\Pi_f^{\gamma Z}$, we replace both the leptonic and hadronic corrections by a

dispersive approach used by Jegerlehner [40]. At the tree level, the mixing angle is just the ratio of EM to weak coupling constants: $\sin^2\theta_W = e/g$. Thus:

$$\sin^2\theta_W(Q^2) = \frac{\alpha(Q)}{\alpha_2(Q)}. \tag{4.57}$$

Furthermore, the loop corrections to α & α_2 can be put into the general form (by a geometric series):

$$\alpha(Q^2) = \frac{\alpha}{1-\Delta\alpha(Q)}. \tag{4.58}$$

It follows to $\mathcal{O}(\alpha)$ then, that the shift in $\sin^2\theta_W$ due to these running constants can be written as:

$$\sin^2\theta_W(Q^2) = \Big(\Delta\alpha(Q) - \Delta\alpha_2(Q)\Big)\sin^2\theta_W(0). \tag{4.59}$$

The same formula may also be applied for the choice of renormalizing from the Z-pole as well. Regardless of renormalization choices, the LHS is the same function (a running EW parameter). Both $\Delta\alpha(Q)$ and $\Delta\alpha_2(Q)$ are available from [40], and have been separated into 3 parts:

$$\Delta\alpha = \Delta\alpha_{\text{lep}} + \Delta\alpha_{\text{had}} + \Delta\alpha_{\text{top}}. \tag{4.60}$$

As shown in Figure 4.3 below, the Jegerlehner parameterization agrees very well with a recent Lattice calculation [56]; and thus it appears to be much

more reliable than simply putting the effective quark masses into $\Pi_f^{\gamma Z}(q^2)$. The total shift (Scattering-Thomson) in the weak mixing angle due to the

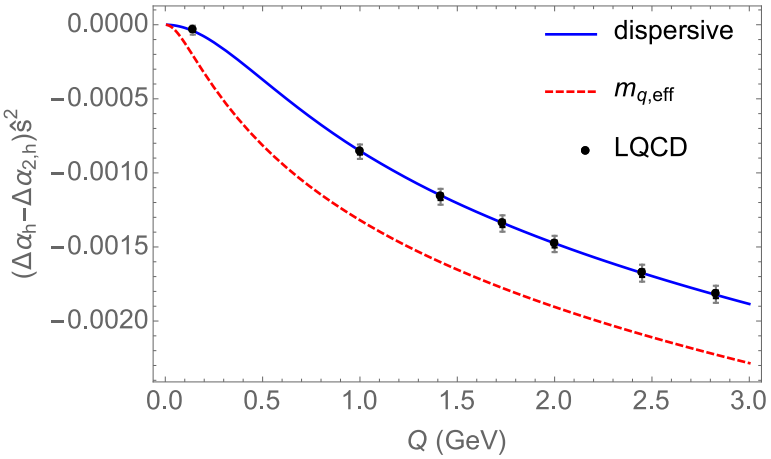

Figure 4.3: Comparison of the difference to the running of $\sin^2\theta_W(q^2)$ from the fermionic loops between the perturbative result of (254) and two non-perturbative calculations.

fermionic and hadronic loops using the dispersive analysis of Jegerlehner is:

$$\delta \sin^2\theta_W(Q^2 = .025\text{GeV}^2) = -.0002\ . \tag{4.61}$$

Next, we turn our attention to the bosonic contributions $(1-6)$, which we will each evaluate separately. Starting with diagram 1:

$$\Pi_1^{\gamma Z\,\mu\nu}(q^2) \;=\;$$

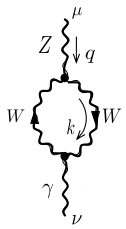

$$\begin{aligned}
&= (-1)^5 i^6 e g c_W g_{\mu\rho} g_{\omega\nu} g_{\tau\alpha} g_{\gamma l} \mu^{2\epsilon} \int \frac{d^d k}{(2\pi)^d} \\
&\quad \times [g^{\tau\gamma}(q-2k)^\rho + g^{\gamma\rho}(k-2q)^\tau + g^{\rho\tau}(q+k)^\gamma] \\
&\quad \times \frac{[g^{\alpha l}(q-2k)^\omega + g^{\alpha\omega}(k+q)^l + g^{\omega l}(k-2q)^\alpha]}{(k^2 - M_W^2)[(q+k)^2 - M_W^2]} \\
&= g^2 s_W c_W g_{\tau\alpha} g_{\gamma l} \mu^{2\epsilon} \int \frac{d^d k}{(2\pi)^d} [g^{\tau\gamma}(q-2k)^\mu + g^{\gamma\mu}(k-2q)^\tau + \\
&\quad g^{\mu\tau}(q+k)^\gamma] \times \frac{[g^{\alpha l}(q-2k)^\nu + g^{\alpha\nu}(k+q)^l + g^{\nu l}(k-2q)^\alpha]}{(k^2 - M_W^2)[(q+k)^2 - M_W^2]} \\
&= \frac{c_W s_W g^2}{6} \Bigg\{ g^{\mu\nu} \big[(19q^2 + 32M_W^2) B_0(q^2; M_W, M_W) + 22 A_0(M_W) \\
&\quad + 10(-2M_W^2 + p^2/3) \big] + \frac{q^\mu q^\nu}{q^2} \big[(-22q^2 - 20M_W^2) B_0(q^2; M_W, M_W) \\
&\quad + 20 A_0(M_W) + 10(-2M_W^2 + p^2/3) \big] \Bigg\}. \qquad (4.62)
\end{aligned}$$

$$\Pi_2^{\gamma Z\mu\nu}(q^2) = \quad$$

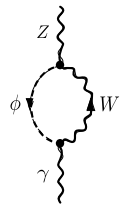

$$= 2i^6(-1)^5 egM_W M_Z s_W^2 g_{\mu\nu} g^{\alpha\gamma} g^{\rho\tau} g_{\alpha\tau} g_{\gamma\rho} \mu^{2\epsilon} \int \frac{d^dk}{(2\pi)^d} \frac{1}{(k^2 - M_W^2)[(q-k)^2 - M_W^2]}$$

$$= 2g^2 s_W^3 \frac{M_W^2}{c_W} g_{\mu\nu} u^{2\epsilon} \int \frac{d^dk}{(2\pi)^d} \frac{1}{(k^2 - M_W^2)[(q-k)^2 - M_W^2]}$$

$$= \frac{2g^2 M_W^2 s_W^3 g^{\mu\nu}}{c_W} B_0(q^2; M_W, M_W). \tag{4.63}$$

$$\Pi_3^{\gamma Z\mu\nu}(q^2) = \quad$$

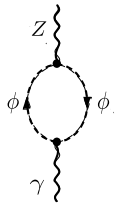

$$= i^6(-1)^4 eg \frac{\cos(2\theta_W)}{2c_W} g_{\mu\beta} g_{\alpha\nu} \mu^{2\epsilon} \int \frac{d^dk}{(2\pi)^d} \frac{(2k-q)^\beta (q-2k)^\alpha}{(k^2 - M_W^2)[(q-k)^2 - M_W^2]}$$

$$= \frac{g^2 s_W}{2c_W} (c_W^2 - s_W^2) \mu^{2\epsilon} \int \frac{d^dk}{(2\pi)^d} \frac{(2k-q)^\mu (q-2k)^\beta}{(k^2 - M_W^2)[(q-k)^2 - M_W^2]}$$

$$= \frac{g^2 s_W (c_W^2 - s_W^2)}{6c_W} \Bigg\{ g^{\mu\nu} \Big[(4M_W^2 - q^2) B_0(q^2; M_W, M_W) + 2A_0(M_W^2)$$

$$+2(-2M_W^2 + p^2/3) \Big] + \frac{q^\mu q^\nu}{q^2} \Big[(q^2 - 4M_W^2) B_0(q^2; M_W, M_W)$$

$$+4A_0(M_W) + 2(-2M_W^2 + p^2/3) \Big] \Bigg\}. \tag{4.64}$$

$$\Pi_4^{\gamma Z\mu\nu}(q^2) = \quad$$

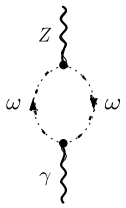

$$= 2(-1)^2 i^6 e g c_W g_{\mu\beta} g_{\alpha\nu} \int \frac{d^dk}{(2\pi)^d} \frac{(k-q)^\beta k^\alpha}{(k^2-M_W^2)[(q-k)^2-M_W^2]}$$

$$= -2g^2 s_W c_W \mu^{2\epsilon} \int \frac{d^dk}{(2\pi)^d} \frac{(k-q)^\mu k^\nu}{(k^2-M_W^2)[(q-k)^2-M_W^2]}$$

$$= -\frac{c_W s_W g^2}{6} \Bigg\{ g^{\mu\nu} \Big[(4M_W^2 - q^2) B_0(q^2; M_W, M_W) + 2A_0(M_W)$$
$$+2(-2M_W^2 + p^2/3) \Big] + \frac{q^\mu q^\nu}{q^2} \Big[-(2q^2 + 4M_W^2) B_0(q^2; M_W, M_W)$$
$$+4A_0(M_W) + 2(-2M_W^2 + p^2/3) \Big] \Bigg\}. \qquad (4.65)$$

$$\Pi_5^{\gamma Z\mu\nu}(q^2) = \quad$$

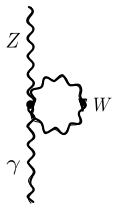

$$= -i^4 e g c_W g_{\mu\alpha} g_{\delta\nu} g_{\tau\gamma} \mu^{2\epsilon} \int \frac{d^dk}{(2\pi)^d} \frac{(2g^{\tau\gamma} g^{\delta\alpha} - g^{\tau\delta} g^{\gamma\alpha} - g^{\tau\alpha} g^{\gamma\delta})}{k^2 - M_W^2}$$

$$= -g^2 s_W c_W \mu^{2\epsilon} \int \frac{d^dk}{(2\pi)^d} \frac{[2g^{\tau\gamma} g_{\mu\nu} - g_\mu^\gamma g_\nu^\tau - g_\mu^\tau g_\beta^\gamma] g_{\tau\gamma}}{k^2 - M_W^2}$$

$$= -6 c_W s_W g^2 g^{\mu\nu} A_0(M_W). \qquad (4.66)$$

$$\Pi_5^{\gamma Z\,\mu\nu}(q^2) = \quad$$

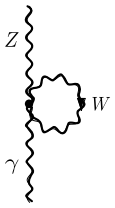

$$\begin{aligned}
&= -i^4 g e \frac{\cos(2\theta_W)}{c_W} g_{\mu\beta} g_{\alpha\nu} g^{\beta\alpha} \mu^{2\epsilon} \int \frac{d^d k}{(2\pi)^d} \frac{1}{k^2 - M_W^2} \\
&= -g^2 s_W g_{\mu\nu} \frac{(c_W^2 - s_W^2)}{c_W} \mu^{2\epsilon} \int \frac{d^d k}{(2\pi)^d} \frac{1}{k^2 - M_W^2} \\
&= -g^2 \frac{s_W (c_W^2 - s_W^2)}{c_W} g_{\mu\nu} A_0(M_W). \qquad (4.67)
\end{aligned}$$

We now need the sum of these 6 amplitudes for the total unrenormalized bosonic γZ self energy, which we will decompose into transverse (T) and longitudinal (L) parts:

$$\Pi_{Bos}^{\gamma Z\ \mu\nu} = \left(g^{\mu\nu} - \frac{q^\mu q^\nu}{q^2} \right) \Pi_{Bos,T}^{\gamma Z} + \frac{q^\mu q^\nu}{q^2} \Pi_{Bos,L}^{\gamma W}, \qquad (4.68)$$

where:

$$\begin{aligned}
\Pi_{Bos,T}^{\gamma Z}(q^2) &= \frac{g^2 s_W}{6 c_W} \Big\{ [(18 c_W^2 + 1) q^2 + 8(3 c_W^2 + 1) M_W^2] B_0(q^2; M_W, M_W) \\
&\quad + 4(1 - 6 c_W^2)[A_0(M_W) - M_W^2] + 2q^2/3 \Big\}, \qquad (4.69) \\
\Pi_{Bos,L}^{\gamma Z}(q^2) &= \frac{2 g^2 M_W^2 s_W}{c_W} B_0(q^2; M_W, M_W) = \frac{\alpha}{2\pi s_W c_W} M_W^2 B_0. \qquad (4.70)
\end{aligned}$$

It is a well-known fact that only the transverse component of a self-energy contributes to S-matrix elements, since the longitudinal part vanishes when

contracted with a polarization vector: $\epsilon_\mu q^\mu = 0$. The first term of (4.68) then obeys the Ward identity $q_\mu \Pi_{Bos}^{\gamma Z\ \mu\nu} = 0$. Therefore, at some point, the longitudinal component must cancel or else this condition will not be obeyed. Our unrenormalized SE in (4.68-4.70) agrees with that attained in [57]. However, rather than renormalize it now, we can form a gauge-invariant self-energy using a method known as the Pinch Technique [58]-[59]. The technique states that the non-Abelian vertices $WW\gamma$ & WWZ of diagrams 7 & 8 in Figure 4.2 each contain a term which effectively "pinches out" the intermediate fermion line in the loop. The remaining diagram resembles a γZ mixing contribution which can then be folded into (4.68). See Figure 4.4 for an illustration of the effect. We can start by writing the full expression of diagram 7, which is:

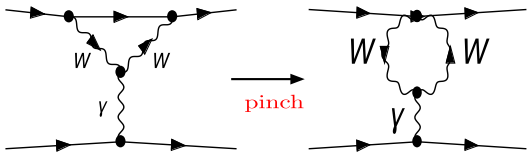

Figure 4.4: The pinch technique applied to the electron's anapole moment vertex diagram reveals a hidden γZ mixing piece after removing the intermediate fermion line.

M_7 =

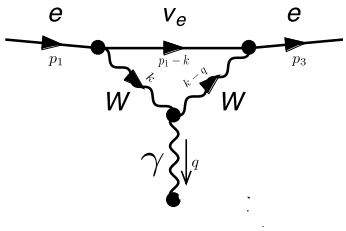

$$
\begin{aligned}
&= \left(\frac{ig}{\sqrt{2}}\right)^2 \int \frac{d^4}{(2\pi)^4}\bar{u}_e(p_3)\gamma^\alpha P_L \frac{i(\not{p}_1 - \not{k})}{(p_1-k)^2}\gamma^l P_L u_e(p_1)\left(\frac{-ig_{l\gamma}}{k^2-M_W^2}\right) \\
&\times\left(\frac{-ig_{\alpha\tau}}{(k-q)^2-M_W^2}\right)\left(\frac{-ig_{\delta\beta}}{q^2-\lambda^2}\right)(-ie)[g^{\tau\gamma}(q-2k)^\delta \\
&+g^{\gamma\delta}(k+q)^\tau + g^{\delta\tau}(k-2q)^\gamma]. \qquad (4.71)
\end{aligned}
$$

The non-Abelian γWW vertex, which is in square brackets, contains two terms which generate a pinching effect: k^τ and k^γ. So let's isolate them for now, denoting $|_p$ for the pinch part they constitute:

$$
\begin{aligned}
M_7|_p &= -\frac{g^2 e}{2}\int \frac{d^4k}{(2\pi)^4}\bar{u}_e(p_3)\gamma^\alpha P_L \frac{1}{\not{p}_1 - \not{k}}\gamma^l P_L u_e(p_1) \\
&\times \frac{g_{l\gamma}g_{\alpha\tau}g_{\delta\beta}(g^{\gamma\delta}k^\tau + g^{\delta\tau}k^\gamma)}{(k^2-M_W^2)[(k-q)^2-M_W^2](q^2-\lambda^2)} \\
&= \frac{ig^2 e}{2(q^2-\lambda^2)}\int \frac{d^4k}{(2\pi)^4}\bar{u}_e(p_3)\gamma^\alpha P_L \frac{1}{\not{p}_1 - \not{k}}\gamma^l P_L u_e(p_1) \\
&\times \frac{(g_{l\beta}k_\alpha + g_{\alpha\beta}k_l)}{(k^2-M_W^2)[(k-q)^2-M_W^2} \\
&= -\frac{ig^2 e}{2(q^2-\lambda^2)}\int \frac{d^4k}{(2\pi)^4}\bar{u}_e(p_3)\left[\not{k}P_L\frac{1}{\not{p}_1-\not{k}}\gamma_\beta P_L\right. \\
&\left.+\gamma_\beta P_L \frac{1}{\not{p}_1-\not{k}}\not{k}P_L\right]u_e(p_1)\frac{1}{(k^2-M_W^2)[(k-q)^2-M_W^2]}. \qquad (4.72)
\end{aligned}
$$

We can then us the simple identities:

$$\not{k} P_L = -P_L \not{k}, \tag{4.73}$$

$$-\not{k} = (\not{p}_1 - \not{k}) - \not{p}_1, \tag{4.74}$$

in which case the terms inside the square brackets reduces to:

$$\begin{aligned} & P_L \frac{[(\not{p}_1 - \not{k}) - \not{p}_1]}{\not{p}_1 - \not{k}} \gamma_\beta P_L - \gamma_\beta P_L \frac{[(\not{p}_1 - \not{k}) - \not{p}_1]}{\not{p}_1 - \not{k}} P_L \\ = & P_L \left(1 - \frac{\not{p}_1}{\not{p}_1 - \not{k}} \right) \gamma_\beta P_L - \gamma_\beta P_L \left(1 - \frac{\not{p}_1}{\not{p}_1 - \not{k}} \right) P_L. \end{aligned} \tag{4.75}$$

In the forward limit one has $\not{p}_1 \approx \not{p}_3$, and we are also "sandwiching" this expression between the external spinors in (4.72). Thus we have:

$$\begin{aligned} & \bar{u}_e(p_3) \left[P_L \left(1 - \frac{\not{p}_1}{\not{p}_1 - \not{k}} \right) \gamma_\beta P_L - \gamma_\beta P_L \left(1 - \frac{\not{p}_1}{\not{p}_1 - \not{k}} \right) P_L \right] u_e(p_1) \\ & = \bar{u}_e(p_3) \left[-\gamma_\beta P_L^2 + \frac{\not{p}_1 P_L \gamma_\beta P_L}{\not{p}_1 - \not{k}} - \gamma_\beta P_L^2 - \frac{\gamma_\beta P_L^2 \not{p}_1}{\not{p}_1 - \not{k}} \right] u_e(p_1) \\ & \approx -2 \bar{u}_e(p_1) \gamma_\beta P_L u_e(p_1), \end{aligned} \tag{4.76}$$

where we have used the massless fermion limit: $\not{p}_1 u_e(p_1) \approx 0$ and $P_L^2 = P_L$. (4.72) then reduces to:

$$M_7|_p = \frac{2ig^2 e}{2q^2} \int \frac{d^4k}{(2\pi)^4} \bar{u}_e(p_1) \gamma_\beta P_L u_e(p_1) \frac{1}{(k^2 - M_W^2)[(k-q)^2 - M_W^2]}. \tag{4.77}$$

The remaining leptonic current $J_\beta^3 = \bar{u}_e(p_1) \gamma_\beta P_L u_e(p_1)$ is an unphysical one

for the electron. Nonetheless, we may express it in terms of physical ones:

$$J^3_\beta = 2(J^Z_\beta + s^2_W J^\gamma_\beta), \tag{4.78}$$

where J^Z_μ and J^γ_μ are the neutral and EM currents without their coupling constants. Since it is a photon (purely vector) which couples to the proton here, in order to attain a PV effect, we need the J^Z_β term from (4.78). Therefore:

$$\begin{aligned} M_7|^{PV}_p &= \frac{2ig^2e}{q^2}\int \frac{d^4k}{(2\pi)^4}\frac{1}{(k^2-M^2_W)[(k-q)^2-M^2_W]}\bar{u}_e J^Z_\beta u_e \\ &= \frac{ig^2e}{q^2}\left(\frac{2i}{16\pi^2}\right)B_0(q^2;M_W,M_W)\bar{u}_e J^Z_\beta u_e \\ &= -\frac{e}{q^2}\left(\frac{\alpha}{2\pi s^2_W}B_0(q^2;M_W,M_W)\right)\bar{u}_e J^Z_\beta u_e, \end{aligned} \tag{4.79}$$

which gets multiplied by the proton's photon current $\bar{u}_p J^\gamma_\beta u_p$ in the full scattering amplitude. This implicitly means that this is a contribution to the γZ SE. We next need to evaluate the pinch part of the proton vertex in diagram

8:

M_8 =

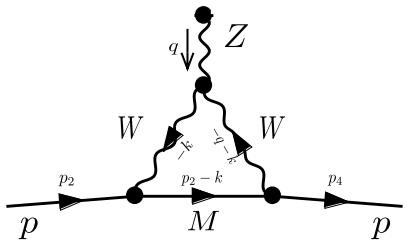

$$= \int \frac{d^4k}{(2\pi)^4}\left(\frac{-ig^{\mu\rho}}{q^2-M_Z^2}\right) igc_W[g_{\delta\tau}(2k+q)_\rho - g_{\tau\rho}(k+2q)_\delta + g_{\rho\delta}(q-k)_\tau]$$
$$\times\left(\frac{-ig^{\alpha\delta}}{k^2-M_W^2}\right)\left(\frac{-ig^{\tau\beta}}{(k+q)^2-M_W^2}\right)\bar{u}_p(p_4)\frac{ig}{\sqrt{2}}\gamma_\beta P_L i\frac{(\not{p}_2 - \not{k} + M)}{(p_2-k)^2-M^2}\frac{ig}{\sqrt{2}}$$
$$\times\gamma_\alpha P_L u_p(p_2). \qquad (4.80)$$

This expression assumes that the nucleons are pure spin-1/2 Dirac fermions, while in fact, nothing forces this to be true. Fortunately this loop expression involves:

$$M_8 \sim \int d^4k \frac{\text{numerator}}{(k^2-M_W^2)[(k+q)^2-M_W^2][(p_2-k)^2-M^2]}. \qquad (4.81)$$

The two W-boson propagators implies that this integral is dominated at high k^2 momentum scales – a limit in which the nucleon behaves like free quarks.

Therefore, our vertex approximately behaves as (taking $\alpha_S = 0$):

$M_8(\text{proton}) =$ 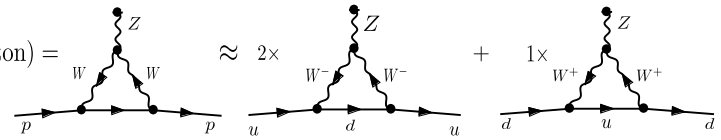 (4.82)

So let us proceed with the up quark contribution:

$$\begin{aligned} M_8(u) &= \frac{-i^7 g^3 c_W}{2(q^2 - M_Z^2)} \int \frac{d^4k}{(2\pi)^4} \bar{u}_u(p_4)\gamma_\beta P_L \frac{1}{\not{p}_2 - \not{k}} \gamma_\alpha P_L u_u(p_2) \\ &\quad \times \frac{g^{\mu\rho} g^{\alpha\delta} g^{\tau\beta} [g_{\delta\tau}(2k+q)_\rho - g_{\tau\rho}(k+2q)_\delta + g_{\rho\delta}(q-k)_\tau]}{(k^2 - M_W^2)[(q+k)^2 - M_W^2]}. \end{aligned} \tag{4.83}$$

The pinch terms originate from k_δ and k_τ here, and so the pinch part of this diagram will be:

$$\begin{aligned} M_8(u)|_p &= -\frac{ig^3 c_W}{2(q^2 - M_Z^2)} \int \frac{d^4k}{(2\pi)^4} \bar{u}_u(p_4)\gamma_\beta P_L \frac{1}{\not{p}_2 - \not{k}} \gamma_\alpha P_L u_u(p_2) \\ &\quad \times \frac{g^{\mu\rho} g^{\alpha\delta} g^{\tau\beta} [g_{\tau\rho} k_\delta + g_{\rho\delta} k_\tau]}{(k^2 - M_W^2)[(q+k)^2 - M_W^2]} \\ &= -\frac{ig^3 c_W}{2(q^2 - M_Z^2)} \int \frac{d^4k}{(2\pi)^4} \bar{u}_u(p_4)\gamma_\beta P_L \frac{1}{\not{p}_2 - \not{k}} \gamma_\alpha P_L u_u(p_2) \\ &\quad \times \frac{[g^{\beta\mu} k^\alpha + g^{\alpha\mu} k^\beta]}{(k^2 - M_W^2)[(q+k)^2 - M_W^2]}. \end{aligned} \tag{4.84}$$

This expression is identical to that of $M_7|_p$, but with a slightly different

prefactor outside the integral. They are related by:

$$\begin{aligned} M_8(u)|_p &= M_7|_p\left(\frac{e}{q^2} \to \frac{gc_W}{q^2 - M_Z^2}\right), \qquad (4.85) \\ \Rightarrow M_8(u)|_p &= \frac{ig^3 c_W}{q^2 - M_Z^2}\int \frac{d^4k}{(2\pi)^4}\bar{u}_u(p_4)\gamma^\mu P_L u_u(p_2)\frac{1}{(k^2 - M_W^2)[(q+k)^2 - M_W^2]}, \end{aligned}$$

and in this case we now need the EM part of the J_3^μ current for a PV contribution:

$$\begin{aligned} M_8(u)|_p^{PV} &= \frac{2is_W^2 g^3 c_W}{q^2 - M_Z^2}\int \frac{d^4k}{(2\pi)^4}\frac{\bar{u}_u J_\gamma^\mu u_u}{(k^2 - M_W^2)[(q+k)^2 - M_W^2]} \\ &= \frac{2igc_W e^2}{q^2 - M_Z^2}\bar{u}_u J_\gamma^\mu u_u \frac{i}{16\pi^2}B_0(q^2; M_W, M_W) \\ &= -\frac{\alpha}{2\pi}\frac{gc_W}{q^2 - M_Z^2}\bar{u}_u J_\gamma^\mu u_u B_0(q^2; M_W, M_W). \qquad (4.86) \end{aligned}$$

The full EM currents of the up and down quarks are:

$$\bar{u}_u J_\gamma^\mu u_u = +\frac{2e}{3}\bar{u}_u\gamma^\mu u_u, \qquad (4.87)$$

$$\bar{u}_d J_\gamma^\mu u_d = -\frac{e}{3}\bar{u}_d\gamma^\mu u_d, \qquad (4.88)$$

$$\Rightarrow 2\bar{u}_u J_\gamma^\mu u_u + \bar{u}_d J_\gamma^\mu u_d = +e\bar{u}\gamma^\mu u = \bar{u}_p J_\gamma^\mu u_p. \qquad (4.89)$$

Therefore:

$$M_8(\text{proton})|_p^{PV} = -\frac{g}{c_W(q^2 - M_Z^2)}\left(\frac{\alpha c_W^2}{2\pi}\right)\bar{u}_p J_\gamma^\mu u_p B_0(q^2; M_W, M_W), \quad (4.90)$$

and this expression will get multiplied by the electron's neutral current

$\bar{u}_e J^Z_\mu u_e$ in the scattering amplitude to also contribute to the γZ SE. To recap our PT results, we now have the two expressions:

$$\begin{aligned} M_7|_p^{PV} &= -\frac{e}{q^2}\frac{\alpha}{2\pi s_W^2} B_0(q^2; M_W, M_W)\bar{u}_e J^Z_\beta u_e, \\ M_8|_p^{PV} &= -\frac{g}{(q^2 - M_Z^2)}\frac{\alpha c_W}{2\pi} B_0(q^2; M_W, M_W)\bar{u}_p J^\mu_\gamma u_p. \end{aligned}$$

However, in order to make sense of these results, we should consider the full scattering amplitudes, and make sure that the currents present include their respective coupling constants: $J^Z_\beta \sim g/c_W$, $J^\mu_\gamma \sim e$. Doing so gives for the S-matrix elements:

$$\begin{aligned} M_7|_p^{PV} &\xrightarrow{\text{scattering}} -\frac{1}{q^2}\left(\frac{\alpha c_W}{2\pi s_W}\frac{1}{q^2 - M_Z^2} B_0(q^2; M_W, M_W)\right)\bar{u}_e J^Z_\beta u_e \bar{u}_p J^\beta_\gamma u_p, \\ M_8|_p^{PV} &\xrightarrow{\text{scattering}} -\frac{1}{q^2 - M_Z^2}\left(\frac{\alpha c_W}{2\pi s_W}\frac{1}{q^2} B_0(q^2; M_W, M_W)\right)\bar{u}_e J^Z_\mu u_e \bar{u}_p J^\mu_\gamma u_p, \end{aligned}$$

and their contribution to the γZ SE comes from the quantities in round parenthesis once the common mixing propagator has been factored out. Thus our total PT part of the γZ self energy is:

$$\begin{aligned} \Delta_p &= \frac{\alpha c_W}{2\pi s_W} B_0(q^2; M_W, M_W)\left(\frac{1}{q^2 - M_Z^2} + \frac{1}{q^2}\right) \\ &= \frac{\alpha}{2\pi s_W c_W}\frac{c_W^2 q^2 + c_W^2(q^2 - M_Z^2)}{q^2(q^2 - M_Z^2)} B_0(q^2; M_W, M_W) \\ &= \frac{\alpha}{2\pi s_W c_W}[2q^2 c_W^2 - M_W^2] B_0(q^2; M_W, M_W). \end{aligned} \tag{4.91}$$

Note that the M_W^2 term of Δ_p has exactly equal and opposite sign to $\Pi^{\gamma Z}_{Bos,L}$ in (4.70). This renders the sum $\Pi^{\gamma Z\ \mu\nu}_{Bos} + g^{\mu\nu}\Delta_p$ gauge invariant. This total forms now our unrenormalized transverse γZ PT self energy. The resulting function, which we'll call $\Pi^{\gamma Z}_{Bos+PT,T}(q^2)$, is UV-divergent and it must be renormalized before it is inserted into an observable quantity. In order to understand how it is renormalized, the γZ mixing propagator is defined as:

$$D_{\gamma Z}(q^2) \approx \frac{-i\Pi^{\gamma Z}(q^2)}{q^2(q^2 - M_Z^2)} = \quad , \tag{4.92}$$

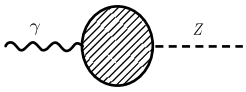

and its renormalization conditions require that:

$$\Pi^{\gamma Z}(0) = 0, \tag{4.93}$$

$$\mathrm{Re}\Pi^{\gamma Z}(M_Z^2) = 0. \tag{4.94}$$

Therefore, in the on-shell (OS) renormalization scheme, the renormalized γZ SE is constructed as follows:

$$\hat{\Pi}^{\gamma Z}(q^2) = \Pi^{\gamma Z}(q^2) - \Pi^{\gamma Z}(0) - \frac{q^2}{M_Z^2}[\mathrm{Re}\Pi^{\gamma Z}(M_Z^2) - \Pi^{\gamma Z}(0)], \tag{4.95}$$

and so the counter terms are effectively functions of $\Pi^{\gamma Z}(0)$ and $\mathrm{Re}\Pi^{\gamma Z}(M_Z^2)$. Rather than employing the OS scheme, we choose to use the $\bar{\mathrm{M}}$S scheme which begins with the OS counterterms, but only keeps their $\Delta_\epsilon = \frac{2}{\epsilon} - \gamma_E + \ln 4\pi$ terms in the renormalization subtraction. This renormalization process equally applies to the fermionic expression as it does the bosonic,

and so I include both below for completeness reasons. Inserting $\Pi_T^{\gamma Z} = \Pi_{fer,T}^{\gamma Z} + \Pi_{bos,T}^{\gamma Z} + \Delta_p$ into the $\bar{\text{MS}}$ scheme gives one:

$$\begin{aligned}
\hat{\Pi}_{ferm}^{\gamma Z} &= \frac{\alpha}{2\pi s_W c_W}\left\{\frac{1}{3}\Sigma_f N_c^f Q_f (I_f^3 - 2s_W^2 Q_f)\left[-(q^2+2m_f^2)B_0(q^2;m_f,m_f)\right.\right. \\
&\quad \left.\left. +2m_f^2 B_0(0;m_f,m_f) + \frac{q^2}{3}\right]\right\}, \qquad (4.96) \\
\hat{\Pi}_{bos+PT}^{\gamma Z} &= \frac{\alpha}{2\pi s_W c_W}\left\{\left[\left(\frac{7c_W^2}{2}+\frac{1}{12}\right)q^2 + \left(2c_W^2 - \frac{1}{3}\right)M_W^2\right]B_0(q^2;M_W,M_W)\right. \\
&\quad \left. -\left(2c_W^2-\frac{1}{3}\right)M_W^2 B_0(0;M_W,M_W) + \frac{q^2}{18}\right\}. \qquad (4.97)
\end{aligned}$$

Finally, we can insert both these expressions into the formula for $\kappa(Q^2)$, as well as insert the analytical expressions for the PaVe functions to get:

$$\kappa^{PT}(q^2;\mu = M_Z) \equiv \kappa_f(q^2) + \kappa_b^{PT}(q^2) - 1. \qquad (4.98)$$

The -1 term simply ensures we don't double-count 1's in κ_f & κ_b^{PT}, as each is given by:

$$\begin{aligned}
\kappa_f(q^2) &= 1 - \frac{\alpha}{2\pi s_W^2}\left\{\frac{1}{3}\Sigma_f N_c^f Q_f (I_f^3 - 2s_W^2 Q_f)\left[\ln\frac{m_f^2}{M_Z^2} - \frac{5}{3} - 4z_f\right.\right. \\
&\quad \left.\left. +(1+2z_f)p_f \ln\left(\frac{p_f+1}{p_f-1}\right)\right]\right\}, \qquad (4.99) \\
z_f &\equiv \frac{m_f^2}{q^2} < 0, \qquad (4.100) \\
p_f &= \sqrt{1-4z_f}, \qquad (4.101)
\end{aligned}$$

$$\kappa_b^{PT}(q^2) = 1 - \frac{\alpha}{2\pi s_W^2}\left\{ -\frac{42c_W^2+1}{12}\ln c_W^2 + \frac{1}{18} - \left(\frac{p}{2}\ln\frac{p+1}{p-1} - 1\right)\left[(7+4z)c_W^2 + \frac{1}{6}(1-4z)\right]\right\}, \quad (4.102)$$

$$z \equiv \frac{M_W^2}{q^2} < 0, \quad (4.103)$$

$$p = \sqrt{1-4z}. \quad (4.104)$$

It then follows that we predict the running parameter: $\sin^2\theta_W^{PT}(q^2) = \kappa^{PT}(q^2)s_W^2$, where $s_W^2 \equiv \sin^2\theta_W(M_Z^2)$. The contributions from the fermionic, bosonic+PT, and total are all plotted in Figure 4.5.

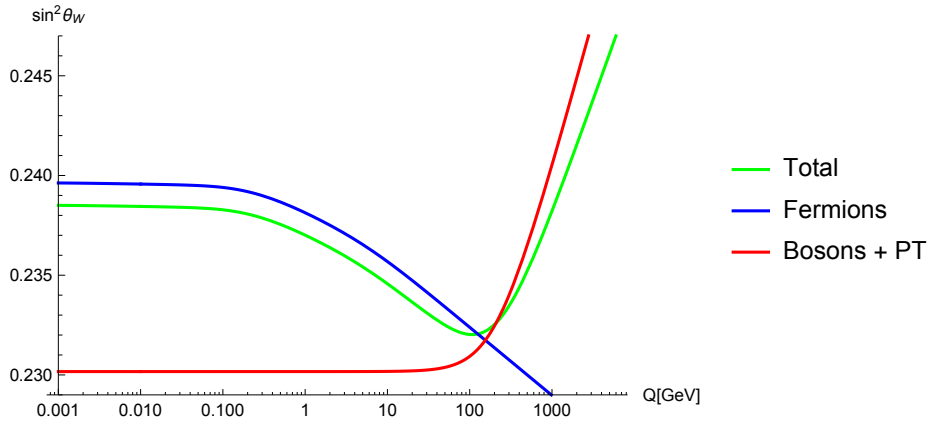

Figure 4.5: The fermionic contribution to $\sin^2\theta_W(Q^2)$ is relevant at low Q, while the bosonic part sets in above the Z-pole mass.

As one can see in the figure, the fermionic part is large at low Q only, while the bosonic is large at high Q only. This is easily understood as the Q^2 flowing into the loop must be large enough to produce the paired W-bosons

around their mass scale, whereas the light fermions require a much lower Q^2 in order to be produced in the loop. Another observation of these results is seen by evaluating $\kappa_f(q^2 \gg m_f^2)|_{m_f=m_e}$. which is the contribution to the weak mixing angle by the electron/positron pair at the scattering limit, where:

$$\begin{aligned}\kappa_f(q^2 \gg m_f^2)|_{m_f=m_e} &= 1 - \frac{\alpha}{2\pi s_W^2}\frac{1}{3}(-1)\left(\frac{1}{2} - 2s_W^2\right)\left[\ln\frac{m_e^2}{M_Z^2} - \frac{5}{3} - \ln\frac{m_e^2}{Q^2}\right] \\ &= 1 + \frac{1}{4s_W^2}\frac{\alpha}{3\pi}(1-4s_W^2)\left(\ln\frac{m_e^2}{M_Z^2} + \ln\frac{Q^2}{m_e^2} - \frac{5}{3}\right),\end{aligned} \tag{4.105}$$

which is remarkably similar to $\Delta_e'(Q^2)$, and the connection isn't exactly obvious. In fact, I find that their relative shift between the Thomson and scattering limits is equal: $\kappa_f^{\rm scat} - \kappa_f^{\rm Thom} = \Delta_e'^{\,\rm Scatt} - \Delta_e'^{\,\rm Thom} = \frac{\alpha}{3\pi}(1-4s_W^2)[\ln(Q^2/m_e^2) - 5/3]$. The main advantage of defining $\sin^2\theta_W^{PT}$ is that not only is it a gauge-invariant quantity (which EW Lagrangian parameters aren't necessarily), but it's also process-independent. Therefore, if all SM precision tests adopt this definition, they are all in fact extracting/using the same quantity, regardless of what experiment is involved.

4.6 Δ_{NP} Correction:

The remaining terms in M_7 also contributes to a PV effect and it must be calculated. This will be called the non-pinch (NP) vertex correction, which is given by:

$$\begin{aligned} M_7|_{NP} &= -\frac{ig^2e}{2}\int\frac{d^4k}{(2\pi)^4}\bar{u}_e(p_3)\gamma^\alpha P_L\frac{(\not{p}_1-\not{k})}{(p_1-k)^2}\gamma^l P_L u_e(p_1)g_{l\gamma}g_{\alpha\tau}g_{\delta\beta} \\ &\quad\times[g^{\tau\gamma}(q-2k)^\delta+g^{\gamma\delta}q^\tau-2g^{\delta\tau}q^\gamma] \\ &\to -\frac{\alpha e}{2\pi s_W^2}\lim_{q^2\to 0}\left(\frac{\Gamma_{2W}^{ee\gamma}(q^2)-\Gamma_{2W}^{ee\gamma}(0)}{q^2}\right), \end{aligned} \tag{4.106}$$

which is the renormalized PV part of the vertex, and the embedded vertex function is defined as:

$$\begin{aligned} \Gamma_{2W}^{ee\gamma}(q^2) &= \left(\frac{M_W^2}{q^2}+2\right)B_0(0;0,M_W)-\left(\frac{2M_W^2}{q^2}+3\right)B_0(q^2;M_W,M_W) \\ &\quad +M_W^2\left(\frac{M_W^2}{q^2}+2\right)C_0(0,0,q^2;M_W,0,M_W). \end{aligned} \tag{4.107}$$

This expression is well-behaved in the limit above, and it simplifies considerably to give:

$$\lim_{q^2\to 0}\left(\frac{\Gamma_{2W}^{ee\gamma}(q^2)-\Gamma_{2W}^{ee\gamma}(0)}{q^2}\right)=-\frac{4}{9M_W^2}. \tag{4.108}$$

The $M_8|_{NP}$ amplitude is equivalent, and with the two, now we just need to take the ratio with the M_Z PV amplitude to find the corresponding correction

to $Q_W(p)$:

$$\begin{aligned}\Delta_{NP} &= \frac{\left(\frac{-\alpha e}{2\pi s_W^2}\right)(e)\left(\frac{-4(2)}{9M_W^2}\right)}{\frac{e^2}{c_W^2 s_W^2}\frac{g_A^e}{M_Z^2}} \\ &= \frac{8\alpha}{9\pi}. \end{aligned} \tag{4.109}$$

This expression represents a process-dependent correction to the weak charge of the proton, which must effectively be added to the RHS of (4.2).

4.7 $\Box_{ZZ}$ Correction

We are now left with the task of evaluating the Box corrections to $Q_W(p)$. The same technical difficulties which plagued the γW box in the CC process also affect the γZ box. Before looking at that case, however, we will calculate the somewhat simpler "doubly-massive" two boson exchange (TBE) amplitudes: $\Box_{ZZ}$, $\Box_{WW}$. The general amplitude for the ZZ box in the forward limit is:

$M^{box}_{ZZ}|_{fwd}$ =

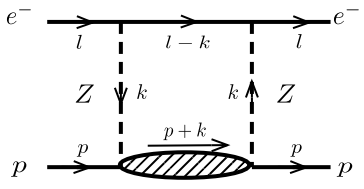

$$= \frac{ig^4}{16c_W^4}\int\frac{d^4k}{(2\pi)^4}\bar{u}_e(l)(g_V^e\gamma_\nu - g_A^e\gamma_\nu\gamma_5)(\not{l}-\not{k})(g_V^e\gamma_\mu - g_A^e\gamma_\mu\gamma_5)u_e(l)$$
$$\times\frac{\bar{u}_p(p)(g_V^p\gamma^\nu - g_A^p\gamma^\nu\gamma_5)(\not{p}+\not{k}+M)(g_V^p\gamma^\mu - g_A^p\gamma^\mu\gamma_5)u_p(p)}{(l-k)^2[(p+k)^2-M^2](k^2-M_Z^2)^2}, \tag{4.110}$$

which is a daunting expression indeed. The proton has been idealized here to the level of a Dirac fermion. However, just as in $M_8|_p$, this is justified, as the high k^2 which probes the hadron means we can calculate M_{ZZ} for free quarks and the combination $2u+d$ yields the proton result once again. There are also many terms which this numerator will generate, and among them all, only contributions of the form: $(V \text{ or } A)_e \times (V^2 \text{ or } A^2)_{had}$ and $(V^2 \text{ or } A^2)_e \times (V \text{ or } A)_{had}$ can generate a PV effect.

Unlike vertex corrections, it is often simpler to work with cross sections when dealing with box diagrams. Defining the box correction as the ratio of cross sections (3.3), gives for the PV ZZ box:

$$\Box_{ZZ}^{Box} \equiv \frac{\sum\limits_{\text{spins}} M_\gamma^* M_{ZZ}^{box,PV}}{\sum\limits_{\text{spins}} M_\gamma^* M_Z^{PV}}. \tag{4.111}$$

Where the denominator here is given by:

$$\sum_{\text{spins}} M_\gamma^* M_Z^{PV} = -\frac{2 g_V^p s^2}{M_Z^2 q^2}. \tag{4.112}$$

Until now, we have been essentially using (4.111) to evaluate our $Q_W(p)$ corrections, as in the forward limit, the M_γ^*'s essentially cancel. We will not do this here, as (4.111) allows one to write their box expression as a product of leptonic and hadronic tensors as was done in (3.29). I have found that this correction has the following general crossing symmetry:

$$\Box_{ZZ}^{xbox}|_{u\to s,\, g_A^e \to -g_A^e} = \Box_{ZZ}^{box}(s). \tag{4.113}$$

A direct loop calculation of (4.110) and its crossed box can also be done exactly in the forward limit, but the PaVe expression is excessively large to include here. In the massless quark limit, and omitting coupling constants

and integration prefactors reveals that:

$$\Box_{ZZ}^{\rm box} + \Box_{ZZ}^{\rm xbox} \sim -\frac{6g_A^e({g_A^e}^2 + {g_V^e}^2)}{g_A^e}. \tag{4.114}$$

Let us see if we can use dispersive techniques to reproduce this result. To do so, it will be helpful to split the box correction into 2 terms:

$$\Box_{ZZ}^{box} = \Box_{ZZ,(1+2)}^{box} + \Box_{ZZ,(3)}^{box}, \tag{4.115}$$

where (1+2) denotes the total V coupling to the hadron while (3) denotes the A coupling to the hadron. Each of these terms has the following imaginary part:

$$\mathrm{Im}\Box_{ZZ,(1+2)}(r) \sim \frac{2\pi g_V^e({g_A^q}^2 + {g_V^q}^2)}{g_V^q}\frac{[2(1+r)^2\ln(1+r) - r(2+3r+2r^2)]}{r^2(1+r)}, \tag{4.116}$$

$$\mathrm{Im}\Box_{ZZ,(3)}(r) \sim \frac{2\pi g_A^q({g_A^e}^2 + {g_V^e}^2)}{g_A^e}\frac{[2(1+r)^2\ln(1+r) - r(2+3r)]}{r^2(1+r)}, \tag{4.117}$$

$$r = \frac{s}{M_Z^2}. \tag{4.118}$$

Then we can use the following intermediate result of section 3.2:

$$\mathrm{Re}\Box(s) = \frac{1}{\pi}\int_0^\infty ds'\left(\frac{\mathrm{Im}\Box(s')}{s'-s} - \frac{\mathrm{Im}\Box(-s')}{s'+s}\right). \tag{4.119}$$

The first term corresponds to the box while the second term corresponds to the crossed box where $u \approx -s$ in the forward limit. Then using the crossing relation of (4.113) gives us:

$$\mathrm{Im}\Box^{ZZ}_{(1+2)}(-s') = \mathrm{Im}\Box^{ZZ}_{(1+2)}(s'), \tag{4.120}$$

$$\Rightarrow \quad \left(\frac{\mathrm{Im}\Box^{ZZ}_{(1+2)}(s')}{s'-s} - \frac{\mathrm{Im}\Box^{ZZ}_{(1+2)}(-s')}{s'+s} \right) = 2s \frac{\mathrm{Im}\Box^{ZZ}_{(1+2)}(s')}{s'^2-s^2} \to 0, \tag{4.121}$$

$$\mathrm{Im}\Box^{ZZ}_{(3)}(-s') = -\mathrm{Im}\Box^{ZZ}_{(3)}(s'), \tag{4.122}$$

$$\Rightarrow \quad \left(\frac{\mathrm{Im}\Box^{ZZ}_{(3)}(s')}{s'-s} - \frac{\mathrm{Im}\Box^{ZZ}_{(3)}(-s')}{s'+s} \right) = 2s' \frac{\mathrm{Im}\Box^{ZZ}_{(3)}(s')}{s'^2-s^2}. \tag{4.123}$$

Therefore only the axial-vector part of the ZZ boxes contributes and the real part of $\Box^{ZZ}$ at the zero energy limit is:

$$\begin{aligned} \mathrm{Re}\Box^{ZZ}_{tot}(0) &= \frac{2}{\pi} \int_0^\infty ds' \frac{\mathrm{Im}\Box^{ZZ}_{(3)}(s')}{s'} \\ &\sim \frac{2}{\pi} M_Z^2 (-2\pi g_A^q) \frac{({g_A^e}^2 + {g_V^e}^2)}{g_A^e} \int_0^\infty dr \frac{[2(1+r)^2 \ln(1+r) - r(2+3r)]}{M_Z^2 r^3 (1+r)} \\ &= -\frac{6 g_A^q ({g_A^e}^2 + {g_V^e}^2)}{g_A^e}. \end{aligned} \tag{4.124}$$

This result now includes the crossed ZZ box also – a subtle convenience for analytically continuing to negative energies in the dispersion relation. Then we can insert the appropriate prefactors to get the official correction:

$$\Box^{ZZ}_{tot}(0) = \frac{3\alpha}{2\pi} \frac{({g_A^e}^2 + {g_V^e}^2)}{c_W s_W} g_V^q g_A^q. \tag{4.125}$$

Finally, we can take the proton sum: $\sum_{q=2u+d}$ to get the sought proton result. It was also stated by the authors of [51] that this box amplitude can be perturbatively corrected by QCD interactions (we will see how this gets determined, but for the WW box in the following section), which leads to an additional factor of $1 - \alpha_S(M_Z)/\pi$:

$$\Box_{ZZ} = \frac{\alpha}{16\pi c_W^2 s_W^2}(9 - 20s_W^2)(1 - 4s_W^2 + 8s_W^4)\left(1 - \frac{\alpha_S(M_Z)}{\pi}\right). \quad (4.126)$$

4.8 $\Box_{WW}$ Correction

The WW box amplitude M^{box}_{WW} can be attained from M^{box}_{ZZ} under the substitution:

$$M^{box}_{WW} \sim M^{box}_{ZZ}|_{g_A \to 1/2,\, g_V \to 1/2}, \tag{4.127}$$

with the understanding that there is also a different overall prefactor due to slightly different coupling constants. The axial and the vector couplings apply to both the electron and proton in (4.127) - hence their lack of superscripts. Despite this simple translation, there is a subtle difference between the greater $\Box_{ZZ}$ & $\Box_{WW}$ quantities which must be accounted for. To demonstrate this, we begin by writing down the diagrams for the WW box amplitudes:

$M^{box}_{WW} =$ 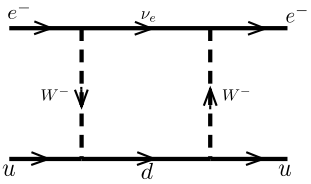

, (4.128)

$M^{xbox}_{WW} =$ 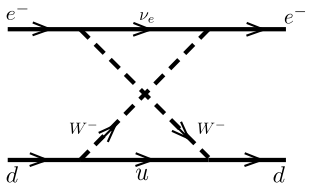

. (4.129)

Since we need the combination $2u + d$, this means that for the proton:

$$\Box_{WW} = 2\Box^{box}_{WW} + \Box^{xbox}_{WW}, \tag{4.130}$$

due to the flavour constraints of the diagrams above. For $\Box_{ZZ}$, both the up and down quarks have a box and crossed box. This weighted expression in (4.130) means that in the dispersion integrand for $\Box_{WW}$ we will have a contribution proportional to $\mathrm{Im}\Box^{WW}_{(1+2)}$, of which the very last term reads:

$$\Box_{WW} \sim \frac{1}{\pi}\int_0^\infty dr \frac{1}{1+r} \to \infty. \tag{4.131}$$

Of course, we don't really need to calculate $\Box_{WW}$ dispersively, as the direct loop calculation is already known, giving:

$$\Box^{box}_{WW}(s) \sim \frac{8}{c_W^2}\left[2 - \frac{s}{(M_W^2+s)}\ln\Big(\frac{-s}{M_W^2}\Big)\right] \to \frac{16}{c_W^2}, \tag{4.132}$$

$$\Box^{xbox}_{WW}(s) = -\frac{\Box^{box}_{WW}}{4} \to -\frac{4}{c_W^2}. \tag{4.133}$$

However, it will be re-assuring to demonstrate the fact that the dispersive technique can be adapted to compute $\Box_{WW}$ just as well here. This adaption is known as a subtracted dispersion relation. Applying Cauchy's integral theorem to the closed contour of Figure 4.6 gives us the relation:

$$f(s_x) = f(s_0) + \frac{s_x - s_0}{\pi}\int_{s_{th}}^\infty ds \frac{\mathrm{Im}f(s)}{(s-s_0)(s-s_x)}, \tag{4.134}$$

where s_0 is called the subtraction point, s_x is the point of interest and $f(s_0)$ is the subtraction constant. One glaring limitation of this equation is that we are now required to know the full function f at an arbitrary point in order

to get it everywhere else, where as the unsubtracted relation only asks that we know the imaginary part as input.

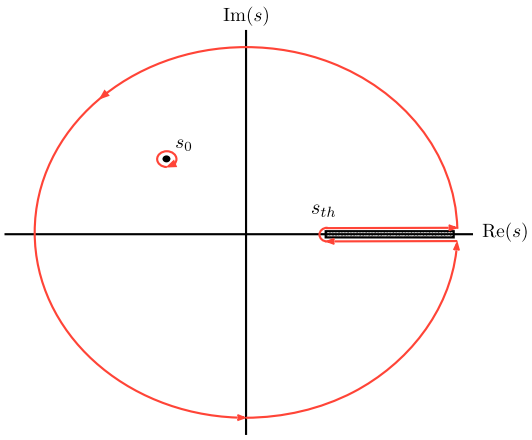

Figure 4.6: The contour chosen to derive (332) where s_x is any point inside the infinite circle.

We will apply the subtracted relation in the extreme case of $s_0 \approx 0 = s_{th}$. From (4.116-4.118) we have that $\mathrm{Im}\Box^{box}_{WW} = 8\pi/c_W^2(M_W^2 + s)$ and we get:

$$\begin{aligned}
\Box^{box}_{WW}(s_x) &= \Box^{box}_{WW}(0) + \frac{s_x}{\pi}\int_0^\infty ds \frac{\mathrm{Im}\Box^{box}_{WW}(s)}{s(s-s_x)} \\
&= \frac{8(2)}{c_W^2} + \frac{s_x}{\pi}\int_0^\infty ds \frac{-8\pi s}{c_W^2 s(M_W^2+s)(s-s_x)} \\
&= \frac{8(2)}{c_W^2} - \frac{8s_x[\ln M_W^2 - \ln(-s_x)]}{c_W^2(M_W^2+s_x)} \\
&= \frac{8}{c_W^2}\left[2 - \frac{s_x \ln(-s_x/M_W^2)}{M_W^2+s_x}\right] \to \frac{16}{c_W^2},
\end{aligned} \tag{4.135}$$

as we already know. Now let's add the crossed box and officially compute

the correction to $Q_w(p)$. The prefactor for each is:

$$\Box_{WW} \sim \frac{M_{WW}^{PV}}{M_Z^{PV}} \sim \frac{g^4/(2\sqrt{2})^4(1/\pi^2)}{(g/c_W)^2} = \frac{\alpha c_W^2}{16\pi s_W^2}, \tag{4.136}$$

$$\Rightarrow \quad \Box_{WW}^{box} = \frac{\alpha}{\pi s_W^2}, \tag{4.137}$$

$$\Rightarrow \quad \Box_{WW}^{xbox} = -\frac{\alpha}{4\pi s_W^2}. \tag{4.138}$$

Then (4.130) finally leads to the known result:

$$\Box_{WW} = \frac{7\alpha}{4\pi s_W^2}. \tag{4.139}$$

There is a further improvement that can be made to this result, and one that somewhat honours the fact that the quarks inside the proton can interact via the strong interaction. To begin, let us look closely at the expressions of $M_{WW}^{\rm box}$ & $M_{WW}^{\rm xbox}$ found from (4.128-4.129). The former being given by:

$$\begin{aligned} M_{WW}^{box} \quad = \quad & \frac{i^8 g^4}{2^6} \int \frac{d^4k}{(2\pi)^4} \left[\bar{u}_e(p_3)\gamma_\nu(1-\gamma_5)\frac{(\not{p}_1 - \not{k})}{(p_1-k)^2}\gamma_\mu(1-\gamma_5)u_e(p_1) \right] \\ & \times \left[\bar{u}_u(p_4)\gamma^\nu(1-\gamma_5)\frac{(\not{p}_2 + \not{k})}{(p_2+k)^2}\gamma^\mu(1-\gamma_5)u_u(p_2) \right] \\ & \times \frac{1}{(k^2 - M_W^2)[(q-k)^2 - M_W^2]}. \end{aligned} \tag{4.140}$$

Inside the leptonic current we have:

$$\begin{aligned}
&\bar{u}_e(p_3)\gamma_\nu(1-\gamma_5)(\not{p}_1-\not{k})\gamma_\mu(1-\gamma_5)u_e(p_1)\\
&\quad=2\bar{u}_e(p_3)\gamma_\nu(\not{p}_1-\not{k})\gamma_\mu(1-\gamma_5)u_e(p_1)\\
&\quad\approx-2\bar{u}_e(p_3)\gamma_\nu\not{k}\gamma_\mu(1-\gamma_5)u_e(p_1).
\end{aligned}\tag{4.141}$$

$$\begin{aligned}
\Rightarrow M_{WW}^{\text{box}}\approx-\frac{g^4}{16}\int\frac{d^4k}{(2\pi)^4}\bar{u}_e(p_3)\gamma_\nu\gamma_\beta\gamma_\mu k^\beta(1-\gamma_5)u_e(p_1)\frac{1}{k^2(k^2-M_W^2)^2}\\
\times\bar{u}_u(p_4)\gamma^\nu\frac{1}{\not{k}}\gamma^\mu(1-\gamma_5)u_u(p_2).
\end{aligned}\tag{4.142}$$

We can then use the Chisolm identity inside our lepton current, which states that:

$$\begin{aligned}
\gamma_\nu\gamma_\beta\gamma_\mu k^\beta &= (\gamma_\mu k_\nu+\gamma_\nu k_\mu)-g_{\nu\mu}\not{k}+i\epsilon_{\nu\beta\mu\alpha}\gamma^\alpha\gamma_5 k^\beta\\
&\equiv P_{\mu\nu}+(NP)_{\mu\nu}.
\end{aligned}\tag{4.143}$$

The first & second terms refer to "pinch" & "non-pinch" respectively for their effect on the intermediate quark propagator in M_{WW}^{box}. In the literature [58]-[59] the so-called "pinch technique" refers to the same mathematical effect as $P_{\mu\nu}$ above. However, here it will not be used to form a gauge-invariant SE – and so I will call this the "superficial pinch technique" (SPT)

to distinguish the two. Keeping only the pinch term gives the pinch part of the box:

$$\begin{aligned} M_{WW}^{\rm box}|_p &= -\frac{g^4}{16}\int\frac{d^4k}{(2\pi)^4}\bar{u}_e(p_3)(\gamma_\mu k_\nu+\gamma_\nu k_\mu)(1-\gamma_5)u_e(p_1)\frac{1}{k^2(k^2-M_W^2)^2} \\ &\quad\times\bar{u}_u(p_4)\gamma^\nu\frac{1}{\not{k}}\gamma^\mu(1-\gamma_5)u_u(p_2) \\ &= -\frac{g^4}{8}\int\frac{d^4k}{(2\pi)^4}\bar{u}_e(p_3)\gamma_\mu(1-\gamma_5)u_e(p_1)\frac{1}{k^2(k^2-M_W^2)^2} \\ &\quad\times\bar{u}_u(p_4)\gamma^\nu(1-\gamma_5)u_u(p_2) \\ &= \bar{u}_e(p_3)\gamma_\mu(1-\gamma_5)u_e(p_1)\bar{u}_u(p_4)\gamma^\nu(1-\gamma_5)u_u(p_2) \\ &\quad\times\left[-\frac{g^4}{8}\int\frac{d^4k}{(2\pi)^4}\frac{1}{k^2(k^2-M_W^2)^2}\right]. \end{aligned} \tag{4.144}$$

Then using:

$$\int\frac{d^4k}{(2\pi)^4}\frac{1}{k^2(k^2-M_W^2)^2}=\eta\frac{M_W^2B_0(0;M_W,M_W)-A_0(M_W)}{M_W^4}=-\frac{\eta}{M_W^2}, \tag{4.145}$$

with $\eta=-1/\pi^2$, our pinched box is fully reduced as:

$$M_{WW}^{\rm box}|_p=\bar{u}_e(p_3)\gamma_\mu(1-\gamma_5)u_e(p_1)\bar{u}_u(p_4)\gamma^\nu(1-\gamma_5)u_u(p_2)\left(\frac{-g^4}{8\pi^2M_W^2}\right). \tag{4.146}$$

We will also need to calculate the non-pinch part of (4.142) and it is:

$$\begin{aligned} M_{WW}^{box}|_{NP} &= -\frac{g^4}{16}\int\frac{d^4k}{(2\pi)^4}\frac{\bar{u}_e(p_3)(-g_{\nu\mu}\not{k}+i\epsilon_{\nu\beta\mu\alpha}\gamma^\alpha\gamma_5 k^\beta)(1-\gamma_5)u_e(p_1)}{k^2(k^2-M_W^2)^2} \\ &\quad\times\bar{u}_u(p_4)\gamma^\nu\frac{1}{\not{k}}\gamma^\mu u_u(p_2) \\ &= \frac{g^4}{16}\int\frac{d^4k}{(2\pi)^4}\Bigg[\bar{u}_e(p_3)\gamma^\delta(1-\gamma_5)u_e(p_1)\bar{u}_u(p_4)\gamma^\nu\gamma^\alpha\gamma^\mu(1-\gamma_5)u_u(p_2) \\ &\quad\times\frac{g_{\nu\mu}k_\delta k_\alpha}{k^{2^2}(k^2-M_W^2)^2}-\bar{u}_e(p_3)\gamma^\alpha\gamma_5(1-\gamma_5)u_e(p_1) \\ &\quad\times\bar{u}_u(p_4)\gamma^\nu\gamma^\tau\gamma^\mu(1-\gamma_5)u_u(p_2)\frac{i\epsilon_{\nu\beta\mu\alpha}k^\beta k_\tau}{k^{2^2}(k^2-M_W^2)^2}\Bigg]. \end{aligned} \tag{4.147}$$

Then using:

$$\int\frac{d^4k}{(2\pi)^4}\frac{k^\mu k^\nu}{k^{2^2}(k^2-M_W^2)^2} = \frac{1}{4}\int\frac{d^4k}{(2\pi)^4}\frac{g^{\mu\nu}}{k^2(k^2-M_W^2)^2} \tag{4.148}$$

$$= \frac{1}{4\pi^2M_W^2}g^{\mu\nu}, \tag{4.149}$$

allows us to get our reduced non-pinched box:

$$\begin{aligned} M_{WW}^{box}|_{NP} = \frac{g^4}{64\pi^2M_W^2}\big[&\bar{u}_e(p_3)\gamma_\alpha(1-\gamma_5)u_e(p_1)\bar{u}_u(p_4)\gamma^\nu\gamma^\alpha\gamma_\nu(1-\gamma_5)u_u(p_2) \\ &-i\bar{u}_e(p_3)\gamma^\alpha\gamma_5(1-\gamma_5)u_e(p_1)\bar{u}_e(p_4)\gamma^\nu\gamma^\beta\gamma^\mu(1-\gamma_5)u_u(p_2)\epsilon_{\nu\beta\mu\alpha}\big]. \end{aligned} \tag{4.150}$$

We could further simplify the first term using $\gamma^\nu\gamma^\alpha\gamma_\nu = -2\gamma^\alpha$, but the term $\sim \gamma^\nu\gamma^\beta\gamma^\mu\epsilon_{\nu\beta\mu\alpha}$ is irreducible. So far, we have been using a ratio of

amplitudes to derive our $Q_W(p)$ corrections, but it will be instructional to use a ratio of cross sections here, just as (3.3) suggests. For the tree-level amplitudes, we have:

$$\begin{aligned} M_\gamma^*(\lambda) &= \frac{ie^2}{q^2}\bar{u}_u(p_2)\gamma_\alpha u_u(p_4)\bar{u}_e^\lambda(p_1)\gamma^\alpha u_e(p_3) && (4.151)\\ M_Z(\lambda) &= -\frac{ig^2}{c_W^2(q^2-M_Z^2)}\bar{u}_e(p_3)\gamma_\mu(g_V^e-g_A^e\gamma_5)u_e^\lambda(p_1) \\ &\quad \times\bar{u}_u(p_4)\gamma^\mu(g_V^p-g_A^p\gamma_5)u_u(p_2). && (4.152)\end{aligned}$$

With these two expressions, we can evaluate the Born cross section:

$$\begin{aligned} \sigma_{\rm Born}(\lambda) &= \sum_{spins} M_\gamma^* M_Z \approx \frac{e^4}{2s_W^2c_W^2q^2M_Z^2}{\rm Tr}[\not{p}_2\gamma_\alpha\not{p}_4\gamma^\mu(g_V^p-g_A^p\gamma_5)] \\ &\quad \times{\rm Tr}[(1+\lambda\gamma_5)\not{p}_1\gamma^\alpha\not{p}_3\gamma_\mu(g_V^e-g_A^e\gamma_5)] \\ &= \frac{16e^4}{s_W^2c_W^2M_Z^2q^2}\big\{(p_1\cdot p_4)(p_2\cdot p_3)[g_V^e(g_A^p\lambda+g_V^p)-g_A^e(g_A^p+g_V^p\lambda)] \\ &\quad +(p_1\cdot p_2)(p_3\cdot p_4)[g_A^e(g_A^p-g_V^p\lambda)+g_V^e(g_V^p-g_A^p\lambda)].\big\} && (4.153)\end{aligned}$$

Then we will take the PV combination: $(\lambda=-1)-(\lambda=+1)$ as well as use:

$$p_1\cdot p_4 \approx -\frac{u}{2} \approx p_2\cdot p_3, \qquad (4.154)$$

$$p_1\cdot p_2 \approx \frac{s}{2} \approx p_3\cdot p_4, \qquad (4.155)$$

to get:

$$\sigma_{Born}^{PV} = \frac{8e^4}{s_W^2c_W^2M_Z^2q^2}[u^2(g_A^eg_V^p-g_A^pg_V^p)+s^2(g_A^eg_V^p+g_A^pg_V^e)]. \qquad (4.156)$$

At forward scattering $s^2 \approx u^2$, so we simply get:

$$\sigma_{Born}^{PV} \approx \frac{16e^4 s^2}{s_W^2 c_W^2 M_Z^2 q^2} g_A^e g_V^p. \tag{4.157}$$

Meanwhile, in the numerator of our correction, we must compute:

$$\sigma_{WW}^{box}|_p = \sum_{\text{spins}} M_\gamma^* M_{WW}^{box}|_p, \tag{4.158}$$

$$\begin{aligned}
\Rightarrow \sigma_{WW}^{box}|_p &= \left(\frac{ie^2}{q^2}\right)\left(\frac{-ig^4}{8M_W^2}\right)\frac{1}{2}\text{Tr}[\not{p}_2\gamma_\alpha \not{p}_4 \gamma^\mu(1-\gamma_5)] \\
&\quad \times \text{Tr}[(1+\lambda\gamma_5)\not{p}_1\gamma^\alpha \not{p}_3 \gamma_\mu(1-\gamma_5)] \\
&= \frac{e^6}{16\pi^2 M_W^2 s_W^4 q^2}[-64(\lambda-1)(p_1\cdot p_2)(p_3\cdot p_4)], \\
\Rightarrow \sigma_{WW}^{box}|_p^{PV} &= \frac{2e^6 s^2}{\pi^2 M_W^2 s_W^4 q^2}.
\end{aligned} \tag{4.159}$$

Thus the correction due to $M_{WW}^{\text{box}}|_p$ will be:

$$\begin{aligned}
\delta_{WW}^{\text{box}}|_p = \frac{\sigma_{WW}^{\text{box}}|_p^{PV}}{\sigma_{Born}^{PV}} &= \frac{2e^6 s^2}{\pi^2 M_W^2 s_W^4 q^2}\frac{s_W^2 c_W^2 M_Z^2 q^2}{16e^4 s^2 g_A^e g_V^p} \\
&= \frac{e^2}{8\pi^2 s_W^2} \\
&= \frac{\alpha}{2\pi s_W^2}.
\end{aligned} \tag{4.160}$$

We can repeat this process for the non-pinch part. The first & second terms

of (4.150) respectively yields:

$$\begin{aligned} \sigma_{WW}^{box}|_{NP}^{PV} &= \frac{e^6 s^2}{2\pi^2 q^2 M_W^2 s_W^4} + \frac{3e^6 s^2}{2\pi^2 q^2 M_W^2 s_W^4} \\ &= \frac{2e^6 s^2}{\pi^2 q^2 M_W^2 s_W^4}, \qquad (4.161) \\ \Rightarrow \delta_{WW}^{box}|_{NP}^{PV} &= \frac{\alpha}{2\pi s_W^2}. \qquad (4.162) \end{aligned}$$

Indeed this entire analysis can be repeated for the crossed box and the final results are nicely organized into Table 4.1 below.

$\delta_{WW} \times \frac{\alpha}{\pi s_W^2}$	Pinch	Non-pinch	Sum
BOX	$\frac{1}{2}$	$\frac{1}{2}$	1
XBOX	$-\frac{1}{2}$	$\frac{1}{4}$	$-\frac{1}{4}$
Proton sum	$\frac{2}{4}$	$\frac{5}{4}$	$\frac{7}{4}$

Table 4.1: $\Box_{WW}$ corrections decomposed between box and crossed box as well as pinch and non-pinch components.

The total proton sum is consistent with (4.139) as we require. The interesting physics here is that the total pinch sum is independent of the details of the strong interaction, as it corresponds to a WW box with the intermediate hadron propagator pinched out. The non-pinch sum, however, is at the mercy of pQCD corrections in α_S. Therefore, we may use these results to generalize (4.139) to:

$$\Box_{WW} = \frac{\alpha}{4\pi s_W^2}\left[2 + 5\Big(1 - \frac{\alpha_S(M_W)}{\pi}\Big)\right]. \qquad (4.163)$$

4.9 $\Box_{\gamma Z}$ Correction

The γZ box correction has been calculated dispersively by a number of groups [60]-[66]. Rather than give a detailed explanation of the computation of this correction, I will simply give a quick summary, as the work of this dissertation did not focus on this particular RC. In the case of $e^- p$ scattering, both the V coupling and A coupling to the hadron makes a contribution to $Q_W(p)$. Furthermore, their energy dependence is of interest unlike the $\Box^{\gamma W}$ correction, which only matters at zero energy. Concerning the dispersion relations, the vector and axial-vector corrections have the following general relations [64]:

$$\mathrm{Re}\Box^V_{\gamma Z}(E) = \frac{2E}{\pi} P \int_0^\infty dE' \frac{1}{E'^2 - E^2} \mathrm{Im}\Box^V_{\gamma Z}(E'), \tag{4.164}$$

$$\mathrm{Re}\Box^A_{\gamma Z}(E) = \frac{2}{\pi} P \int_0^\infty dE' \frac{E'}{E'^2 - E^2} \mathrm{Im}\Box^A_{\gamma Z}(E'). \tag{4.165}$$

Due to the factor of E in (4.164), the vector correction goes to 0 as $E \to 0$, while the axial correction remains finite in this limit – as we have seen from (3.56). The imaginary parts of $\Box^V_{\gamma Z}$ and $\Box^A_{\gamma Z}$ have been calculated, and in

terms of structure functions, they are given by [65]:

$$\begin{aligned}
\mathrm{Im}\Box^V_{\gamma Z}(E) &= \frac{1}{(s-M^2)^2}\int_{W_\pi^2}^{s} dW^2 \int_0^{Q^2_{max}} dQ^2 \frac{\alpha(Q^2)}{1+Q^2/M_Z^2} \\
&\quad \times \left[F_1^{\gamma Z} + \frac{s(Q^2_{max}-Q^2)}{Q^2(W^2-M^2+Q^2)} F_2^{\gamma Z} \right], \qquad (4.166) \\
\mathrm{Im}\Box^A_{\gamma Z}(E) &= \frac{1}{(s-M^2)^2}\int_{W_\pi^2}^{s} dW^2 \int_0^{Q^2_{max}} dQ^2 \frac{v_e(Q^2)\alpha(Q^2)}{1+Q^2/M_Z^2} \\
&\quad \times \left[\frac{2ME}{W^2-M^2+Q^2} - \frac{1}{2} \right] F_3^{\gamma Z}, \qquad (4.167)
\end{aligned}$$

where $v_e(Q^2) = 1 - 4s^2_W(Q^2)$, $s = M^2 + 2ME$ and $Q^2_{max} = 2ME(1 - W^2/s)$. The $F^{\gamma Z}_{1,2,3}$ interference structure functions have been modeled with various parameterizations from SBMTH [61] - [63], GHRM [64] - [65], CR [66] and their results for the vector part are given in Table 4.2.

Authors	$\Box^V_{\gamma Z}(E = 1.165\mathrm{GeV}) \times 10^{-3}$
SBMTH	5.57 ± 0.36
GHRM	5.46 ± 2.0
CR	5.7 ± 0.9

Table 4.2: $\Box^V_{\gamma Z}$ corrections computed by 3 separate research groups.

The axial box has been computed as well. (4.167) can be substituted into (4.165) and the $\int dE'$ integration evaluated. The details of this procedure have already been described for $\Box^{\gamma W}_A$ in section 3.2. This time we can keep

the energy dependence in, and the result is [61]:

$$\Box^A_{\gamma Z}(E) = \frac{2}{\pi}\int_0^\infty dQ^2 \frac{v_e(Q^2)\alpha(Q^2)}{Q^2(1+Q^2/M_Z^2)}\int_0^1 dx F_3^{\gamma Z}(x,Q^2) f(x,Q), \tag{4.168}$$

$$f(x,Q) = \frac{1}{t^2}\left[\ln\left(1-\frac{t^2}{r^2}\right) + 2t\tanh^{-1}\left(\frac{t}{r}\right)\right], \tag{4.169}$$

$$t \equiv \frac{4MEx}{Q^2}, \tag{4.170}$$

$$r \equiv 1+\sqrt{1+4M^2x^2/Q^2}, \tag{4.171}$$

which simply reduces to (3.104) when $\{v_e \to 1,\ M_Z \to M_W,\ E \to 0\}$. In 2011, the authors of [61] found this contribution at zero energy to be: $\Box^A_{\gamma Z}(0) = (4.4 \pm .4)\times 10^{-3}$ and to have a rather mild energy dependence. At the Qweak beam energy the axial corrections are shown in Table 4.3, which are again, all very complementary to one another.

Authors	$\Box^A_{\gamma Z}(E = 1.165\text{GeV}) \times 10^{-3}$
SBMTH	$3.7 \pm .4$
EGRM*	$3.97 \pm .22$
CR	$4.0 \pm .5$

Table 4.3: $\Box^A_{\gamma Z}$ corrections computed by 3 separate research groups. *EGRM is a recently updated value [67].

4.10 Updating $Q_W(p)$

Putting together the results of sections 4.2 - 4.9 we can state the following expression for the 1-loop corrected weak charge of the proton:

$$\begin{aligned} Q_W^{p,NLO}(Q^2) &= (\rho_{NC}^{NLO} + \Delta_e)\left[1 - 4\sin^2\theta_W^{PT}(Q^2) + \Delta_e'(Q^2) + \Delta_{NP}\right] \\ &\quad + \Box_{WW} + \Box_{ZZ} + \Box_{\gamma Z}(E). \end{aligned} \tag{4.172}$$

Q_W^p is only defined at $Q^2 = 0$, in accordance to equation (1.76). However, both $\sin^2\theta_W^{PT}$ and Δ_e' were found to have a Q^2-dependence between the Thomson and scattering limits. Since no $e^- p \to e^- p$ PVES experiment can be done at $Q^2 = 0$, we keep the full Q^2 dependence where it is due here. The catch being that any explicit Q^2-dependence in the RHS of (4.172) must be placed into the 2nd term on the RHS of (1.76) when $Q_W(p)$ is extracted from a fit to PVES cross section data. In Table 4.4, I have included all of the terms of the RHS of (4.172), to summarize my findings. For the parameter ρ_{NC}^{NLO}, I use an updated value of from the Particle Data Group [68].

Correction	Expression	$Q^2 = 0$	$Q^2 = .025\text{GeV}^2$
ρ_{NC}^{NLO}	(206-207)	1.00066	1.00066
$\sin^2\theta_W^{PT}$	(252),(296),(297-302)	0.23867	0.23847
Δ_e	(243),(249)	0.00116	0
Δ_e'	(243),(249)	-0.00141	-0.00084
Δ_{NP}	(307)	.00221	.00221
$\Box_{WW}$	(361)	.01831	.01831
$\Box_{ZZ}$	(324)	.00183	.00183
$\Box_{\gamma Z}\vert_{E=0}$	(362-363)	.0044	.0044
$Q_W^{NLO}(p)$	(370)	.07069	undefined

Table 4.4: Radiative corrections to $Q_W(p)$ considered at both the Thomson and Scattering limits.

A meaningful goal from this analysis is to extract the weak mixing angle from a measurement of $Q_W(p)$ as suggested by (1.75). We will use an updated version of (1.75) which comes from our (4.172), as we would like to use the gauge-invariant pinch technique definition of $\sin^2\theta_{W,PT}$. This was done by the authors of [53], who quote their experimental value of the weak charge of the proton as:

$$Q_W(p)|_{\text{Qweak}} = 0.0719 \pm .0045\ . \tag{4.173}$$

Using this experimental value together with the results of Table 4.4 at $Q^2 = 0$, I find consistent results with [53] for the weak mixing angle at the Thomson limit:

$$\sin^2\theta_{W,PT}(0) = 0.2384 \pm .0011\ . \tag{4.174}$$

This result is in agreement with the SM prediction of [52]: $\sin^2\theta_W(0) = 0.23867 \pm .00016$, which is claimed to be commensurate with the pinch technique definition. It is recommended to those with available data on A_{LR}^{ep} to re-extract $Q_W(p)$ with the newly-determined Q^2-dependent RCs provided in this dissertation, and repeat this test of $\sin^2\theta_W$.

Chapter 5

Conclusion and Remarks

Now that all of the important radiative corrections have been calculated, it is time to understand what conclusions they lead to. We have already discussed the effect of the RCs to the proton's weak charge in chapter 4, and so in chapter 5 we will now study our results for $\Box_A^{\gamma W}$, which was computed in chapter 3. First I will revise the CKM matrix element V_{ud} and its effect on the unitarity condition. Next, I discuss a relationship between the CC valence structure function to the NC ones, which allows a comparison of this work to previous work on the γZ box. Finally, I will detail new constraints which can be placed on a few SM extensions (BSM physics).

5.1 Revising V_{ud}

Our job now is to take the computed radiative corrections of section 3 and apply them to update V_{ud}. The Δ_R^V inside (1.80) is given by:

$$\begin{aligned} \Delta_R^V &= \frac{\alpha}{2\pi}\left[3\ln\frac{M_Z}{M} - \ln c_W\right] + 2\Box_A^{\gamma W} \\ &= 0.017007 + 2\Box_A^{\gamma W}, \end{aligned} \tag{5.1}$$

where the .017007 also includes the re-summed logarithm analysis of Marciano & Sirlin [11]. Inserting our new, dispersively computed $\Box_A^{\gamma W}$ from Table 3.3 then gives:

$$\Delta_R^V = .024767 \pm .000184\ . \tag{5.2}$$

Then this will be inserted into (1.80) with $Ft = 3072.07 \pm .63$ to give:

$$|V_{ud}|^2_{\text{superallowed}} = .94799(26)\ . \tag{5.3}$$

The 2018 PDG gives us the other matrix elements of the top CKM row. They are [70]: $|V_{us}|^2 = .05031(16)$ and $|V_{ub}|^2 = .00002(0)$. We can then define the following convenient CKM unitarity test quantity:

$$\Sigma_{CKM}^{3\times 3} \equiv |V_{ud}|^2 + |V_{us}|^2 + |V_{ub}|^2, \tag{5.4}$$

and with our values above, the experimental value of this quantity becomes:

$$\Sigma_{CKM}^{3\times3} = .99832(42), \tag{5.5}$$

which falls short of 1 by $\sim 4\sigma$. Although this is not compelling evidence that the SM is incorrect, indeed tension has been raised with the CKM unitarity condition. Before this dispersive analysis was performed on $\Box_A^{\gamma W}$, the latest consensus from [14] gave $|V_{ud}|^2 = .94907(29)$ which had Σ_{CKM} in agreement with 1. A comparison is shown in Table 5.1 for this unitarity result between 3 research groups, as extracted from the totals in Table 3.3.

Authors	$\Box_{\gamma W}^{A} \times 10^{-3}$	$\Sigma_{CKM}^{3\times3}$
MS '06	3.26(19)	.9994(5)
SGRM '18	3.79(10)	.9984(4)
SBM '19	3.88(13)	.9983(4)

Table 5.1: $\Box_{\gamma W}^{A}$ corrections computed by 3 separate research groups and their effect on the SM CKM unitarity prediction.

The dispersive analysis is one which aims to improve $\Box_A^{\gamma W}$ in both the accuracy of its central value and by reducing the hadronic uncertainty. Looking at Table 5.1, we see that this has essentially been accomplished. Our final uncertainty is largely due to the Regge region, and to a lesser extent, the elastic region. The poor data shown in Figure 3.20 should really be updated, should new low Q^2 data allow it.

Although not as precise as the superallowed β decay case of (1.80), V_{ud} may

also be extracted from neutron lifetime measurements via (1.82). Here we need to know the correction Δ_R, which contains both inner and outer radiative corrections. Combining (2.1) & (2.3) gives us:

$$\Delta_R = \frac{\alpha}{2\pi}\left[3\ln\Big(\frac{M_p}{2E_m}\Big) + \frac{81}{10} - \frac{4\pi^2}{3}\right] + \Delta_R^V. \tag{5.6}$$

We already have our Δ_R^V, and the terms inside the square brackets are:

$$\frac{3\alpha}{2\pi}\ln\Big(\frac{M_p}{2E_m}\Big) = .02094, \tag{5.7}$$

$$\frac{\alpha}{2\pi}\left(\frac{81}{10} - \frac{4\pi^2}{3}\right) = -.005876, \tag{5.8}$$

$$\Rightarrow \frac{\alpha}{2\pi}\bar{g}(E_m) = .015064, \tag{5.9}$$

and this means we will get:

$$\Delta_R = 0.03983(18)\ . \tag{5.10}$$

Meanwhile PDG (2018) gives us for the neutron: $\tau_n = 879.3(9)s$ and $\lambda = -1.2723(23)$. Substituting all of these numbers into (1.82) then gives one:

$$|V_{ud}|^2_{\text{neutron}} = .9524(12), \tag{5.11}$$

which easily agrees with $\Sigma^{3\times3}_{CKM} = 1$ within uncertainty, but it clearly has an absolute uncertainty nearly 3 times greater than that estimated from super-

allowed β decays. Perhaps with improved future λ measurements, $|V_{ud}|_{\text{neutron}}$ can be competitive with (5.3).

5.2 Relating $F_3^{(0)}$ to $F_3^{\gamma Z}$

There is a strong connection between the structure function $F_3^{(0)}$ found in CC processes and the function $F_3^{\gamma Z}$ which is found in NC processes. This was pointed out by the authors of [30], and a detailed proof will be given below. Understanding this connection will allow us to freely compare previous results for $\Box_A^{\gamma Z}$ to our new results for $\Box_A^{\gamma W}$. To begin establishing this relationship, consider the axial current of the W-bosons:

$$A_i^\mu = \bar{q}\gamma^\mu\gamma_5\tau_i q, \tag{5.12}$$

which is a rank 1 tensor in isospin space. This is traditionally decomposed into ladder operators and a z-component via:

$$A_1^{\pm 1,\mu} = \mp\frac{1}{\sqrt{2}}(A_1^\mu \pm iA_2^\mu), \tag{5.13}$$

$$A_1^{0,\mu} = A_3^\mu. \tag{5.14}$$

The axial charged and axial weak currents are defined as:

$$(J_W^\mu)_A = \frac{1}{\sqrt{2}}A_1^{1,\mu}, \tag{5.15}$$

$$(J_Z^\mu)_A = -\frac{1}{2}A_1^{0,\mu}. \tag{5.16}$$

Meanwhile, the Wigner-Eckart theorem states that a spherical tensor's matrix element in angular momentum space is related to a product of a Clebsch-

Gordon coefficient and its "reduced" matrix element which is independent of the z-component substates:

$$\langle jm|T_q^{(k)}|j'm'\rangle = \frac{\langle j'm'kq|jm\rangle}{\sqrt{2j'+1}}\langle j'||T^{(k)}||j\rangle, \tag{5.17}$$

which can perfectly apply to the case of $|jm\rangle$ in isospin space. The hadronic tensor in our γW box is proportional to the interference matrix elements of the isoscalar EM current and the axial weak current:

$$F_3^{(0)} \sim \langle p|J_{EM}^{(0)\mu}(J_W^\nu)_A|n\rangle, \tag{5.18}$$

whilst (5.15) implies that:

$$\begin{aligned}
\langle p|(J_W^\nu)_A|n\rangle &= \Big\langle \frac{1}{2}, +\frac{1}{2}\Big|\frac{1}{\sqrt{2}}A_1^{1,\nu}\Big|\frac{1}{2}, -\frac{1}{2}\Big\rangle \\
&= \frac{1}{\sqrt{2}}\Big\langle \frac{1}{2}, +\frac{1}{2}\Big|A_1^{1,\nu}\Big|\frac{1}{2}, -\frac{1}{2}\Big\rangle, \\
\Rightarrow \langle p|(J_W^\nu)_A|n\rangle &= \frac{1}{\sqrt{2}}C\Big(\frac{1}{2}\ 1\ \frac{1}{2}; -\frac{1}{2}\ 1\ +\frac{1}{2}\Big)\Big\langle \frac{1}{2}\Big|\Big|A_1^{1,\nu}\Big|\Big|\frac{1}{2}\Big\rangle,
\end{aligned} \tag{5.19}$$

where $C(jkj'; mqm') \equiv \langle j'm'kq|jm\rangle$ are the traditional C-G coefficients, and in particular $C\Big(\frac{1}{2}\ 1\ \frac{1}{2}; -\frac{1}{2}\ 1\ +\frac{1}{2}\Big) = \sqrt{2/3}$. Thus:

$$\langle p|(J_W^\nu)_A|n\rangle = \frac{1}{\sqrt{3}}\Big\langle \frac{1}{2}\Big|\Big|A_1^{1,\nu}\Big|\Big|\frac{1}{2}\Big\rangle. \tag{5.20}$$

Meanwhile let's consider the isovector combination of $(J^\nu_Z)_A$ currents:

$$\begin{aligned}
\langle p|(J^\nu_Z)_A|p\rangle - \langle n|(J^\nu_Z)_A|n\rangle &= -\frac{1}{2}\Big\langle \frac{1}{2}, +\frac{1}{2}\Big| A_1^{0,\nu}\Big|\frac{1}{2}, +\frac{1}{2}\Big\rangle \\
&\quad +\frac{1}{2}\Big\langle \frac{1}{2}, -\frac{1}{2}\Big| A_1^{0,\nu}\Big|\frac{1}{2}, -\frac{1}{2}\Big\rangle \\
&= -\frac{1}{2}C\Big(\frac{1}{2}\ 1\ \frac{1}{2}; \frac{1}{2}\ 0\ +\frac{1}{2}\Big)\Big\langle \frac{1}{2}\Big\|A_1^{0,\nu}\Big\|\frac{1}{2}\Big\rangle \\
&\quad +\frac{1}{2}C\Big(\frac{1}{2}\ 1\ \frac{1}{2}; -\frac{1}{2}\ 0\ -\frac{1}{2}\Big)\Big\langle \frac{1}{2}\Big\|A_1^{0,\nu}\Big\|\frac{1}{2}\Big\rangle \\
&= -\frac{1}{2}\left(-\frac{1}{\sqrt{3}}\right)\Big\langle \frac{1}{2}\Big\|A_1^{0,\nu}\Big\|\frac{1}{2}\Big\rangle \\
&\quad +\frac{1}{2}\left(+\frac{1}{\sqrt{3}}\right)\Big\langle \frac{1}{2}\Big\|A_1^{0,\nu}\Big\|\frac{1}{2}\Big\rangle \\
&= \frac{1}{\sqrt{3}}\Big\langle \frac{1}{2}\Big\|A_1^{0,\nu}\Big\|\frac{1}{2}\Big\rangle \\
&= \frac{1}{\sqrt{3}}\Big\langle \frac{1}{2}\Big\|A_1^{1,\nu}\Big\|\frac{1}{2}\Big\rangle. \qquad (5.21)
\end{aligned}$$

Equating (5.20) to (5.21) means that:

$$\langle p|J^{(0)\mu}_{EM}(J^\nu_W)_A|n\rangle = \langle p|J^{(0)\mu}_{EM}(J^\nu_Z)_A|p\rangle - \langle n|J^{(0)\mu}_{EM}(J^\nu_Z)_A|n\rangle, \qquad (5.22)$$

since $J^{(0)\mu}_{EM}$ plays a superfluous role as an isospin operator here. Next, we can think of J^μ_{EM} as the sum of its isoscalar and isovector parts: $J^\mu_{EM} = J^{(0)\mu}_{EM} + J^{(3)\mu}_{EM}$, from which it follows from (5.22):

$$\begin{aligned}
\langle p|J^{(0)\mu}_{EM}(J^\nu_W)_A|n\rangle = \langle p|J^\mu_{EM}(J^\nu_Z)_A|p\rangle - \langle n|J^\mu_{EM}(J^\nu_Z)_A|n\rangle \\
-\langle p|J^{(3)\mu}_{EM}(J^\nu_Z)_A|p\rangle + \langle n|J^{(3)\mu}_{EM}(J^\nu_Z)_A|n\rangle. \qquad (5.23)
\end{aligned}$$

Since $(J_Z^\nu)_A \,\epsilon\, (I=1)$ and $J_{EM}^{(3)\mu} \,\epsilon\, (I=1)$ we can either have $J_{EM}^{(3)\mu}(J_Z^\nu)_A \,\epsilon (I=0)$ or $(I=2)$. The $(I=2)$ case vanishes under $\langle \frac{1}{2}, \pm\frac{1}{2}|...|\frac{1}{2}, \pm\frac{1}{2}\rangle$ and the $(I=0)$ case cancels in the combination $\langle p|...|p\rangle - \langle n|...|n\rangle$, leaving us with just:

$$\langle p|J_{EM}^{(0)\mu}(J_W^\nu)_A|n\rangle = \langle p|J_{EM}^{\mu}(J_Z^\nu)_A|p\rangle - \langle n|J_{EM}^{\mu}(J_Z^\nu)_A|n\rangle. \tag{5.24}$$

The RHS of (5.24) is directly proportional to the interference structure function found in the γZ box between proton and neutron. Taking the other time ordering of this equation into account (which is trivially satisfied in the same way), we recover the following relation between structure functions:

$$F_3^{(0)} = F_{3,p}^{\gamma Z} - F_{3,n}^{\gamma Z}. \tag{5.25}$$

The most precarious region from which we model $F_3^{(0)}$ is the Regge region. The fact that we still have no direct data on $F_3^{\gamma Z}$ in this region means that this relationship has very little chance of improving our model constraints on $F_{3,Reg}^{(0)}$. Instead, in a recent work [67], the axial part of the γZ box was re-computed with the help of the relation:

$$F_3^{\gamma Z} = \frac{1}{2}F_3^{\nu p + \bar{\nu} p} + F_3^{\gamma Z(0)}, \tag{5.26}$$

where $F_3^{\gamma Z(0)}$ is the small isosinglet component of $F_3^{\gamma Z}$. Both terms on the RHS can be modeled analogously to $F_3^{(0)}$ and fitted to the same neutrino data

[50]. Thus, the practical role of (5.25) for us is more of a consistency check at this point until tighter constraints can be put on our Regge region input data. As an exercise, we can see if our prediction for $\Box^{\gamma W}_{A,Reg}$ is consistent with previously used $F^{\gamma Z}_{3,Reg}$.

In [61] a relatively simple model was used for $F_3^{\gamma Z}$ in the Regge region which merely requires it to match the DIS prediction at the Regge-DIS boundary, but one that also forces $F_3^{\gamma Z}(x, Q^2 \to 0) \to 0$:

$$F^{\gamma Z}_{3,Reg} = \frac{1 + \Lambda^2/Q_0^2}{1 + \Lambda^2/Q^2} F^{\gamma Z}_{3,DIS}(x, Q_0^2), \tag{5.27}$$

which, in turn, has an identical x-dependence as the DIS model. Λ^2 is a free parameter which is in the range $(0.4 - 1.0)\mathrm{GeV}^2$. (5.27) can be separately applied to either the proton or neutron [62]. The difference is defined by $F^{\gamma Z}_{3,DIS}$ which is given by:

$$\begin{aligned} F^{\gamma Z}_{3,DIS} &= \Sigma_q 2 e_q g_A^q (q - \bar{q}) \\ &= \begin{cases} \frac{2}{3}u_{\mathrm{v}} + \frac{1}{3}d_{\mathrm{v}}, & \text{proton} \\ \frac{1}{3}u_{\mathrm{v}} + \frac{2}{3}d_{\mathrm{v}}, & \text{neutron} \end{cases} . \end{aligned} \tag{5.28}$$

Applying (5.25) to the RHS of (5.27) gives us:

$$\begin{aligned} F_{3,Reg}^{(0),Toy} &= \frac{1+\Lambda^2/Q_0^2}{1+\Lambda^2/Q^2}\left(F_{3,DIS}^{\gamma Z,p} - F_{3,DIS}^{\gamma Z,n}\right) \\ &= \frac{1+\Lambda^2/Q_0^2}{1+\Lambda^2/Q^2}\left(\frac{u_{\rm v}-d_{\rm v}}{3}\right) \\ &= \frac{1+\Lambda^2/Q_0^2}{1+\Lambda^2/Q^2}F_{3,DIS}^{(0)}. \end{aligned} \tag{5.29}$$

This is a toy model, as it is not rooted/supported by data or fundamental theory. Nonetheless, we can then attempt to compute $\Box_{A,Reg}^{\gamma W}$ from (5.29) for various values of Λ. The results of this exercise are given in Table 5.2.

Λ[GeV]	$\Box_{A,Reg}^{\gamma W} \times 10^{-3}$
.4	.42
.5	.41
.6	.39
.7	.38
.8	.37
.9	.36
1.0	.35

Table 5.2: $\Box_{\gamma W}^{A}$ contributions from the Regge region using the toy model in (5.29)

These values are certainly quite comparable to our $\Box_{A,Reg}^{\gamma W} = (.37 \pm .10) \times 10^{-3}$, and the central value of .37 corresponds to $\Lambda^2 \approx .64\text{GeV}^2$. One possible problem with (5.29) is in its Q^2-dependence. At low W^2, the Christy-Bosted parameterization of $F_3^{(0)}$ is physically motivated by cross section data and it is a monotonically increasing function as $Q^2 \to 0$, where it approaches a

constant at $Q^2 = 0$. $F_{3,Reg}^{(0)}$ as predicted by (3.137) also behaves this way at $W^2 = 4\text{GeV}^2$. On the other hand, $F_{3,Reg}^{(0),Toy}$ does not have this feature as $Q^2 \to 0$. However, it is greater than $F_{3,Reg}^{(0)}$ at intermediate Q^2 values. The end result is that on average, it has a similar area under it over the Regge range $0 \leq Q^2 \leq 2\text{GeV}^2$. As a result, their predictions when integrated inside $\Box_{A,Reg}^{\gamma W}$ are in very good agreement! In any event, it is reassuring to see that a previous $F_{3,Reg}^{\gamma Z}$ model can be reconciled with our new $F_{3,Reg}^{(0)}$ extracted from neutrino scattering data and Regge phenomenology.

5.3 BSM Constraints

One of the big questions we can ask ourselves with discovering a non-unitary CKM matrix is what new BSM physics can explain this. In principle, the total number of allowed fermion generations is not restricted to be 3. If our 3×3 CKM matrix in (1.41) isn't unitary as hinted by the result in (5.5), one possible remedy would be the existence of a 4th quark generation: (t', b'). Then the new CKM matrix would take the form:

$$V_{CKM}^{4\times4} = \begin{pmatrix} V_{ud} & V_{us} & V_{ub} & V_{ub'} \\ V_{cd} & V_{cs} & V_{cb} & V_{cb'} \\ V_{td} & V_{ts} & V_{tb} & V_{tb'} \\ V_{t'd} & V_{t's} & V_{t'b} & V_{t'b'} \end{pmatrix}, \tag{5.30}$$

and first row unitarity would then give:

$$\Sigma_{CKM}^{3\times3} = 1 - |V_{ub'}|^2. \tag{5.31}$$

(5.5) then places a constraint on this new matrix element:

$$|V_{ub'}| \leq .04095\ . \tag{5.32}$$

Furthermore, using global EW precision measurements, additional constraints on both the new matrix elements of (5.30) can be made, as well as minimum allowed masses of the 4th quark generation members. For instance, in [69],

the lower limits of the new quark masses are expected to be:

$$m_{t'} > 256\text{GeV}, \tag{5.33}$$

$$m_{b'} > 128\text{GeV}. \tag{5.34}$$

Global EW analyses are very useful, as introducing a SM extension such as that of a new quark generation will have consequences for many observables. Just as we saw how the heavy (t, b) quark pair affects ρ_{NC} in (4.9), a similar analysis would apply to (t', b'), giving a similar contribution which would involve their masses. We would also have a CKM angle θ_{34} defined by:

$$\begin{pmatrix} |V_{tb}| & |V_{tb'}| \\ |V_{t'b}| & |V_{t'b'}| \end{pmatrix} = \begin{pmatrix} \cos\theta_{34} & \sin\theta_{34} \\ \sin\theta_{34} & \cos\theta_{34} \end{pmatrix}. \tag{5.35}$$

The new mixing angle θ_{34} has been shown to be of the same order as the Cabbibo mixing θ_{12} between the first two quark generations [69]. There are yet other possible ways V_{CKM} can lose its unitarity as well – other candidates being the existence of RH currents or the existence of extra Z-bosons [71]. I will update the constraints on these two possibilities based on our new $|V_{ud}|^2$ value.

Parity violation is considered to be maximal in the SM, but the general form of the weak interaction could be somewhat relaxed to include RH currents.

In [72]-[73] the semileptonic Hamiltonian made such a generalization, where:

$$\begin{aligned} H_{sl} &= a_{LL}(V-A)_l(V-A)_h + a_{LR}(V-A)_l(V+A)_h \\ &\quad + a_{RL}(V+A)_l(V-A)_h + a_{RR}(V+A)_l(V+A)_h, \end{aligned} \tag{5.36}$$

in which (l, h) denotes (lepton,hadron). In the current SM, $a_{LL} = 1$ and $a_{LR} = a_{RL} = a_{RR} = 0$ and hence the 3 extra terms in (5.36) will be presumably very small with respect to the first. In Fermi β decay, the decay rate is given by [71]:

$$\Gamma_\beta \approx |a_{LL}|^2 \left(1 + 2\mathrm{Re}\frac{a_{LR}}{a_{LL}} \right). \tag{5.37}$$

We can also define an analogous Hamiltonian for the purely leptonic weak interactions, where the leptonic coupling constants are instead $c_{LL}, c_{LR}, c_{RL}, c_{RR}$. They are also related to the semileptonic constants via:

$$a_{LL} = c_{LL} V_{ud}^L, \tag{5.38}$$

$$a_{RL} = c_{RL} V_{ud}^L, \tag{5.39}$$

$$a_{LR} = c_{LR} e^{i\alpha} V_{ud}^R, \tag{5.40}$$

$$a_{RR} = c_{RR} e^{i\alpha} V_{ud}^R. \tag{5.41}$$

Since V_{ud} is proportional to the ratio of semileptonic to leptonic decay rates, it follows that:

$$|V_{ud}|^2_{\text{exper}} = \frac{\Gamma_\beta}{\Gamma_\mu} \approx |V^L_{ud}|^2(1 + 2\text{Re}\ \bar{a}_{LR}). \tag{5.42}$$

In fact, if this applies to the other 2 quark generations, we have:

$$\Sigma_{CKM} = 1 + 2\text{Re}\ \bar{a}_{LR}, \tag{5.43}$$

and our (5.5) imposes the following constraint on a_{LR}:

$$.9983(4) = 1 + 2\text{Re}\ \bar{a}_{LR}, \tag{5.44}$$

$$\Rightarrow \text{Re}\ \bar{a}_{LR} = -.0008 \pm .0002, \tag{5.45}$$

which is no longer consistent with being zero. At last, our unitarity result (5.5) can be used to place a lower mass limit on a new Z-boson particle. Were a new Z-boson (Z_χ) to exist, it will have a WZ_χ box diagram correction to the Fermi β decays analogous to the ZW box which enters Δ^V_R. As the authors of [71] explain, the first row unitarity condition can be then modified to:

$$\Sigma^{3\times3}_{CKM} = (.9983 \pm .0004) + \Delta = 1, \tag{5.46}$$

where Δ can be computed from the $Z_\chi W$ box and is:

$$\Delta = -\frac{27\alpha}{40\pi s_W^2}\frac{4}{3}|C_\chi|^2 \ln\frac{X_\chi}{X_\chi - 1}. \tag{5.47}$$

$|C_\chi|^2 = 1/2$ is the $Z_\chi f f$ coupling constant at low energies and $X_\chi \equiv M_{Z_\chi}^2/M_W^2$. We can then combine (5.46) and (5.47) to place a constraint on X_χ:

$$\begin{aligned} (.9983 \pm .0004) + \Delta &= 1, \\ \Rightarrow .0013 \leq \Delta &\leq .0021, \\ \Rightarrow -.4339 \leq \frac{\ln X_\chi}{X_\chi - 1} &\leq -.2686\ . \end{aligned} \tag{5.48}$$

Since M_{Z_χ} must be greater than M_W it simply follows that $\ln X_\chi/(X_\chi - 1)$ is strictly a positive number. Therefore, (5.48) can never be satisfied, which is evidence that a new heavy Z_χ-boson cannot exist.

Besides the obvious improvements to the input parameters of $F_3^{\gamma Z}$ & $F_3^{(0)}$, in a recent paper [74], a proposed new approach using the Feynman-Hellmann theorem together with Lattice techniques could be used to reduce the hadronic uncertainty of $\Box^{\gamma W}$ & $\Box^{\gamma Z}$ even further. This proves that 1 loop semileptonic corrections are still an exciting and active field, and one of great relevance to EW precision tests. As experimental precision tests improve in the future, the need will likely arise to reduce the hadronic uncertainties even further, which could in turn, help our very understanding of the nucleon itself – in fact, we are counting on it.

Appendices

A EW Feynman Rules

The EW Feynman rules can be derived from the full EW Lagrangian. Once this is done in the momentum basis, any future Feynman diagram calculation can start with applying the rules for any arrangement of propagators and interaction vertices. We choose to work exclusively in the Feynman Gauge, where the gauge-fixing parameter is set to 1. Also, for brevity sakes, I will only include the rules which we will actually need in this thesis. For the full set, the reader may find in [75].

A.1 Propagators

$$\mu \overset{\gamma}{\sim\sim} \nu = -\frac{ig_{\mu\nu}}{k^2-\lambda^2+i\epsilon}$$

$$\mu \overset{W}{\sim\sim} \nu = -\frac{ig_{\mu\nu}}{k^2-M_W^2+i\epsilon}$$

$$\mu \overset{Z}{\sim\sim} \nu = -\frac{ig_{\mu\nu}}{k^2-M_Z^2+i\epsilon}$$

$$\overset{f}{\longrightarrow} = -\frac{i(\not{k}+m_f)}{k^2-m_f^2+i\epsilon}$$

$$\overset{\varphi^\pm}{\text{- - - - -}} = -\frac{i}{k^2-M_W^2+i\epsilon}$$

$$\overset{\omega^\pm}{\cdots\cdots} = -\frac{i}{k^2-M_W^2+i\epsilon}$$

A.2 Quartic interactions

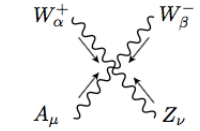

$$= iegc_W[2g_{\alpha\beta}g_{\mu\nu} - g_{\alpha\mu}g_{\beta\nu} - g_{\alpha\nu}g_{\beta\mu}]$$

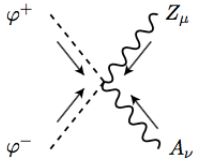

$$= -ieg\frac{\cos(2\theta_W)}{c_W}g_{\mu\nu}$$

A.3 Triple interactions

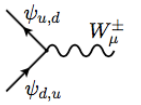

$$= \frac{ig}{\sqrt{2}}\gamma_\mu \frac{(1-\gamma_5)}{2}$$

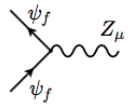

$$= \frac{ig}{2c_W}\gamma_\mu(g_V^f - g_A^f\gamma_5)$$

$$g_V^f \equiv T_f^3 - 2Q_f s_W^2$$

$$g_A^f \equiv T_f^3$$

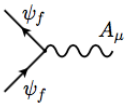

$$= -ieQ_f\gamma_\mu$$

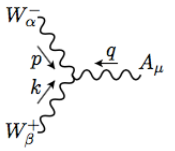

$$= -ie[g_{\alpha\beta}(p-k)_\mu + g_{\beta\mu}(k-q)_\alpha + g_{\mu\alpha}(q-p)_\beta]$$

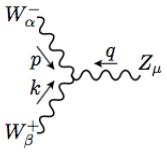

$$= igc_W[g_{\alpha\beta}(p-k)_\mu + g_{\beta\mu}(k-q)_\alpha + g_{\mu\alpha}(q-p)_\beta]$$

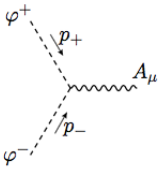

$$= -ie(p_+ - p_-)_\mu$$

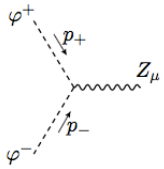

$$= \frac{ig\cos(2\theta_W)}{2c_W}(p_+ - p_-)_\mu$$

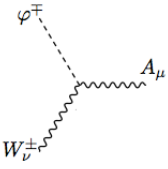

$$= -ieM_W g_{\mu\nu}$$

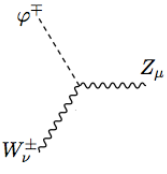

$$= -igM_Z s_W^2 g_{\mu\nu}$$

A.4 Ghost interactions

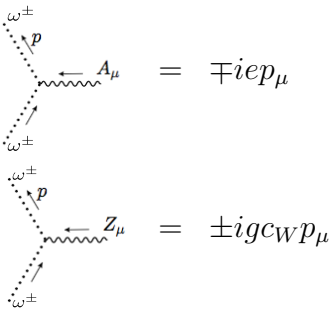

B Deep Inelastic Scattering Definitions

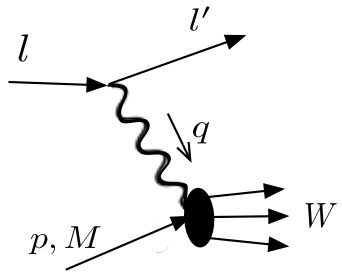

Figure 1: The DIS semileptonic scattering amplitude wherein the exchanged vector boson is potentially γ, W or Z.

$$
\begin{aligned}
Q^2 &= -q^2 = (l - l')^2 \\
\nu &= \frac{q \cdot p}{M} = \frac{W^2 + Q^2 - M^2}{2M} \\
x &= \frac{Q^2}{2M\nu} \\
W^2 &= (p + q)^2 = M^2 + 2M\nu - Q^2 \\
s &= (l + p)^2
\end{aligned}
$$

C Physical Constants Used

C.1 EW Parameters

$$
\begin{aligned}
\alpha_{EM}(0) &= 1/137.036 \\
M_Z &= 91.1876\text{GeV} \\
M_W &= 80.376\text{GeV} \\
M &= 0.93827\text{GeV} \\
s^2_W(M_Z) &= 0.23129 \\
c^2_W &\equiv M^2_W/M^2_Z = 0.77693 \\
m_e &= 0.511\text{MeV} \\
m_\mu &= 0.10566\text{GeV} \\
m_\tau &= 1.7768\text{GeV} \\
m_t &= 173.34\text{GeV} \\
m_b &= 4.199\text{GeV} \\
G_F &= 1.1663787 \times 10^{-5}\text{GeV}^{-2} \\
g_A &= 1.2723 \\
M_A &= 1.05 \pm 0.1\text{GeV}
\end{aligned}
$$

C.2 Resonance & Background Parameters

$D_{13}(1535)$ **Resonance:**

$$
\begin{aligned}
m_{D_{13}} &= 1.52\text{GeV} \\
\Gamma_{D_{13}} &= 0.125\text{GeV} \\
C_3^S(Q^2) &= \frac{1.82/D_V(Q^2)}{1+Q^2/(8.9M_V^2)} \\
C_4^S(Q^2) &= \frac{-0.59/D_V(Q^2)}{1+Q^2/(8.9M_V^2)} \\
C_5^S(Q^2) &= \frac{-0.65}{D_V(Q^2)} \\
C_5^A(Q^2) &= \frac{-2.1/D_A(Q^2)}{1+Q^2/(3M_A^2)} \\
D_V(Q^2) &= (1+Q^2/M_V^2)^2, \;\; M_V = 0.84\text{GeV} \\
D_A(Q^2) &= (1+Q^2/M_A^2)^2, \;\; M_A = 1.05\text{GeV}
\end{aligned}
$$

$\Delta(1232)$ **Resonance:**

$$\begin{aligned} m_\Delta &= 1.232\text{GeV} \\ \Gamma_\Delta &= 0.12\text{GeV} \\ C_3^V(Q^2) &= \frac{1.95/D_V(Q^2)}{1+Q^2/(4M_V^2)} \\ C_4^V(Q^2) &= -C_3^V\frac{M}{\sqrt{W^2}} \\ C_4^A(Q^2) &= -\frac{C_5^A}{4} \\ C_5^A(Q^2) &= \frac{1.2/D_A(Q^2)}{1+Q^2/(3M_A^2)} \end{aligned}$$

Christy-Bosted Parameters

$$\begin{aligned} Q_0^2 &= .05\text{GeV}^2 \\ \sigma_T^{NR,1}(0) &= 246.1\text{GeV}^{-2},\ \ \sigma_T^{NR,2}(0) = -89.4\text{GeV}^{-2} \\ a_1^T &= .0675,\ \ a_2^T = .2098 \\ b_1^T &= 1.3501,\ \ b_2^T = 1.5715 \\ c_1^T &= .1205,\ \ c_2^T = .0907 \\ d_1^T &= -.0038,\ \ d_2^T = .0104 \end{aligned}$$

C.3 Regge Region Parameters

$$\begin{aligned} \nu_0 &= 1\text{GeV} \\ \alpha_0^\rho &= 0.477 \\ \Lambda_{th} &= 1\text{GeV} \\ m_\rho &= .775\text{GeV} \\ m_{a_1} &= 1\text{GeV} \end{aligned}$$

D Plus Prescription

The plus prescription is a recipe for taming the poles of coefficient functions at $x = 1$. For the simple case of integrating these terms with an arbitrary (well-behaved) function we have:

$$\begin{aligned}\int_0^1 dz \frac{h(z)}{(1-z)_+} &= \int_0^1 dz \frac{h(z)-h(1)}{1-z} \\ \int_0^1 dz h(z) \left(\frac{\ln(1-z)}{1-z}\right)_+ &= \int_0^1 dz \big(h(z)-h(1)\big) \frac{\ln(1-z)}{1-z}\end{aligned}$$

However, when one computes the convolution such as that found in (3.113), these relations need to be somewhat generalized where they become:

$$\begin{aligned}\int_x^1 dz h(z,x) \left(\frac{1}{1-z}\right)_+ &= \int_x^1 dz [h(z,x)-h(1,x)] \frac{1}{1-z} \\ &\quad + h(1,x)\ln(1\text{-x}) \\ \int_x^1 dz h(z,x) \left(\frac{\ln(1-z)}{1-z}\right)_+ &= \int_x^1 dz [h(z,x)-h(1,x)] \frac{\ln(1-z)}{1-z} \\ &\quad + \frac{h(1,x)}{2} \ln^2(1-x)\end{aligned}$$

E Passarino Veltman Functions

All loop diagrams in the SM can be decomposed into a basis of 4 fundamental scalar loops through a process known as the Passarino Veltman reduction [76]. The evaluation of many of the Feynman diagrams in this thesis have been aided by 2 significant software packages: FeynCalc©[79], and Package X©[80]. The basis of 4 fundamental scalar loops are defined as:

$$A_0(m) = \frac{1}{i\pi^2}\int d^4k \frac{1}{k^2-m^2+i\epsilon}$$

$$B_0(p_1; m_0, m_1) = \frac{1}{i\pi^2}\int d^4k \frac{1}{(k^2-m_0^2+i\epsilon)[(k+p_1)^2-m_1^2+i\epsilon]}$$

$$C_0(p_1^2, (p_1-p_2)^2, p_2^2; m_0, m_1, m_2) = \frac{1}{i\pi^2}\int d^4k \frac{1}{(k^2-m_0^2+i\epsilon)[(k+p_1)^2-m_1^2+i\epsilon][(k+p_2)^2-m_2^2+i\epsilon]}$$

$$D_0(p_1^2, (p_1-p_2)^2, (p_2-p_3)^2, p_3^2, p_2^2, (p_1-p_3)^2; m_0, m_1, m_2, m_3) = \frac{1}{i\pi^2}\int d^4k$$

$$\times \frac{1}{(k^2-m_0^2+i\epsilon)[(k+p_1)^2-m_1^2+i\epsilon][(k+p_2)^2-m_2^2+i\epsilon][(k+p_3)^2-m_3^2+i\epsilon]}$$

When going from 1 point (A_0) up to 4 point (D_0) integrals, their evaluation rapidly becomes more difficult in the general case, and it is beneficial to just evaluate the 2-4 point functions for special cases, which are given below. There is also a very useful technique for regulating their UV divergences known as Dimensional Regularization, where the following extension is made:

$$\int \frac{d^4k}{(2\pi)^4} \to \mu^\epsilon \int \frac{d^dk}{(2\pi)^d}, \quad \epsilon = 4-d$$

where μ is an arbitrary mass scale called the t'Hooft mass, and we recover our reality in the limit $\epsilon \to 0$. Defining the UV-divergent quantity $\Delta_\epsilon = 2/\epsilon - \gamma_E + \ln 4\pi$, some useful PaVe functions used in this thesis are:

E.1 1 point

$$A_0(m) = m^2\left[\Delta_\epsilon - \ln\frac{m^2}{\mu^2} + 1\right]$$

E.2 2 point

$$\begin{aligned}
B_0(p^2;0,m) &= \Delta_\epsilon - \ln\frac{m^2}{\mu^2} + 2 + \frac{m^2-p^2}{p^2}\ln\left(\frac{m^2-p^2}{m^2}\right)\\
B_0(0;0,m) &= \Delta_\epsilon - \ln\frac{m^2}{\mu^2} + 1\\
B_0(m^2;0,m) &= \Delta_\epsilon - \ln\frac{m^2}{\mu^2} + 2\\
B_0(p^2;0,0) &= \Delta_\epsilon - \ln\left(\frac{-p^2}{\mu^2}\right) + 2\\
B_0(p^2;m,m) &\approx \Delta_\epsilon - \ln\frac{m^2}{\mu^2} + \frac{p^2}{6m^2}, \quad |p^2|, \ll m^2\\
B_0'(m^2;\lambda,m) &\equiv \frac{d}{dp^2}B_0(p^2;\lambda,m)\Big|_{p^2=m^2} \approx -\frac{1}{m^2}\left(\ln\frac{\lambda}{m} + 1\right)
\end{aligned}$$

E.3 3 point

$$
\begin{aligned}
C_0(m^2,m^2,0;m,\lambda,m) &\approx \frac{1}{m^2}\ln\frac{\lambda}{m}, \quad \lambda \ll m \\
C_0(0,0,q^2;0,\lambda,0) &= \frac{1}{q^2}\mathrm{Li}_2\left(\frac{\lambda^2}{q^2}\right)+\frac{1}{2q^2}\ln^2\left(\frac{-\lambda^2}{q^2}\right)+\frac{\pi^2}{6q^2} \\
C_0(m^2,m^2,t;m,M_Z,m) &\approx -\frac{1}{12m^4(M_Z^2-4m^2)^2}\Bigg\{4m^2t(M_Z^2-4m^2) \\
&\quad +(M_Z^2-4m^2)^2(6m^2+t)\ln\frac{m^2}{M_Z^2} \\
&\quad +2M_Z\sqrt{M_Z^2-4m^2}\big[-24m^4+6m^2(M_Z^2-t) \\
&\quad +M_Z^2t\big]\ln\left(\frac{\sqrt{M_Z^2-4m^2}+M_Z}{2m}\right)\Bigg\}, \quad \text{small } t
\end{aligned}
$$

F Renormalized Perturbation Theory

When one computes correlation functions (Feynman amplitudes) at the 1 loop level or beyond, they will inevitably find UV divergences from using the initial (bare) Lagrangian, which we'll denote with a 0 subscript. Renormalized perturbation theory prescribes that we rescale all our Lagrangian parameters to fix this dilemma. In our case, we can restrict this to the following parameters:

$$A_0^\mu = \sqrt{Z_A}A^\mu, \quad \text{photon field} \tag{49}$$

$$\psi_0 = \sqrt{Z_\psi}\psi, \quad \text{electron field} \tag{50}$$

$$m_0 = Z_m m, \quad \text{electron mass} \tag{51}$$

$$e_0 = Z_e e, \quad \text{electron charge} \tag{52}$$

We then expand the renormalization constants to $O(\alpha)$:

$$Z_i = 1 + \delta Z_i = 1 + O(\alpha) \tag{53}$$

After substituting (49-53) into the bare Lagrangian, one finds new terms called counterterms. These counterterms are then found from the renormalization conditions, which act like physical boundary conditions on our correlation functions. In particular for the Zee vertex of (4.10) the addition

of the counterterm gives:

$\hat{\Lambda}_\mu^{Zee} =$ 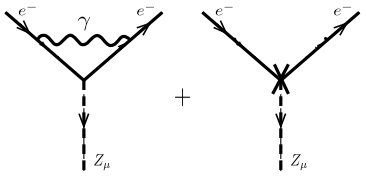

(54)

and the renormalization condition we must invoke is:

$$\hat{\Lambda}_\mu^{Zee}(p_1, p_3)|_{p_1=p_3} = 0 \tag{55}$$

The vertex counterterm is simply found by finding the net counterterm version of the γee coupling in the renormalized Lagrangian, and its vector part is:

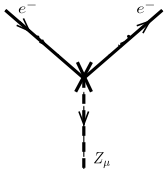

$= g_V^e ig\gamma_\mu \Big(\delta Z_\psi + \delta Z_e + \frac{1}{2}\delta Z_A\Big)$ (56)

Then we have:

$$\hat{\Lambda}_\mu^{Zee} = \Lambda_\mu^{Zee} + \gamma_\mu \Big(\delta Z_\psi + \delta Z_e + \frac{1}{2}\delta Z_A\Big) \tag{57}$$

Without proving it here, it is a rudimentary property of QED that $Z_e = Z_A^{-1/2}$ to all orders in perturbation theory, due to the Ward identity $\Lambda_\mu^{Aee}(p,p) = \frac{d}{dp^\mu}\Sigma^{\bar{e}e}(p)$ and thus $\delta Z_e = -\frac{1}{2}\delta Z_A$. Therefore (57) reduces to:

$$\hat{\Lambda}_\mu^{Zee} = \Lambda_\mu^{Zee} + \gamma_\mu \delta Z_\psi \tag{58}$$

We will next turn our attention to a derivation of δZ_ψ so that we may proceed. Before we can do that, we need to take a close look at the electron's SE correction:

$\Sigma^{\bar{e}e}(p)$ =

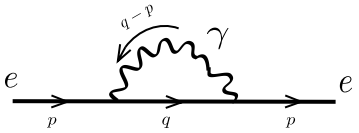

$$= ie^2 \int \frac{d^4q}{(2\pi)^4} \frac{\gamma_\alpha(\not{q}+m)\gamma^\alpha}{(q^2-m^2)[(q-p)^2-\lambda^2]} \tag{59}$$

The Dirac algebra is simply: $\gamma_\alpha(\not{q}+m)\gamma^\alpha = -2\not{q}+4m$, thus

$$\begin{aligned}
\Sigma^{\bar{e}e}(p) &= ie^2 \int \frac{d^4q}{(2\pi)^4} \frac{(-2\not{q}+4m)}{(q^2-m^2)[(q-p)^2-\lambda^2]} \\
&= -\frac{\alpha}{4\pi}\Big\{\not{p}[2B_1(p^2;m,\lambda)+1] + m[4B_0(p^2;m,\lambda)-2]\Big\} \\
&= -\frac{\alpha}{4\pi}\Big\{\not{p}\frac{[A_0(m)-(p^2+m^2)B_0(p^2;m,\lambda)+p^2]}{p^2} \\
&\quad +m[4B_0(p^2;m,\lambda)-2]\Big\}
\end{aligned} \tag{60}$$

To finish our task, we now can derive our counterterm δZ_ψ. To find it, we invoke the renormalization condition which requires the wave function of the

electron propagator to be unity when it is on shell:

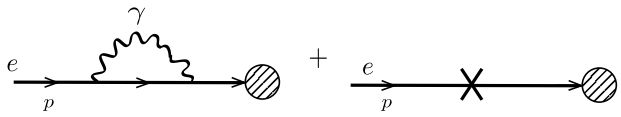

$$= 0 \qquad (61)$$

$$\Rightarrow \left[\lim_{p^2\to m^2} \frac{i}{\not p - m}\hat{\Sigma}^{\bar{e}e}(p)\right] u_e(p) = 0$$

$$\lim_{p^2\to m^2} \frac{i}{\not p - m}[\not p \Sigma_V^{\bar{e}e}(p^2) + m\Sigma_S^{\bar{e}e}(p^2) + \delta Z_\psi(\not p - m) - \delta m]u_e(p) = 0$$

$$\left[\Sigma_V^{\bar{e}e}(m^2) + \delta Z_\psi + m\lim_{p^2\to m^2} \frac{1}{\not p - m}\left(\Sigma_V^{\bar{e}e}(p^2) + \Sigma_S^{\bar{e}e}(p^2) - \frac{\delta m}{m}\right)\right] u_e(p) = 0$$

where δm is found by demanding that the electron's corrected propagator coincides with its physical, renormalized mass $\Rightarrow \delta_m = \Sigma_V^{\bar{e}e}(m^2) + \Sigma_S^{\bar{e}e}(m^2)$. Then we get:

$$\Big\{\Sigma_V^{\bar{e}e}(m^2)+\delta Z_\psi+m\lim_{p^2\to m^2}\frac{(\not{p}+m)}{p^2-m^2}\Big[\Sigma_V^{\bar{e}e}(p^2)-\Sigma_V^{\bar{e}e}(m^2)$$
$$+\Sigma_S^{\bar{e}e}(p^2)-\Sigma_S^{\bar{e}e}(m^2)\Big]\Big\}u_e(p) = 0$$
$$\Big\{\delta Z_\psi+\Sigma_V^{\bar{e}e}+2m^2\big(\Sigma_V^{\bar{e}e\prime}(m^2)+\Sigma_S^{\bar{e}e\prime}(m^2)\big)\Big\}u_e(p)=0$$
$$\Rightarrow \delta Z_\psi=-\Sigma_V^{\bar{e}e}(m^2)-2m^2\big(\Sigma_V^{\bar{e}e\prime}(m^2)+\Sigma_S^{\bar{e}e\prime}(m^2)\big)$$
$$\delta Z_\psi=\frac{\alpha}{4\pi}\frac{1}{m^2}[A_0(m)-2m^2B_0(m^2;m,\lambda)+m^2]$$
$$-2m^2\Bigg[-\frac{\alpha}{4\pi}\frac{d}{dp^2}\left(\frac{1}{p^2}[A_0(m)-(p^2+m^2)B_0(p^2;m,\lambda+p^2)]\right)\Bigg|_{p^2=m^2}$$
$$-\frac{\alpha}{4\pi}\frac{d}{dp^2}[4B_0(p^2;m,\lambda)-2]|_{p^2=m^2}\Bigg]$$

This expression exactly reduces fully to:

$$\delta Z_\psi=\frac{\alpha}{4\pi}\left[1-\frac{A_0(m)}{m^2}+4m^2B_0'(m^2;m,\lambda)\right] \tag{62}$$

Bibliography

[1] S.Glashow, Nucl. Phys. **22**, 579 (1961).

[2] M.D. Schwartz, *"Quantum Field Theory and the Standard Model",* Cambridge University Press (2014).

[3] M.E. Peskin and D.V. Schroeder, *"An Introduction to Quantum Field Theory",* Perseus Books (1995).

[4] A. H. Snell, F. Pleasonton and R.V. McCord, Phys. Rev. **78**, 310 (1950).

[5] J.M. Robson, Phys. Rev. **78**, 311, (1950).

[6] J.M. Robson, Phys. Rev. **83**, 349, (1951).

[7] J.C. Hardy and I.S. Towner, Phys. Rev. C **91**, 025501 (2015).

[8] A.Czarnecki, W.J. Marciano and A. Sirlin, Phys. Rev. Lett. **120**, 202002 (2018).

[9] A. Sirlin, Rev. Mod. Phys. **50**, 3 (1978).

[10] A. Sirlin and A. Ferroglia, Rev. Mod. Phys. **85**, 263 (2013).

[11] A. Czarnecki, W.J. Marciano and A. Sirlin, Phys. Rev. D**70**, 093006 (2004).

[12] I.S. Towner, Nuc. Phys. A. **540**, 478 (1992).

[13] A. Sirlin, Phys. Rev. Lett. **19**, 15 (1967).

[14] W.J. Marciano and A. Sirlin, Phys. Rev. Lett. **96**, 032002 (2006).

[15] A. Sibirtsev, P.G. Blunden, W. Melnitchouk and A.W. Thomas, Phys. Rev. D **82**, 013011 (2010).

[16] R. E. Cutkosky, Phys. Rev. 112, 1027 (1958).

[17] B. Rislow (2013), *Low Energy Tests of the Standard Model* (Doctoral dissertation), College of William and Mary.

[18] B. Bhattacharya, R.J. Hill and G. Paz, Phys. Rev. D **84**, 073006 (2011).

[19] R. Gupta, Y. Jang, H. Lin, B. Yoon and T. Bhattacharya, Phys. Rev. D **96**, 114503 (2017).

[20] Z. Ye, J. Arrington, R.J. Hill and G. Lee, Phys. Lett. B **777**, 8 (2018).

[21] M. Tanabashi et al., Phys. Rev. D **98**, 030001 (2018).

[22] O. Lalakulich and E.A. Paschos, Phys. Rev. D **71**, 074003 (2005).

[23] O. Lalakulich, E.A. Paschos and G. Piranishvili, Phys. Rev. D **74**, 014009 (2006).

[24] D. Dreschel, S.S. Kamalov and L. Tiator, Eur. Phys. J **A34**, 69 (2007).

[25] L. Tiator et al., Chinese Phys. C **33**, 1069 (2009).

[26] T. Leitner et al., Phys. Rev. C **79**, 034601 (2009).

[27] M.E. Christy and P.E. Bosted, Phys. Rev. C **81**, 055212 (2010).

[28] LHA PDF sets, https://lhapdf.hepforce.org

[29] C. Seng, M. Gorchtein, H. Patel and M.J. Ramsey-Musolf, Phys. Rev. Lett. **121**, 241804 (2018).

[30] C. Seng, M. Gorchtein and M.J. Ramsey-Musolf, Phys. Rev. D **100**, 013001 (2019).

[31] S.A. Larin and J.A. Vermaseren, Phys. Lett. B **259**, 345 (1991).

[32] R.K. Ellis, W.J. Stirling and B.R. Webber, *"QCD and Collider Physics"*, Cambridge University Press (1996).

[33] W.A. Bardeen, A.J. Buras, D.W. Duke and T. Muta, Phys. Rev. D **18**, 11 (1978).

[34] G. Altarelli, R.K. Ellis and G. Martinelli, Nuc. Phys. B **157**, 461 (1979).

[35] J.F. Owens, A. Accardi and W. Melnitchouk, Phys. Rev. D **87**, 094012 (2013).

[36] MMHT14 PDFs, L.A. Harland-Lang, A.D. Martin, P. Motylinski and R.S. Thorne, arXiv:1412.3989.

[37] CT14 NNLO PDFs, S. Dulat et al., arXiv:1506.07443.

[38] HERA 20 PDFs, H. Abramowicz et al., arXiv:1506.06042.

[39] S.Alekhin, J. Blumlein, Phys. Rev. D **81**, 014032 (2010).

[40] F. Jegerlehner, arxXiv:1905.05078v1 (2017).

[41] F. Jegerlehner software, www-com.physic.hu_berlin.de/ fjeger/software.html

[42] P.D.B. Collins, *"An Introduction to Regge Theory and High Energy Physics"*, Cambridge University Press (1977).

[43] J. Schwinger, Phys. Rev. **73**, 416L (1948).

[44] F. Bloch and A. Nordsieck, Phys. Rev. **52**, 54 (1937).

[45] V.L. Kashevarov, M. Ostrick and L. Tiator, Phys. Rev. C **86**, 035207 (2017).

[46] C.A. Piketty and L. Stodolsky, Nucl. Phys. B **15**, 571 (1970).

[47] J.J. Sakurai and D. Schildknecht, Phys. Lett. B **40**, 121 (1972).

[48] J. Alwall and G. Ingelman, Phys. Lett. B **596**, 77 (2004).

[49] P. Lichard, Phys. Rev. D **55**, 5385 (1997).

[50] T. Bolognese, P. Fritze, J. Morfin, D.H. Perkins, K. Powell and W.G. Scott, Phys. Rev. Lett. **50**, 224 (1983).

[51] J. Erler, A. Kurylov and M.J. Ramsey-Musolf, Phys. Rev. D **68**, 016006 (2003).

[52] J. Erler and M. J. Ramsey-Musolf, Phys. Rev. D **72**, 073003 (2005).

[53] D. Androić et al., Precision measurement of the weak charge of the proton, Nature **557**, 207-211 (2018).

[54] R.D. Carlini et. al., Jefferson Lab experiment E08-016 (Q_{weak}), http://www.jlab.org/qweak/

[55] A. Ferroglia, G. Ossola and A. Sirlin, Eur. Phys. J. **C34**, 165 (2004).

[56] F. Burger et al., JHEP **1511**, 215 (2015).

[57] M. Bohm and H. Spiesberger, Fortschr. Phys. **34**, 11, 687 (1986).

[58] J.M. Cornwall, J. Papavassiliou and D. Binosi, *"The Pinch Technique and its Applications to Non-Abelian gauge Theories"*, Cambridge University Press (2011).

[59] G. Degrassi and A. Sirlin, Phys. Rev. D **46**, 7 (1992).

[60] J. Arrington, P.G. Blunden and W. Melnitchouk, Prog. Part. Nucl. Phys. **66**, 782 (2011).

[61] P.G. Blunden, W. Melnitchouk and A. Thomas, Phys. Rev. Lett. **107**, 081801 (2011).

[62] P.G. Blunden, W. Melnitchouk and A. Thomas, Phys. Rev. Lett. **109**, 262301 (2012).

[63] N.L. Hall, P.G. Blunden, W. Melnitchouk, A.W. Thomas and R. Young, Phys. Lett. B **731**, 287 (2014).

[64] M. Gorchtein and C. Horowitz, Phys. Rev. Lett. **102**, 091806 (2009).

[65] M. Gorchtein, C. Horowitz and M.J. Ramsey-Musolf, Phys. Rev. C **84**, 015502 (2011).

[66] B.C. Rislow and C.E. Carlson, Phys. Rev. D **83**, 113007 (2011).

[67] J. Erler, M. Gorchtein, O. Koshchii, C. Seng and H. Spiesberger, arXiv:1907.07928v1

[68] Particle Data Group, Review of particle physics, Chinese Phys. C **40**, 100001 (2016).

[69] B.Holdum et al., *"Four Statements about the 4th Quark Generation"*, PMC Physics A, 3:4 (2009).

[70] C. Patrignani et al. (Particle Data Group), Chin. Phys. C, **40**, 100001 (2016).

[71] I.S. Towner and J.C. Hardy, Rep. Prog. Phys. **73**, 046301 (2010).

[72] P. Herczeg, Phys. Rev. D **34**, 3449 (1986).

[73] P. Herczeg Prog. Part. Nucl. Phys. **46**, 413 (2001).

[74] C. Seng and U-G, Meiβner, arXiv:1903.07969v1 (2019).

[75] J.C. Romao, *"Advanced Quantum Field Theory"*, Instituto Superior Tecnico.

[76] G. 't Hooft and M.J. Veltman, Nucl. Phys. B **153**, 365 (1979).

[77] L. Mankiewicz, G. Piller and T. Weigl, Phys. Rev. D **59**, 017501 (1998).

[78] W.J. Marciano and A. Sirlin, Phys. Rev. D **27**, 552 (1983); 29, 75 (1984).

[79] V. Shtabovenko, R. Mertig and F. Orellana, Comput. Phys. Commun., **207C**, 432-444 (2016); R. Mertig, M. Bohm and A. Denner, Comput. Phys. Commun., **64**, 345-359 (1991).

[80] H. Patel, Comput. Phys. Commun., **197** (2015).